Multiple Input Multiple Output (MIMO) Systems Channel Modeling and Analysis

by

Arghavan Emami Forooshani

A thesis Submitted to the Faculty of Graduate Studies in partial fulfillment of the requirements for the degree of

Master of Science

in

Department of Electrical and Computer Engineering

The University of Manitoba

THE UNIVERSITY OF MANITOBA

FACULTY OF GRADUATE STUDIES

*****

COPYRIGHT PERMISSION

Multiple Input Multiple Output (MIMO) Systems Channel Modeling and Analysis

by

Arghavan Emami Forooshani

A Thesis/Practicum submitted to the Faculty of Graduate Studies of The University of Manitoba in partial fulfillment of the requirement of the degree

of

Master of Science

Abstract

This study focuses on the Multiple Input Multiple Output (MIMO) systems, the new technology which has recently received a great deal of attention because of its possible applications in Digital Television (DTV), Wireless Local Area Networks (WLANs), Metropolitan Area Networks (MANs), and mobile communications.

MIMO system is a technology for wireless communications in which multiple antennas are combined at both transmitter and receiver sides to minimize errors and optimize data speed. The success of MIMO systems is due to the fact that they exploit the spatial dimension of the available radio spectrum more than previous systems.

In conventional wireless systems, a single antenna is used at both transmitter and receiver sides which in some cases, this can cause problems with multipath effects. In fact, in digital communications systems such as wireless Internet, it can cause a reduction in speed of data and an increase in the number of errors. The use of two or more antennas, eliminates the troubles caused by multipath wave propagation, and can even take advantage of this effect.

In this study, it is shown that for some applications the MIMO performance may be further improved by using multi-beams rather than multi-antenna elements. This type of MIMO system utilizes angle diversity instead of space diversity. In this type of MIMO, beams can efficiently be pointed towards the best directions to give the highest capacity in the desired directions while do not create interference for other directions. Therefore, it

can be very attractive for environments where interference should be minimized such as hospitals where the radio frequency interference can cause problems through interfering with medical monitoring equipment. Therefore, multi-beam MIMO can be a new and efficient solution which improves wireless communications in critical environments.

Table of Contents

List of Figures

List of Tables

List of Abbreviations

3G	Third Generation
AWGN	Additive White Gaussian Noise
BER	Bit Error Rate
BLAST	Bell Labs Layered Space Time
BTS	Base Station
DOA	Direction Of Arrival
EDGE	Enhanced Data for GSM Evolution
GBSBC	Geometrically Based Single Bounce Circular
GBSBE	Geometrically Based Single Bounce Elliptical
HDTV	High Definition TV
HPBW	Half Power Beam Width
HSDPA	High Speed Downlink Packet Access
IEEE	Electrical and Electronics Engineers
i.i.d	independently identically distributed
LOS	Line Of Sight
MAC	Medium Access Control
MIMO	Multiple Input Multiple Output
MISO	Multiple Input Single Output
MS	Mobile Station

NLOS	Non Line Of Sight
OFDM	Orthogonal Frequency Division Multiplexing
PDA	Personal Digital Assistant
PDF	Probability Density Function
PER	Packet Error Rate
RF	Radio Frequency
SIMO	Single Input Multiple Output
SISO	Single Input Single Output
SISTER	Single Interaction ScatTEring Reflecting
SNR	Signal to Noise Ratio
STBC	Space Time Block Codes
STTC	Space Time Trellis Codes
TE	Transverse Electric Field
TM	Transverse Magnetic Field
UMTS	Universal Mobile Telecommunications System
WiSE	Wireless System Engineering
WLAN	Wireless Local Area Network
WLL	Wireless Local Loop

Acknowledgments

I would like to express my most sincere gratitude to my adviser, Professor S. Noghanian for her kind support and help throughout this research project. For certain, without her intelligent suggestions, encouragement and inspiration during my research this work was not possible.

Also, I would like to extend my gratitude thank to the committee members, Dr. E. Liu and Dr. E. Hossein who took the time to read this dissertation.

Finally, I would like to acknowledge University of Manitoba which has provided the research infrastructure and Natural Sciences and Engineering Research Council of Canada which has supported this research financially.

To my beloved parents

whose prayers and encouragement,

despite of the long distance,

made this work possible.

Chapter1: Introduction

1.1 Chapter Introduction

This chapter briefly describes background of Multiple Input-Multiple Output (MIMO) systems to convey the novel idea and the knowledge of this new technology to the reader. Different diversity schemes are also introduced and finally to become more familiar with MIMO, its applications, advantages and concerns are addressed.

1.2 Background and Motivation

Nowadays, the glory of wireless communication engineering can be seen everywhere in our surroundings, either far away from our planet for Mars exploration rover mission or so close for Internet browsing using Wireless Local Area Network (WLAN) in an indoor environment. For various applications, many different methods of communication are developed. Therefore the main concern of a today's communication engineer, more than finding new ways to communicate, is finding new ways to increase throughput, range, spectral efficiency and reliability of existing systems.

In conventional wireless systems, Single Output-Single Input (SISO), for instance, a single antenna is used at the transmitter (Tx), and another single antenna is used at the receiver (Rx). These systems had to be improved since in some cases, the presence of adverse propagation conditions such as multipath fading and interference can cause problems and hence decrease the system performance. In fact, when an electromagnetic field is met with obstructions such as hills, buildings, utility wires and etc. in an outdoor environment and walls and common obstacles in an indoor environment, the wavefronts are scattered, and thus they take many paths to reach the destination. The late arrival of scattered portions of the signal gives rise to some problems such as fading. In digital communications systems e.g. wireless Internet, it can cause a reduction in data speed and an increase in the number of errors. Different diversity schemes are employed to combat this problem caused by multipaths and it is worth getting familiar with these diversity methods before continuing our discussion.

Diversity Schemes:

- *Frequency Diversity*

  Frequency diversity is achieved by transmitting the same narrowband signal at different carrier frequencies, where the carriers are separated by the coherence bandwidth of the channel.

- *Time Diversity*

Time diversity is achieved by transmitting the same signal at different times, where the time difference is greater than the channel coherence time (the inverse of the channel Doppler spread).

- *Polarization Diversity*

  Polarization diversity is achieved by using either two transmitter antennas or two receiver antennas with different polarization (e.g. vertically and horizontally polarized waves).

- *Space/Antenna Diversity*

  Space or antenna diversity is achieved by using multiple transmitter or receiver antennas (antenna array) where the elements of the array are separated in distance.

- *Angle/Pattern/Beam Diversity*

  Directional antennas offer angle diversity by restricting receiver or transmitter antenna beamwidth to a given angle.

All these methods help to overcome multipath fading, however, polarization diversity method is limited to the number of orthogonal polarizations and is difficult to implement and frequency and time processing are approaching their limits and also bandwidth is expensive. Therefore, among them, space and angle diversities which can be considered as fundamental basis for the advent of MIMO systems, have been more heavily studied for the last two decades as hinted by the impressive body of literature devoted to them. This new area has motivated the wireless academic community and industry by promising to increase capacity and performance with acceptable Bit Error Rate (BER) and efficiently use of bandwidth.

1.3 Space Diversity in Nature

The fundamental innovation of MIMO systems can be found in nature. Far from being a new trick, this has been around for the odd hundred million years.

Creatures with two ears, including us, not only can tell what direction a sound is coming from but also can concentrate on that sound even when there's a lot of extraneous noise appearing from other directions. We can even filter out sounds at the same frequency and with very similar information [1].

Imagine two speakers who are talking in a dark room. The listener among the two persons is capable of determining the location of the speaker because of the delays of the voice received by the two acoustic sensors, ears. Then brain, the human signal processor computes the direction of the speaker from the delay of two signals. Furthermore, if additional speakers join in the conservation, the brain can tune out unwanted interferes and concentrate on one conversation at a time.

1.4 Space Diversity in Communications

Space diversity can be achieved by employing multiple antenna elements at one end only (at the receiver side: SIMO ≡ Single-Input Multiple-Output, or at the transmitter side: MISO ≡ Multiple-Input Single-Output) and combining them in order to offer a more reliable communication link in the presence of multipath fading and interference (Figure 1.1). In the conventional terminology, these signal processing techniques using the data captured by multiple antenna elements are identified as *Smart Antennas* [2]. The main idea of smart antennas is the combination of signals in the spatial dimension (which naturally extends the temporal dimension) and exploiting spatial diversity. If one can estimate the response of each antenna element to a desired transmitted signal, one can optimally combine the elements with weights selected as a function of each element response. One then can maximize the average combined signal level and minimize the level of other components (noise and/or interference). Furthermore, in the presence of multipath fading, the probability of losing the signal altogether vanishes exponentially with the number of antenna elements. The diversity order is then given by the number of those elements.

In these configurations, only a single antenna is used at any point. Although there may be two or more antennas, there is only one set of components to process the signal, or Radio Frequency (RF) chain. The receiver has a single input chain, and the transmitter has a single output chain. The next step beyond diversity is to attach an RF chain to each antenna in the system. This is the basis of MIMO technology. Each RF chain is capable of simultaneous reception or transmission, which can dramatically improve throughput. Furthermore, simultaneous receiver processing has benefits in resolving multipath interference, and may improve the quality of the received signal far beyond simple diversity. Each RF chain and its corresponding antenna are responsible for transmitting a spatial stream. A single frame can be broken up and multiplexed across multiple spatial streams, which are reassembled at the receiver.

As a result, in modern communication systems such as MIMO systems, by exploiting the spatial properties of the multipath channel rather than combating it, a new dimension is offered which can be used to enhance the performance.

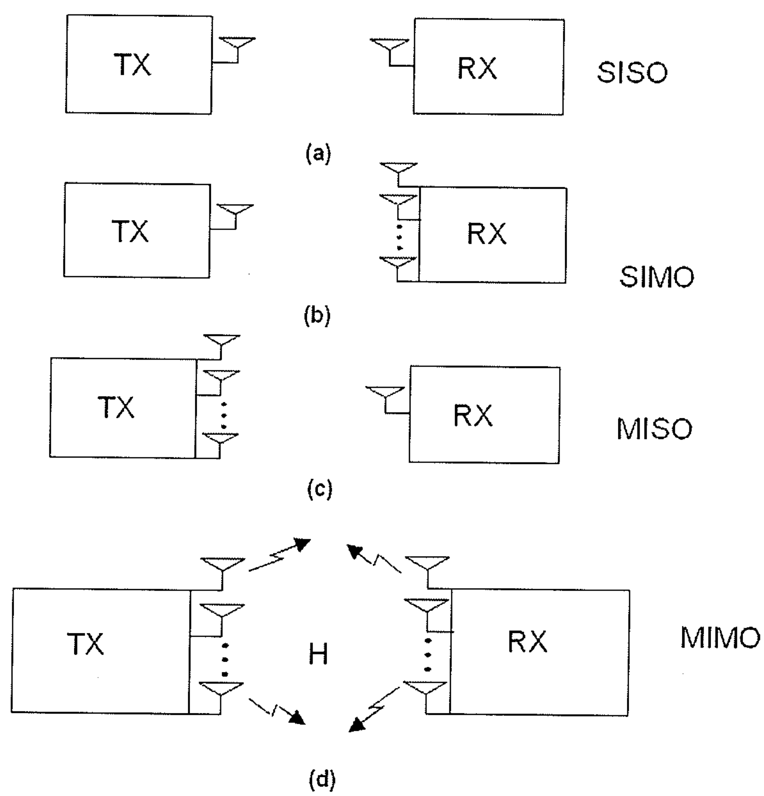

Figure 1.1 **Different configurations of multiple antenna systems: (a) SISO, (b) SIMO, (c) MISO and (d) MIMO.**

1.5 *MIMO Applications*

MIMO systems are currently considered for application in the 2nd and 3rd generation of broadband wireless fixed cellular networks. The next great application of MIMO is undoubtedly the next generation broadband mobile packet-based cellular networks (Universal Mobile Telecommunications System (UMTS) and beyond).

Some of MIMO promising applications are summarized as follows [2]:

- Indoor WLANs
- Wireless Local Loop (WLL)
- Metropolitan voice/data wireless networks (UMTS, Enhanced Data for GSM Evolution (EDGE), 3rd Generation (3G) and beyond networks)
- Very-high-speed fixed and mobile wireless (point to multipoint)
- Acoustic communications
- Broadcast systems (High Definition TV (HDTV), etc.)

MIMO can also be used in conjunction with Orthogonal Frequency Division Multiplexing (OFDM), and will be part of the Institute of Electrical and Electronics Engineers (IEEE) 802.11n high-throughput standard which is expected to be finalized in mid 2007. Moreover, standardization of MIMO to be used in 3G standards such as High-Speed Downlink Packet Access (HSDPA) is currently underway [3].

1.6 MIMO Advantages

During the last few years, MIMO technology has attracted a lot of attention in the area of wireless communications because of the possibility of significant increases in throughput and range at the same bandwidth and same overall transmit power expenditure. In the other word, it increases the spectral efficiency of a wireless communication system.

In fact, MIMO methods make use of multi-element antenna arrays at both transmitter and receiver sides of a radio link to significantly improve the capacity over more traditional SISO, MISO or SIMO systems. MISO or SIMO channels can provide *diversity gain, array gain,* and *interference canceling gain*. In addition to these advantages, MIMO links can offer a so-called *multiplexing gain* by opening parallel spatial data channels within the same frequency band at no additional power costs [4].

Interestingly, MIMO systems work best in multipath rich environments, as they can treat each arriving signal as an independent link from which information can be extracted. Fortunately, at the microwave frequencies used by WLANs and broadband data links where multipath is naturally rich, MIMO is the right technique coming along at the right time.

Main advantages of MIMO systems can be summarized as follows;

- Exploiting spatial properties of the multipath channel rather than combating it
- Extending the range
- Increasing spectral efficiency
- Reducing the interference

- Increasing the channel capacity (Delivering higher data rates)
- Increasing reliability of the communication system

1.7 MIMO Concerns

Despite the recent progress, MIMO research has largely yet to mature and contains a number of unsolved problems in areas as diverse as channel modeling, communication theory, signal processing, antenna design and cellular applications.

Questions such as the followings are the main concerns of MIMO specialists:

"How can one best exploit the properties of MIMO links in cellular networks to improve the spectrum efficiency (bps/Hz), the coverage (cell radius), or the quality (BER, Packet Error Rate (PER)). What is the right trade-off between interference suppression algorithm and data rate increase algorithms using MIMO? How to minimize the additional interference created by having additional antennas, etc.? What is the optimal antenna configuration? ".

Furthermore, as an antenna related issue, MIMO antennas have to have a reasonable physical separation to work well which is not practical to some extent. For large equipment such as laptops with a MIMO-enhanced 2.4 GHz or 5 GHz wireless LAN, separation of antennas may not be a real concern but for a Personal Digital Assistant (PDA) or mobile phone with MIMO system, there may not be enough room. However, extra RF cost will not be an issue in near future while progress in RF integration as well as ever increasing production volumes suggest the barriers will fall soon. In addition, new progresses in creating multiple phase centers for an antenna or using multimode antenna, where several modes are excited separately on the same antenna structure have made it possible to virtually set up a MIMO system without the need for extra space.

There are many other open problems in MIMO but from networking point of view, we can point to the following items:

- MIMO algorithms coping with fast time varying channels, induced by user mobility.
- Interaction between MIMO-based physical layer and Medium Access Control (MAC) layer.

Consequently, there is still plenty of work to be done in finding the best ways to model MIMO systems, designing the physical channel and other communication layers for MIMO such as finding out the best antenna configuration, modulation and encoding schemes, and finding the most effective tradeoffs between cost and performance.

1.8 Thesis Organization

This thesis is organized into 6 chapters. The first chapter contains a study of the advent of MIMO systems and their relation to the traditional diversity techniques to improve the performance of wireless systems. The motivations for MIMO study are presented here.

Chapter 2 is dedicated to positioning this study relative to other works. Two general fields of interest in MIMO are introduced and different types of communication channel are studied. At the end, gaps and limitations in current knowledge and previous works are recognized and objective of this dissertation is addressed.

In Chapter 3, our proposed mathematical model which calculates channel capacity for an environment including reflectors and spherical scatterers is described. In addition, detailed mathematical formulations for reflected and scattered fields, antenna pattern and channel capacity calculations, and coordinate transformations are covered in this chapter. Verification of the program code is also done here by comparing obtained results with *Wireless Insite*, a 3-D ray tracing tool by Remcom Inc. [5].

Chapters 4 and 5 are devoted to the numerical results obtained for outdoor and indoor environments, respectively.

Finally, Chapter 6 contains conclusions for this research and recommendations to be considered for the future work.

1.9 Chapter Summary

Digital communication using MIMO is emerging as one of the most promising research areas in wireless communications. MIMO systems exploit the channel spatial degrees of freedom to increase communication performance. In traditional antenna diversity, these resources are used to transmit and/or receive duplicate copies of a single information stream to increase the reliability of detection. In contrast, spatial multiplexing i.e. sending distinct information streams over the channels increases the throughput and spectral efficiency. The mix of diversity and spatial multiplexing accomplished with a MIMO system will depend on the throughput and quality-of-service requirements of the application.

In fact, MIMO antenna technology exploits multipath propagation to increase data throughput and range, or reduce bit error rates, rather than attempting to eliminate effects of multipath propagation as traditional SISO communication systems seek to do. MIMO wireless research has key applications in the high-speed high-spectrum efficiency wireless networks (3G and beyond). Despite recent progress, MIMO research has largely yet to mature and contains a number of unsolved problems in different areas such as channel modeling, communication theory, signal processing, antenna design and cellular applications.

Chapter2: Literature Review

2.1 Chapter Introduction

In this chapter, this study is positioned relative to other works and also strengths, weaknesses, gaps and limitations in current knowledge and previous works are identified. First a brief history and some overview of needed definitions for MIMO systems can be helpful to follow further details.

2.2 Quick Review of MIMO History in Radio Communications

At Bell Laboratories, formerly known as AT&T Bell Laboratories and Bell Telephone Laboratories, Winters and many others published articles on MIMO in the period from 1986 to 1995 [3]. Before then, it has been for decades that traditional MISO or SIMO channels have been employed to obtain diversity, array, and interference canceling gain. Later in 1996, Greg Raleigh and Gerard J. Foschini invented new approaches to MIMO which increased its efficiency [3]. Foschini and Gans showed in addition to advantages achieved from MISO and SIMO, MIMO links can offer the so-called *multiplexing gain* by opening parallel spatial data channels within the same frequency band at no additional power costs. In the presence of a rich multipath environment, leading to antenna decorrelation and full channel rank, MIMO links offer capacity gains that are proportional to the minimum of the number of transmitter and receiver antennas [6].

In fact, exploiting the spatial properties of the multipath channel, MIMO systems offer a new dimension which can be used to enhance communication performance. This exploitation takes the form of multiple; spatially parallel communication modes that depend on the eigenvalue distribution of the channel complex impulse response matrix which is used to calculate the channel capacity.

In the following section, two general fields of MIMO study will be introduced which the ultimate goal in both is increasing channel capacity through decorrelating the parallel channels.

2.3 Two General Fields of Interest in MIMO Systems

MIMO research can be categorized in two main fields of interest as follows;

1) *Coding and Signal Processing*
2) *Channel Propagation and Antenna Design*

While coding and signal processing are key factors to successful implementation of a MIMO system, the channel propagation and antenna design represent major parameters that ultimately impact system performance. As a result, considerable research has recently been devoted to these two areas. Evaluating the performance potential of MIMO systems, for instance, requires a new level of understanding concerning multipath channel and scatterers' characteristics. Moreover, while there is extensive information available concerning the behavior of antenna diversity in multipath channels, latest activity surrounding MIMO communications has shown new issues related to the impact of antenna properties and array design on system performance [7].

In this thesis, the main focus is on the antenna and propagation side of MIMO systems, therefore, different issues and concerns reflected here are mostly related to MIMO literatures involving channel propagation and antenna design, and coding and signal processing of MIMO will be briefly treated.

2.4 *Wireless Communication System for MIMO*

Figure 2.1 represents a general model of a MIMO communication system showing the "propagation channel and antenna" and also "coding and signal processing" parts. For simplicity, in many studies, the channel is assumed to be time invariant over the interval of a transmission block. Since antenna elements and RF components influence the end-to-end transfer function ($H(\omega)$), they are embedded in the channel.

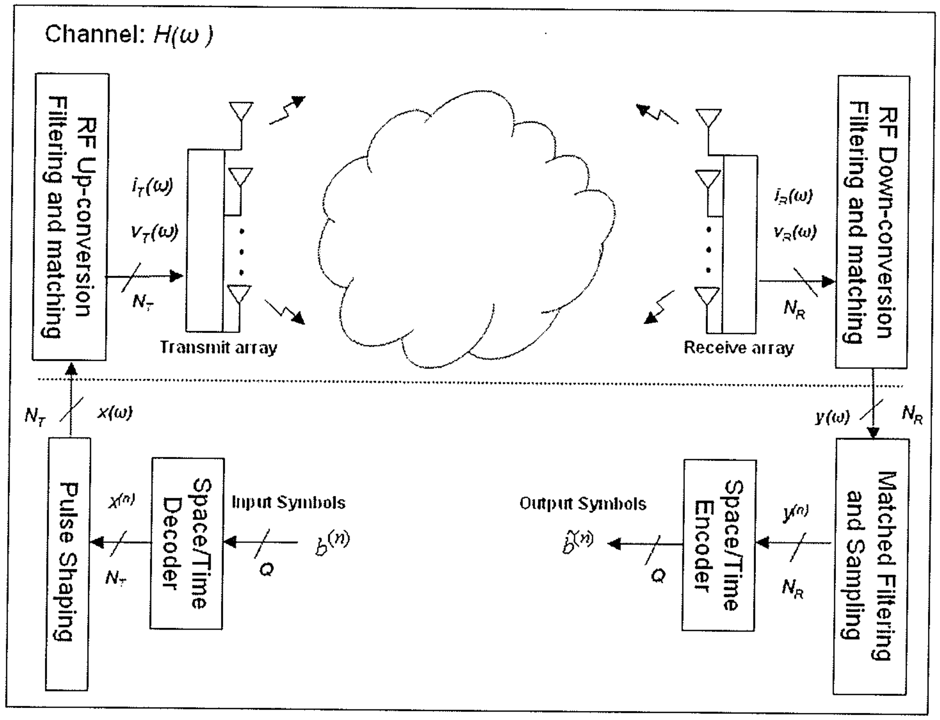

Figure 2.1 **Block diagram of a MIMO wireless system.**

In this system, symbol vector $b^{(n)}$ (n is a time index) represents a set of Q independent data streams encoded into N_T discrete-time complex baseband streams, $x^{(n)}$, at the transmitter. The coding can distribute the input symbols over the N_T outputs (space) and/or over samples (time). The pulse-shaping block converts the discrete-time samples into continuous-time baseband waveforms $x(\omega)$ and feeds them to the N_T channel inputs (RF chains and antennas). The channel combines the input signals to obtain the N_R element output (receive) waveform vector $y(\omega)$. Then at the receiver side matched filter produces the discrete-time baseband sample stream $y^{(n)}$, and the space/time decoder generates estimates of the Q transmitted streams $\hat{b}^{(n)}$.

As a result, for linear channel elements, the MIMO channel input–output relationship may be written as:

$$\underset{N_R\times 1}{y(\omega)}=\underset{N_R\times N_T}{H(\omega)}\;\underset{N_T\times 1}{x(\omega)}+\underset{N_R\times 1}{\eta(\omega)} \tag{2-1}$$

where η is additive noise produced by the channel and includes the interference from the RF front end. $H(\omega)$ *is* complex impulse response of the channel. Each of its elements, $h_{ij}(\omega)$ represents the transfer function between the jth transmitter and ith receiver antennas. Since the transmitter vector $x(\omega)$ is projected onto $H(\omega)$ in (2-1), the number of independent data streams Q that can be supported must be at most equal to the rank of $H(\omega)$ or equivalently $Q \leq min\ (N_T\ , N_R\ )$.

More generally, the properties of $H(\omega)$, such as the distribution of its singular values, determine the performance potential for the MIMO system. Factors such as multipath propagation and scatterers' characteristics, antenna impedance matching, array size and configuration, element pattern, polarization properties and mutual coupling influence these properties. Therefore, poor design of system components or incorrect assumptions about the channel could lead to drastic reduction in system performance.

For convenience, the frequency dependence ω will be usually dropped and hence the system is considered narrowband which is reasonable when the channel response is constant over the system bandwidth (flat fading) or when signals are divided into narrowband frequency bins and processed independently. This highlights the effect of the spatial dimension, a unique factor of MIMO communications, and ignores the complexity of the wide-band channel response [7].

2.5 *Typical Assumptions in Wireless Channel Modeling*

Various approaches to characterize the wireless channel rely on different assumptions which result in either simpler or more applicable models. Following section addresses different possible assumptions which are considered in most studies devoted to channel analysis.

- **Channel Noise**

  In most MIMO research papers channel noise is considered uncorrelated Additive White Gaussian Noise (AWGN) which is the worst kind of noise and it is not predictable.

- **Non Line Of Sight (NLOS) and Line Of Sight (LOS) Scenarios**

  In general, most of the models depend on the assumption that the MIMO channel coefficients (*H*-matrix entries) are Rayleigh distributed, which is reasonable in NLOS scenarios as long as there are no dominant paths. The Rayleigh channel model for *H* has independently identically distributed (i.i.d) complex, zero mean and unit variance entries shown in (2-2) and (2-3). Consequently, $|h_{ij}|^2$ is a χ_2^2 variate (Chi-square distribution with two degrees of freedom) but normalized so $E|h_{ij}|^2=1$.

$$H(\omega) = \begin{bmatrix} h_{11} & \cdots & \cdots & h_{1N_T} \\ \vdots & \ddots & \vdots & \vdots \\ \vdots & \vdots & \ddots & \vdots \\ h_{N_R1} & \cdots & \cdots & h_{N_RN_T} \end{bmatrix} \tag{2-2}$$

$$h_{ij} = Normal(0, \frac{1}{\sqrt{2}}) + jNormal(0, \frac{1}{\sqrt{2}}) \tag{2-3}$$

where $Normal(0, \frac{1}{\sqrt{2}})$ represents the Gaussian distribution with mean=0 and variance=0.5. Regarding the i.i.d. assumption, independence is usually just an approximation which improves as array element spacing becomes large compared to λ (wavelength). However, it is expected that with the i.i.d. idealization capacity estimates can be useful even for spacings as small as $\lambda/2$, because good diversity performance maintains even for correlation as high as 0.5 [6].

However, many scenarios can be described as LOS where the direct path between the receiver and transmitter dominates the channel. In such cases, the channel is Ricean (noncentral chi-square or generalized Rayleigh distribution) distributed rather than Rayleigh distributed. Because of the LOS component, the Ricean fading distribution is less "random" and has a lighter tail than the Rayleigh distribution with the same average channel gain. As a consequence, diversity gain is significantly smaller in the Ricean case compared to the Rayleigh case (Figure 2.2).

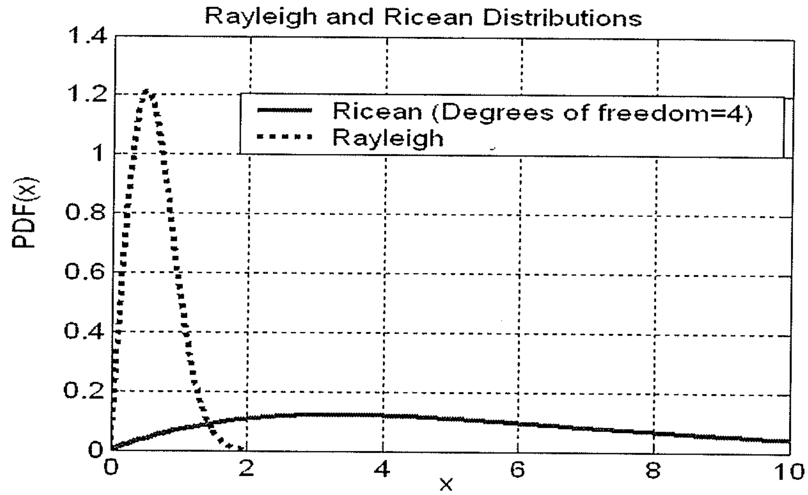

Figure 2.2 **Rayleigh and Ricean distributions.**

- **Transmitter and Receiver Knowledge about the Channel**

Channel information available at Rx, Tx or both is extremely helpful to accurately model the radio channel which can significantly enhance the performance of wireless communication systems. Therefore, most of MIMO detection schemes are based on perfect channel knowledge being available at the receiver; however, this is never achievable in reality.

In practice, the channel estimation procedure is aided by transmitting pilot symbols that are known at the receiver. Use of these symbols, on the other hand, causes reduction in spectral efficiency. Therefore, to increase spectral efficiency, it is desirable to limit the number of transmitted pilot symbols.

If transmitter is informed about the channel, *water filling* method allocates power to the high-gain channels and in general does not use the weaker channels. In contrast, if the transmitter does not know H, it *evenly* divides the power among the N_T transmitter antennas to form independent streams [7].

In the case that transmitter is not informed about the channel; power is allocated to all the available channels evenly.

- **Different Distributions for Scatterers**

In systems which employ spatial filtering such as switched beam systems or adaptive antennas, distribution of the multipath components is important in determining the performance of the channel [8]. To simulate these systems without using measured data or site specific propagation prediction techniques, a model must be used to generate multipath channel parameters. Therefore, a number of realistic spatial channel models are introduced and the defining equations (or geometry) are described in [8]. Some of these models are illustrated in Figure 2.3 to Figure 2.5.

In Lee's model shown in Figure 2.3, scatterers are distributed on a circular ring. Each scatterer is intended to represent the effect of many scatterers within the region and hence each scatterer is referred to as effective scatterer [8]. This model is only good for environments such as outdoors where the scatterers are mostly around the Mobile Station (MS).

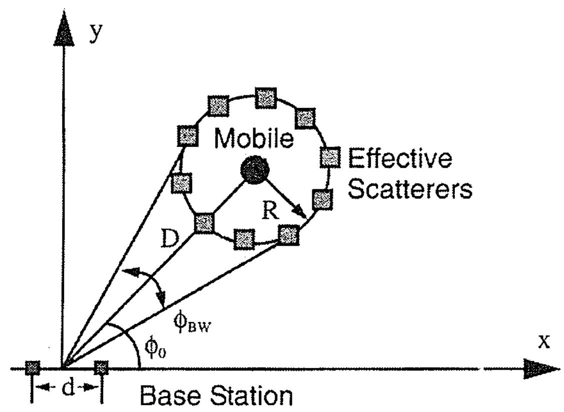

Figure 2.3 **Lee's model [8].**

In Geometrically-Based Single-Bounce Circular Model (GBSBC), it is assumed that scatterers lie within radius R_m about the mobile (Figure 2.4). This model is based on the assumption that in macrocell environments where antenna heights are relatively high, there will be no scattering from the area around the Base Station (BTS) [8]. Again, this model is only good for environments such as outdoors where the scatterers are mostly around the MS.

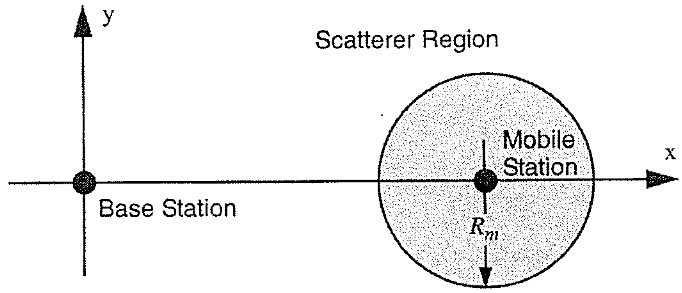

Figure 2.4 **GBSBC model [8].**

In Geometrically-Based Single-Bounce Elliptical Model (GBSBE), scatterers are uniformly distributed within an ellipse as shown in Figure 2.5. This model is developed for microcell and picocell environments where antenna heights are low and hence scattering for both BTS and MS are the same [8]. This model is good for the environments such as indoors where Tx and Rx have almost the same height and scatterers are distributed around both Tx and Rx.

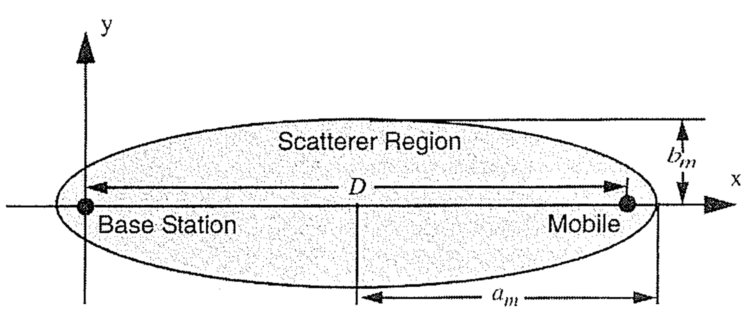

Figure 2.5 **GBSBE model [8].**

Single Interaction ScatTEring Reflecting (SISTER) Model

All models mentioned above are valid for special environments with specific assumptions. The motivation of this work was the need for a general model that is valid for both outdoor and indoor environments. Also a model that includes antenna characteristics in the channel model is required to make realistic conclusions about different environments. Therefore, in this thesis, a model is developed that responds to both shortcomings of previous models. It is worth mentioning that ray-tracing is another modeling method that is very accurate in terms of scattering environment and antenna characteristics, but it is site-specific, i.e. it needs exact information about environment and it is computationally intensive, needing long run-time. If general conclusions about system configuration based on statistics of the channel are required, ray-tracing is not a practical tool. The proposed model (SISTER) not only is general in terms of different fading channels and antenna configuration but also is simple and can be run in a reasonable computation time. In SISTER model, scatterers are located in an enclosed area which includes Tx and Rx; besides, any numbers and distributions including uniform and cluster forms can be defined for scatterers. Moreover, to have even more accurate model, reflections are also included in our modeling.

To keep this model simple, only single interaction from each scatterer (or reflector) is considered and the interactions between scatterers (or reflectors) are neglected. At first glance, it might seem that this assumption makes the model nonideal since it fails to model multiple interactions which do exist in reality. While this is true to some extent, it should be noted that the goal of developing this model was to let the designers to obtain a general view about the channel and specify the procedure guidelines properly. A more precise design can be developed based on these guidelines by using more accurate models which results in a faster implementation of the system.

2.6 Coding and Signal Processing

2.6.1 Coding for MIMO

Forward error correction coding constitutes an important part of MIMO research. In the increasingly popular space-time coding techniques [9], the coding of symbols is performed in an interleaved manner across the transmitter antennas in order to provide the same average level of protection to each antenna. This allows extracting a diversity gain out of the MIMO channel. Typical schemes use computationally-involved convolutional codes; however, simpler linear codes have been also proposed which unfortunately work only for the case of two transmitter antennas [10].

As a result, space-time coding introduces redundancy in space, by adding multiple antennas, and redundancy in time, through channel coding. Two main space-time coding techniques are *Space Time Block Codes* (STBC) and *Space Time Trellis Codes* (STTC).

STBC provide diversity gain, with very low decoding complexity, whereas STTC provide both diversity and coding gains at the cost of higher decoding complexity [9].

2.6.2 Signaling Schemes and Receiver Design for MIMO

A usual drawback of information theoretic analysis is that it does not reflect the performance realized by actual transmission-reception systems, since it is an upper bound realized by ideal algorithms/codes only. Therefore, a real problem is the study of actual signaling schemes and receiver algorithms specially developed for MIMO systems. Current signaling or transmission schemes typically fall into two categories; *Spatial Multiplexing* which maximizes the data rate using variants of the Bell Labs Layered Space-Time (BLAST) algorithm and *Diversity Scheme* which minimizes the BER through space time coding ideas.

As a mater of fact, both of them are trying to maximize the spectrum efficiency of the transmission, but in different ways. By diversity schemes, resources are used to transmit and/or receive duplicate copies of a single information stream to increase the reliability of detection. In contrast, spatial multiplexing indicates sending distinct information streams over the channels to increase throughput and spectral efficiency. It is an interesting and useful problem to somehow combine the two approaches through a single unifying scheme. The mix of them accomplished with a MIMO system will depend on the throughput and quality-of-service requirements of the application.

Once a transmission scheme is decided upon, various receiver structures (linear, maximum likelihood, decision feedback, etc.) can be applied. Now the open problem is to find a signal processing structure that represents a good performance/complexity trade-off. This has become a popular problem to work on [2].

In addition to signal processing for power control, *Array Processing* is another attractive topic in MIMO signal processing which is essential in order to find signal *Direction of Arrival* (DOA) and hence to help estimating the communication channel as accurate as possible. Different array-based DOA estimation techniques are broadly divided in to four different groups: *Conventional, Subspace Based, Maximum Likelihood,* and *Integrated* techniques [8]. It is worth noting that adding array processing part will bring complexity to the system which is not desirable for applications where system cost and complexity are the most important issues.

2.7 Propagation Channel and Antenna Design

Since antenna properties such as pattern, polarization, array configuration, and mutual coupling can impact the correlation between the channels and hence the MIMO system performance, it is required to have a closer look at the fundamental physical link, i.e., the link between the antennas and the propagation path in between. In this section, impact of different antenna properties on correlation and the system performance will be discussed by referring to recent studies.

2.7.1 Array Configuration

It is difficult to find a unique array topology which maximizes the capacity or minimizes symbol error rates and interference in all propagation environments since the optimal array shape depends on the site-specific propagation characteristics; however, some general observations are possible for indoor and outdoor environments. In some studies several array types were explored for both the BTS and the MS in an outdoor environment [11]. The BTS antennas included single and dual polarization arrays and multibeam structures. The arrays of the MS were monopoles to obtain spatial, angle, and/or polarization diversity. All of the array configurations showed very similar performance except multibeam BTS antennas which resulted in a 40–50% reduction in measured capacity since generally only one of the beams pointed in the direction of the mobile. These results suggest that average capacity is relatively insensitive to array configuration [7]. However, an adaptive system that intelligently selects the sub-arrays and connects them to the electronic modules has shown great performance by providing improved capacity [12], [13] or lower probability of symbol error [14] relative to the fixed arrays. In these systems either Tx is informed about the radio link through receiving known training sequence periodically or use blind adaptive algorithm. In either ways, complexity is the price which is paid to achieve this high performance in these systems.

2.7.2 Element Polarization

Recent works have shown that six independent communication modes are enabled only for full multipath angle spread in a rich multipath environment. In these systems, three Cartesian vector components of the electric and magnetic fields provide six uncorrelated signals at the receiver [15]. However, constructing a multi-polarized antenna that can achieve this bound is not that easy in practice. Using half wavelength dipoles and full wavelength loops leads to strong mutual coupling and nonideal pattern characteristics that can reduce the number of independent channels. One interesting geometry is a cube consisting of dipole antennas to obtain a high-degree of polarization diversity in a compact form [16]. Finally, in the common case where two polarizations are used, typical scattering leads to a co-polarized received signal that is 4 to 10 dB higher than the cross-polarized signal level [17]. The result is an H-matrix that exhibits low correlation coupled with weak channel gain between the two orthogonally polarized channels (reduced Signal to Noise Ratio (SNR)) [18].

The key advantage of using two polarizations is that regardless of the environment, at least two parallel channels are achievable.

2.7.3 Mutual Coupling

Coupling between transmitter and receiver antenna elements is a real issue for MIMO systems which has a great impact on the capacity of a given communication channel.

Although in some research, it has been claimed that in certain cases antenna coupling has a beneficial effect and leads to reduced signal correlation, strong coupling between antenna elements can put to an upper bound on capacity performance. Two main conclusions of recent studies can be summarized as follows [7]:

First, since coupled antennas offer angle diversity in addition to improved power collection, the capacity of two coupled dipoles can be higher than that of uncoupled antennas.

Second, for a fixed-length array, the strong coupling between elements packed into the same physical space results in an upper bound on capacity performance.

Figure 2.6, for instance, plots the capacity as a function of the number of transmitter and receiver half-wavelength dipoles ($N_T=N_R=M$) packed into a linear array of length 5λ [19]. As it can be seen, this analysis predicts significant capacity reduction compared to a system where coupling is neglected for spacing smaller than about 0.5λ, results in an upper capacity bound for a given aperture length.

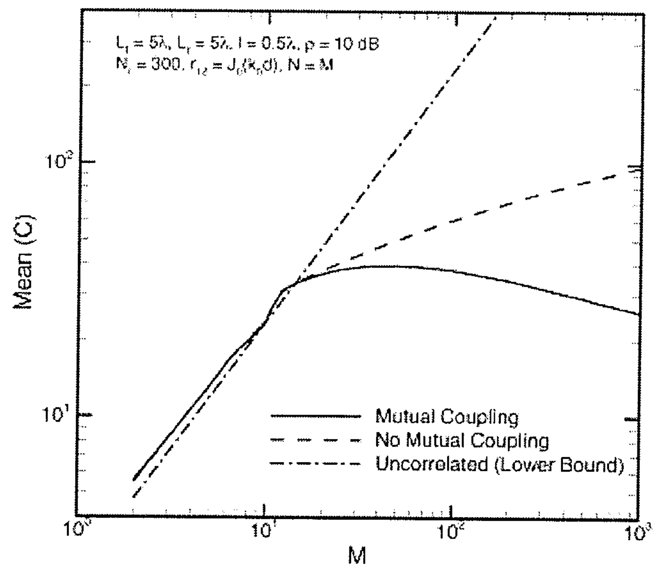

Figure 2.6 **Impact of mutual coupling on arrays of length 5λ as the number of elements increases, (r_{12}=covariance, Nr=number of Mont Carlo realizations, ρ=*SNR*) [19].**

2.7.4 Antenna Pattern

Assuming two antennas with the same or closely spaced phase centers, a single incident wave polarization, and that the arrival angles of the multipath components satisfy a Probability Density Function (PDF), $f_\Omega(\Omega)$, it is desirable that the signal correlation [20]:

$$\rho_P = \int f_\Omega(\Omega) e_1(\Omega) e_2(\Omega) d\Omega \qquad (2\text{-}4)$$

where $e_i(\Omega)$ is the pattern of the *i*th antenna, to be small. Omnidirectional pattern created by most small elements, for instance, results in relatively large values of ρ_P, leading to low capacity. However, when element patterns are properly designed to minimize ρ_P, then capacity gains are possible. Use of multi-mode antennas is one suggested approach where the patterns for different modes exhibit high orthogonality (low correlation) [21]. Finding other antenna topologies such as using a single antenna but with multiple phase centers, which offer this orthogonality in a compact form, remains an area of active research.

In addition to mentioned correlation of antenna elements, the way which the antenna confronts the multipath environment is another important aspect of element radiation pattern. A recent study, as an example has compared the capacity performance of dipole antennas with that of higher-gain spiral antennas whose radiation patterns are more directive towards 45° and 135° in elevation [22]. Figure 2.7 shows different results for channel capacity, obtained from measurement (using a switched array system) and simulation (using a statistical path-based channel model) for the two antennas in an indoor environment.

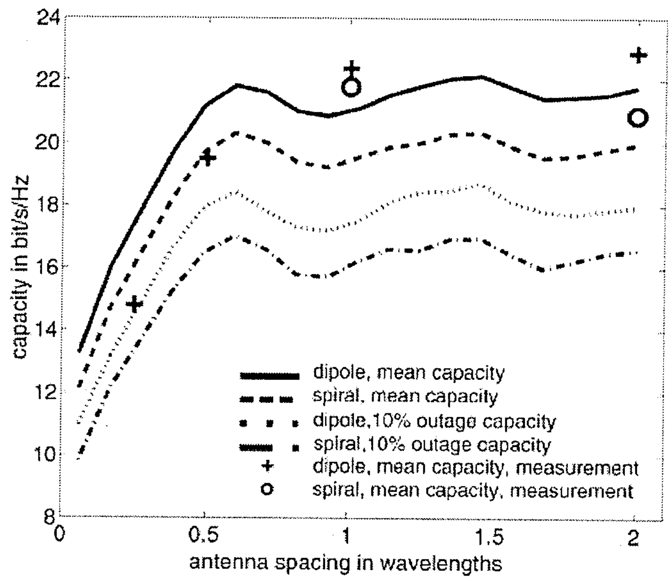

Figure 2.7 **Simulated and measured outage capacities for arrays of 2 dipole and spiral antennas in an indoor environment as a function of antenna spacing [22].**

As it shows the lower gain dipoles offer higher capacity (by about 10%), since these antennas place more energy into the horizontal plane where most of the multipath components are concentrated [7].

2.8 Thesis Objective

To model modern wireless communication systems such as MIMO systems, classical channel models which study received signal power level distribution and Doppler shifts of a single antenna may not be useful anymore. Instead, new types of channel are required to be characterized by modern models which consider spatial properties of radio channel as well as temporal ones.

As it was mentioned frequently, the ultimate goal of the study of MIMO modeling is to maximize the capacity which is achievable if orthogonal channels exist and to minimize the interference with other systems. The system which best satisfies these conditions, will be the most suitable one particularly for indoor environments.

To design such a system, first an accurate channel model should be obtained. In fact, the need to achieve channel models for different wireless radio channels has resulted in a large number of different modeling approaches that can be found in the literature. One reason for the abundance of approaches is that the propagation of a transmitted radio signal is a very complicated process, and modeling all the phenomena in a physically correct manner is virtually impossible. Thus, many different types of simplifications and approximations are necessary in order to obtain a simple yet accurate model of the wireless radio communications channel. Different approaches to channel modeling may roughly be divided in the following categories:

Statistical Models

Statistical models use a very simplified physical analysis to achieve a statistical description of the radio channel. These models are used not only for simulating channel data but also serves as a starting point for designing optimal receivers [23].

Semi-Deterministic Models

These models are more accurate physically. A typical approach is to position scatterers in the study area and then calculate the properties of this deterministic scenario using fundamental physics and corresponding mathematical formulas. By assuming some statistical distribution of the location of these objects and their properties, a semi-deterministic radio channel model is obtained. Similar to the purely statistical models, these models can be used to simulate data and designing receiver algorithms. Their main advantage is that they provide some physical insight of the channel properties while avoiding the intensive computations of ray-tracing schemes [23].

Ray Tracing Models

In these models, by employing optical concepts (treating the waves as rays) the field strength can be calculated and hence it would be possible to accurately predict the radio channel if a detailed map of the study area is available [23].

Currently, different ray tracing tools such as *Wireless Insite* by Remcom Inc., *Wireless System Engineering* (WiSE) by Bell, etc. can be found in the market to simulate the real environments and construct the channel impulse response.

Empirical Models

In this model, no detailed modeling of the area is performed. Instead, simplified versions of ray-tracing are fitted to measured data through a number of parameters [23].

Among all the mentioned methods, ray tracing seems the most attractive and modern one which seems capable of modeling the channel very precisely. However, it is difficult and almost impossible to enter all the details of the study area and using many approximations are inevitable. In fact, their applications are limited to modeling deterministic scenarios where a good map is available. Moreover, they are very computer intensive and sometimes it takes a very long time to run a simulation or see the results of a new run for a changed parameter.

Considering all above, it can be concluded that statistical and semi-deterministic models are suitable at the first stage of design to let the designers obtain an overview about the channel and specify the procedure guidelines properly. Then, they can stay on the right track and continue to go further and improve their primer design by using more accurate models such as ray tracing and empirical models which finally lead to implementation of a high performance system.

In this regard, we chose to develop a mathematical model (SISTER) which falls into semi-deterministic category. This model is applicable to arbitrary antennas and suitable for channel prediction studies in both indoor and outdoor environments. In this model, different distributions for scatterers and in the case of indoor environments, different dimensions for a room can be assumed. The corresponding algorithm calculates the LOS, reflected and scattered electric fields and finally computes the channel capacity in a very short time.

It is worth mentioning that similar study has been done [23] but it does not include different distributions for the scatterers, reflection from the ground and antenna array factor in channel complex impulse response calculations. Moreover, it is not suitable for indoor applications since it does not take into account the reflections from the walls.

SISTER model includes different factors which influence the channel capacity in calculation of channel complex impulse response. Since among these factors, the ones related to antenna properties play a major role in improving the channel capacity, in this dissertation we mostly have focused on antenna pattern impact on channel capacity and how an antenna confronts multipath environment by studying beam selection solution.

Beam Selection, also known as *Angle Diversity* is a promising solution which recently has attracted considerable attention. This approach is a relatively new topic in MIMO channel modeling and falls in the antenna design and channel propagation category which as previously described constructs the physical layer of wireless communication systems. To obtain narrow beams needed in this method, antenna array can be used as MIMO elements at both Tx and Rx sides.

The main advantage of this technique comparing to its other counterparts is that it allocates high capacity not to all the points but the desired ones which results in minimum interference for undesired areas. This is quite beneficial in indoor environments where interference is a real concern. The main difficulty in these systems is finding the optimal angles where the different beams should be directed towards. Some indoor studies suggest that to virtually create a rich multipath environment in order to increase the probability of orthogonality between different paths, the beams should be directed towards the scatterers [24]. However, to find the optimum angles while considering adjacent beams to have the least correlation with each other, demands much more studies. The fact that scanning angle of antenna array starts broadening while scanning towards endfire direction is another issue which should be taken into account in these types of research.

2.9 *Chapter Summary*

In this chapter, it was shown that issues related to "antennas and electromagnetic propagation" and "signal processing" play significant roles in determining MIMO system performance. Popular space-time coding techniques allow extracting a diversity/coding gain by coding of symbols performed in an interleaved manner across the transmitter antennas. It was also discussed that both signal processing approaches, spatial diversity and multiplexing, maximize the spectrum efficiency of the transmission, but in different ways.

In addition, impact of different antenna properties such as pattern, polarization, array configuration, and mutual coupling on correlation were discussed. Recent MIMO research on element pattern show that designing element patterns properly to minimize signal correlation, causes increase in capacity. Using polarization diversity, on the other hand, can increase mutual coupling and leads to nonideal pattern characteristics that can reduce the number of independent channels. Mutual coupling itself is another issue in MIMO systems which can have either positive or negative effects on channel capacity in different conditions. Research on array configuration effects, also has shown that since it is difficult to find a unique array topology which maximizes the capacity or minimizes symbol error rates and interference in all propagation environments the best performance can be obtained through using intelligently-selected sub-arrays.

Finally, objective of this study was briefly introduced. Beam selection was mentioned as a new approach in MIMO channel modeling which not only offers higher capacity for desired areas but also is helpful to decrease the interference. The main concern in this approach is finding the optimum angles while considering adjacent beams to have the least correlation with each other. Also, the fact that scanning angle starts broadening while approaching to endfire state is another issue which should be taken into account.

Chapter3: Theory and Analysis

3.1 Chapter Introduction

In this chapter, first, different steps for developing the SISTER model to characterize the outdoor and indoor environments are briefly explained and after that, as the main body of this chapter, essential mathematical formulas required to model the wireless communication consisting of transmitter, scatterers, reflectors and receiver are described. These formulas consist of reflected and scattered field, antenna pattern and channel capacity calculations and coordinate transformations. At the end, the developed model is validated by a ray tracing tool and the results of received power, electric field amplitude and phase and channel capacity are compared.

3.2 SISTER Model

In SISTER model different locations, configurations, radiation patterns and polarizations can be defined for Tx and Rx antennas. Scatterers' distribution, material and size can also be defined. Simple shape of sphere is chosen for scatterers in order to obtain analytical expressions for scattered fields. Moreover, to keep the simplicity, only a single interaction from each scatterer (or reflector) is considered and the interactions between scatterers (or reflectors) are neglected as it is shown in Figure 3.1.

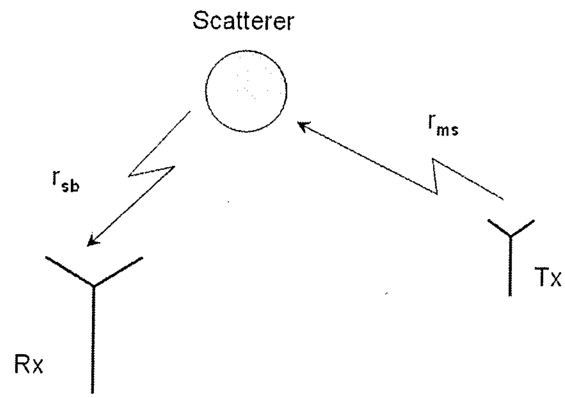

Figure 3.1 **Single interaction for each scatterer is considered.**

This model can be used for both indoor and outdoor applications and there is no limitation on Tx and Rx heights, element spacing and Tx-Rx separation.

Both LOS and NLOS cases are modeled. In the NLOS case, a blocking wall is assumed between Tx and Rx.

Without losing the generality, it is assumed that the MS is the transmitter and the BTS is the receiver. Therefore, the electric waves are generated at the MS and then propagate towards the scatterers (or reflectors) and finally scatter (or reflect) towards the BTS. In order to use far field expressions for antennas, scatterers are located in the far field of both Tx and Rx. From antenna theory, if the distance between the antenna and the object is $r \geq \frac{2D^2}{\lambda}$ where D is the largest dimension of the corresponding antenna and λ is the wavelength, object is located in the far field of the antenna.

3.2.1 Outdoor Model

The SISTER is sufficiently general to be applied to any distributions and locations for the scatterers. However, for the outdoor model, we evaluate the final results for two cases which are common ones in outdoor environments:

1. Case1: Scatterers are uniformly distributed around each end in a cubic volume ($200\lambda \times 150\lambda \times 50\lambda$ or $25 \times 18.75 \times 6.25$ m^3) containing BTS, MS and scatterers as shown in Figure 3.2.

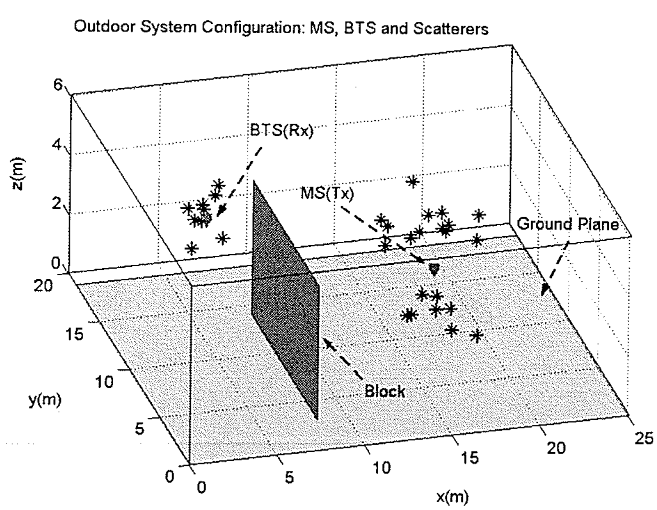

Figure 3.2 System configuration for Case1.

2. Case2: Scatterers are distributed in cluster form in a cubic volume containing MS and BTS as it is shown in Figure 3.3.

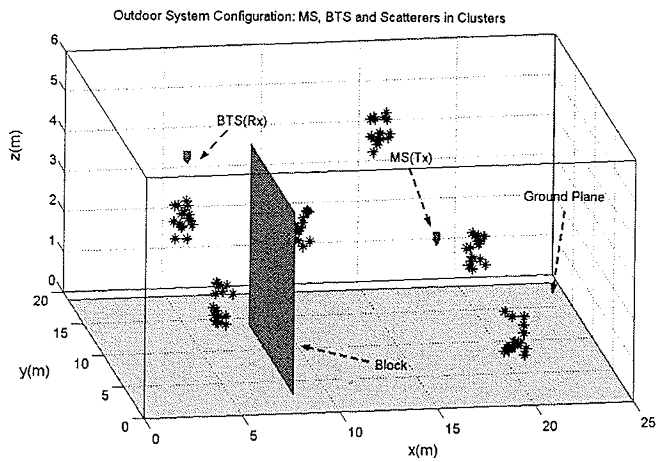

Figure 3.3 **System configuration for Case2.**

3.2.2 Indoor Model

In order to characterize the indoor channel, the outdoor model is enhanced in such a way that it includes not only the scatterers and reflection from the ground but also reflection from the walls as shown in Figures 3.4 and 3.5. Two distributions of uniform and cluster form for scatterers are considered. Two different environments including a typical office area of $5\times4\times3$ m^3 and an amphitheater of $10\times7\times5$ m^3 are studied.

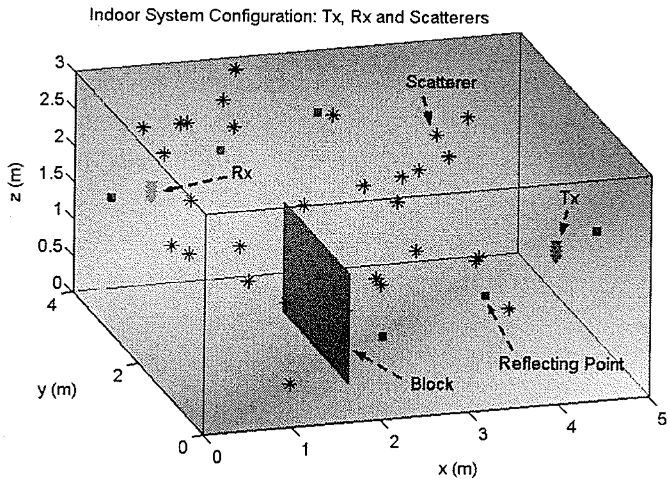

Figure 3.4 3-D schematic of the room including Tx, Rx, reflectors and uniformly distributed scatterers.

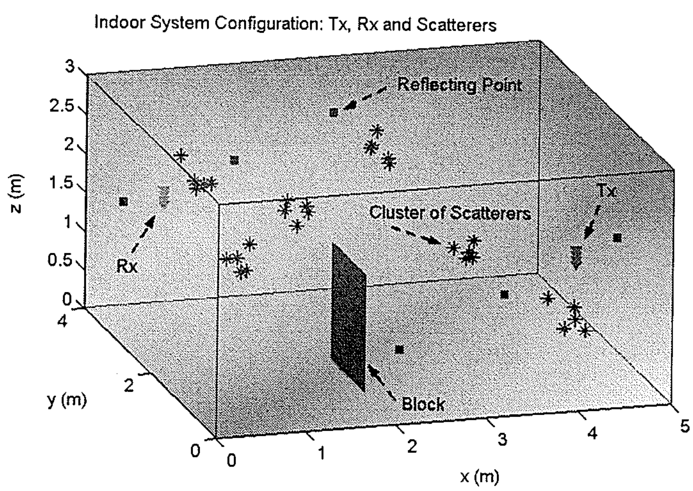

Figure 3.5 3-D schematic of the room including Tx, Rx, reflectors and scatterers in cluster form.

3.3 Analytical Calculations

In this section, first different required calculations will be explained. Then it will be shown how these calculations are used to compute the channel complex impulse response matrix (*H*-matrix) and the channel capacity.

3.3.1 Model Formulation Procedure

By considering a 4×4-MIMO system, *H*-matrix will consist of 16 entries each of which corresponds to a different channel:

$$H = \underbrace{\begin{bmatrix} h_{11} & h_{12} & h_{13} & h_{14} \\ h_{21} & h_{22} & h_{23} & h_{24} \\ h_{31} & h_{32} & h_{33} & h_{34} \\ h_{41} & h_{42} & h_{43} & h_{44} \end{bmatrix}}_{Rx_1 \quad Rx_2 \quad Rx_3 \quad Rx_4} \begin{matrix} Tx_1 \\ Tx_2 \\ Tx_3 \\ Tx_4 \end{matrix} \qquad (3\text{-}1)$$

where h_{ij} is the complex impulse response for each channel which in fact represents the interaction between each of 4 elements at Tx with all the scatterers, reflectors and each of 4 elements at Rx. It should be noted that for space diversity case 4 elements of Tx and Rx represent 4 antennas and for angle diversity case they represent 4 beams.

To calculate each h_{ij}, first radiated electric field from the first Tx antenna (or beam) which is received by the first scatterer should be calculated. After that, scattered field from the scatterers which is received by the first Rx antenna (or beam) should be calculated. This procedure should be repeated for all scatterers, antennas and beams. The scattered fields should be added for all scatterers. If any reflector exists, the reflected field should be calculated and added to it as well. In addition, in the LOS case, electric field for direct path between Tx and Rx should also be added to the summation.

The suggested solution to obtain the scattered field from a sphere is based on an $\vec{x}$ oriented field incident along the $\vec{z}$ axis. However, these conditions will rarely be fulfilled since the same coordinate system is used for all scatterers. By employing a local coordinate system for each scatterer, the mentioned solution can be applied. Thus, throughout the calculation procedure for the electric field, coordinate transformation is frequently performed to convert local coordinates to global one and vice versa.

3.3.2 Transmitter and Receiver Antenna Pattern Calculation

To calculate channel complex impulse response, electric field of the antenna elements used at both ends and array factor in case of using the arrays are needed. The SISTER model can be applied to different antenna patterns but for convenience, the antenna pattern which is presented here is half-wavelength dipole antenna.

Electric field of a z-directed half-wavelength dipole antenna is as follows [25]:

$$E_\theta = j\eta \frac{I_0 e^{-jkr}}{2\pi r}\left[\frac{\cos(\frac{\pi}{2}\cos\theta)}{\sin\theta}\right] \qquad (3\text{-}2)$$

Assuming that the array axis is in z direction, array factor formula can also be obtained by [25]:

$$\begin{cases} AF = \sum_{n=1}^{N} e^{j(n-1)\Psi} \\ \Psi = kd\cos\theta + \beta \end{cases} \tag{3-3}$$

where N, Ψ, k, d, θ and β are the number of array elements, progressive phase, wave number, elements' spacing, elevation angle of observation point and progressive phase lead current excitation, respectively.

When an array is used, different scan angles can be used for different MIMO elements. Recalled from antenna theory, scan angle of θ_0 can be achieved by choosing β as follows [25]:

$$\beta = -kd\cos\theta_0 \tag{3-4}$$

3.3.3 Scattered Field Calculation

Consider a sphere of radius a located at the origin as it is shown in Figure 3.6.

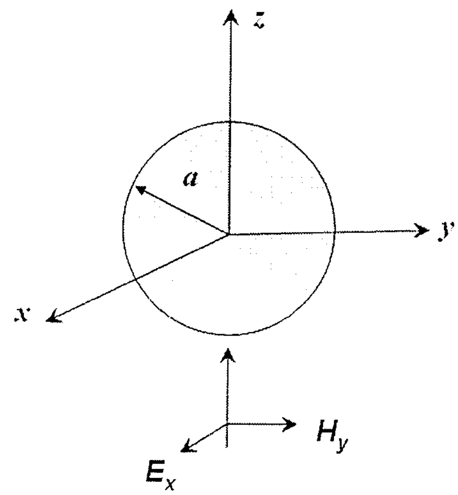

Figure 3.6 **A sphere of radius *a* located at the origin as a scatterer.**

Assuming a uniform plane wave polarized in the x direction traveling along the z-axis is incident upon this sphere, the incident electric field is given by:

$$\begin{cases} E_i = E_0 e^{-jkr} \vec{a}_x \\ k = \omega\sqrt{\mu\varepsilon} \end{cases} \tag{3-5}$$

where E_0 is the incident field amplitude, ω is angular velocity, k, μ and ε are the wave number, electric permeability and permittivity of surrounding medium, respectively. Then the far-field expressions for scattered field from the spherical scatterer at a point (r,θ_i,φ_i) can be written as:

$$\vec{E}^s = E_0 \frac{e^{-jkr}}{r}(E_\theta^s \vec{a}_\theta + E_\varphi^s \vec{a}_\varphi) \tag{3-6}$$

where E_θ^s and E_φ^s are as follows [23]:

$$\begin{cases} \vec{E}_\theta^s = \dfrac{j\cos\varphi_i}{k} \times \sum_{n=1}^{\infty} j^n \dfrac{2n+1}{n(n+1)} [a_n u_1(\theta_i) - b_n u_2(\theta_i)] \\ \vec{E}_\varphi^s = \dfrac{j\sin\varphi_i}{k} \times \sum_{n=1}^{\infty} j^n \dfrac{2n+1}{n(n+1)} [a_n u_2(\theta_i) - b_n u_1(\theta_i) \end{cases} \tag{3-7}$$

where $u_1(\theta_i)$ and $u_2(\theta_i)$ are:

$$\begin{cases} u_1(\theta_i) = \sin\theta_i P_n^{1'}(\cos\theta_i) \\ u_2(\theta_i) = \dfrac{P_n^1(\cos\theta_i)}{\sin\theta_i} \end{cases} \tag{3-8}$$

where, P_n^m is the *Associated Legendre Function* [26] and assuming that the permeability of the sphere is the same as surrounding environment, a_n and b_n can be written as:

$$\begin{cases} a_n = \dfrac{-k^2 j_n(s)[s_1 j_n(s_1)]' + k_1^2 j_n(s_1)[s j_n(s)]'}{k^2 h_n^{(2)}(s)[s_1 j_n(s_1)]' - k_1^2 j_n(s_1)[s h_n^{(2)}(s)]'} \\ b_n = \dfrac{-j_n(s)[s_1 j_n(s_1)]' + j_n(s_1)[s j_n(s)]'}{h_n^{(2)}(s)[s_1 j_n(s_1)]' - j_n(s_1)[s h_n^{(2)}(s)]'} \end{cases} \tag{3-9}$$

where $j_n(x)$ is the *Spherical Bessel Function* of order *n*, $h_n^2(x)$ is the *Spherical Hankel Function* of the second kind of order *n* [26] and a_n, b_n are coefficient dependent on the electrical size of the spherical scatterer and *s* and s_1 are defined by:

$$\begin{cases} s_1 = k_1 a \\ s = k\ a \end{cases} \tag{3-10}$$

where k_1, k and a are the wave number for the spherical scatterer, free space wave number and scatterer radius, respectively.

The infinite summation is approximated by taking only a limited number of terms (n_c). A rule of thumb of how many terms that should be evaluated is [23]:

$$n_c = s + 4.05 s^{1/3} + 2 \tag{3-11}$$

Finally in order to have large amount of scattering, electrical conductivity should be chosen high enough. Therefore, the dielectric properties of the conducting scatterers are assumed as follows:

$$\begin{cases} \varepsilon_s = \varepsilon_0 (1 - j100) \\ \mu = \mu_0 \end{cases} \tag{3-12}$$

where ε_0 and μ_0 are surrounding medium's (air) electrical permittivity and magnetic permeability, respectively.

3.3.4 Reflected Field Calculation

Since a considerable amount of multipaths is generated by reflectors, to characterize the indoor channel more accurately, we enhanced the model in such a way that it includes not only the scatterers but also the reflections from the walls.

To simulate the indoor scenario, transmitter, receiver and the scatterers are located in a simple cubic room, the dimensions of which can be changed. For each single antenna at Tx and Rx in a simple cubic room, six reflecting points exist. For all the sixteen existing channels, 96 reflection points exist.

For each transmitter and receiver set, reflecting points from different walls are found in terms of the dimensions of the wall and the position of Tx and Rx.

To visualize the geometry easier, two reflecting points A_1 and A_5 corresponding to walls1 and 5 and their planes of incidence are shown in Figure 3.7.

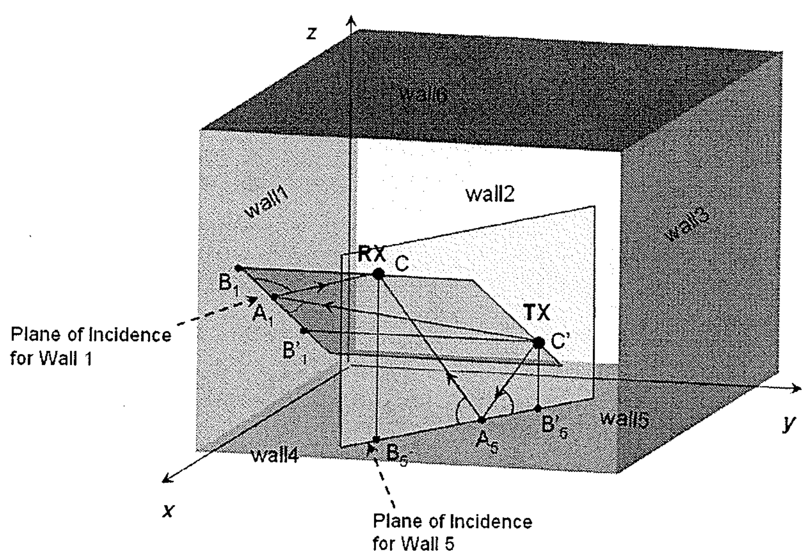

Figure 3.7 3-D geometry of two reflecting points.

As it is shown in Figure 3.8 more clearly, two triangles of ABC and AB'C' are similar and hence reflecting point, A, can be obtained as follows:

$$\begin{cases} \dfrac{AB}{AB'} = \dfrac{BC}{B'C'} = known \\ BA + AB' = BB' = known \end{cases} \Rightarrow AB \text{ and } AB' \text{ can be obtained} \qquad (3\text{-}13)$$

where *BB'* is the distance between projection points of Rx and Tx on the wall and *BC* and *B'C'* are the distances between Rx and Tx and the wall, respectively.

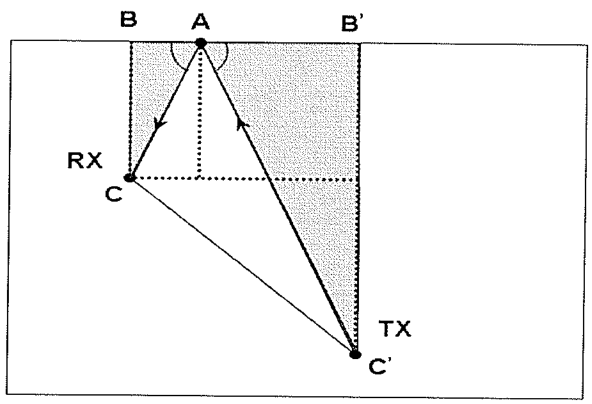

Figure 3.8 **2-D Geometry of reflecting points in the plane of incidence.**

As an example, A_5, reflecting point of wall5 can be found from two equations given below:

$$\begin{cases} \dfrac{A_5B_5}{A_5B'_5} = \dfrac{B_5C_5}{B'_5C'_5} = \dfrac{z_{RX} - z_{wall5}}{z_{TX} - z_{wall5}} \\ B_5A_5 + A_5B'_5 = B_5B'_5 = \sqrt{(x_{RX} - x_{TX})^2 + (y_{RX} - y_{TX})^2} \end{cases} \qquad (3\text{-}14)$$

Other reflecting points can also be found in a similar way.

After finding all the reflecting points, the electric fields originated at Tx side and reflected from theses points and terminated at Rx side can be calculated. These fields must be added to those obtained from scatterers and the direct path between Tx and Rx to get the total electric field.

Since the reflection coefficient is different for transverse or perpendicular (Γ_{TE}) and parallel (Γ_{TM}) polarization of electric field relative to the plane of incidence, received electric field on the boundary should be decomposed in to Transverse Electric Field (TE) and Transverse Magnetic Field (TM) polarizations. As it was shown in Figures 3.7 and 3.8, plane of incidence is the plane containing both a normal to the boundary and the incident wave's propagation direction [27].

To decompose electric field components for wall5, for instance, E_x and E_y, each are split in two polarizations of E_{xTM}, E_{xTE} and E_{yTM}, E_{yTE}, respectively (Figure 3.9):

$$\begin{cases} E_{xTM} = E_x \cos(\psi)\Gamma_{TM} \\ E_{xTE} = E_x \sin(\psi)\Gamma_{TE} \end{cases} \tag{3-15}$$

$$\begin{cases} E_{yTM} = E_y \sin(\psi)\Gamma_{TM} \\ E_{yTE} = E_y \cos(\psi)\Gamma_{TE} \end{cases} \tag{3-16}$$

where $\psi = \arctan\frac{y_{cross}}{x_{cross}}$ and Γ_{TE} and Γ_{TM} are reflection coefficients for TE and TM polarizations, respectively.

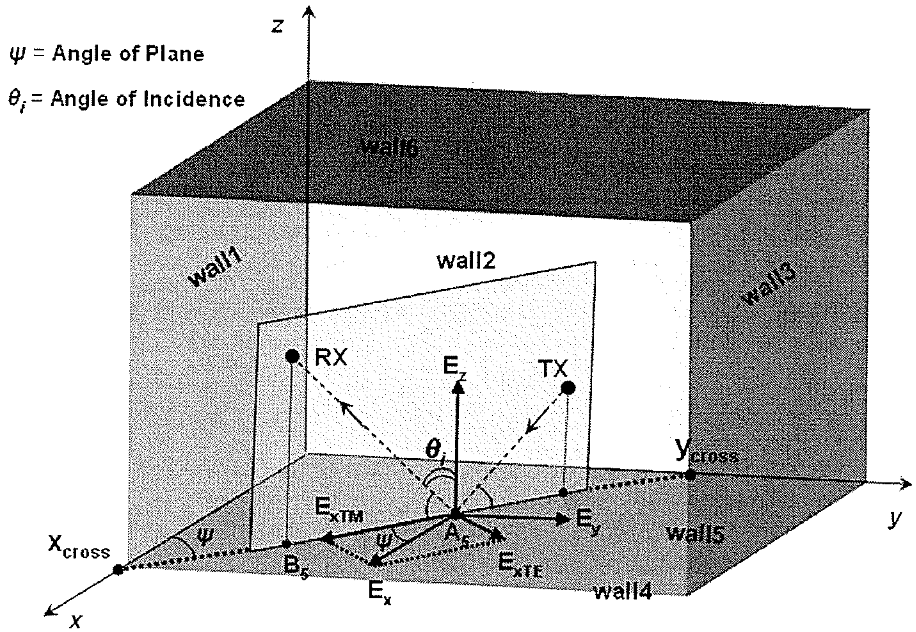

Figure 3.9 **3-D view of electric field decomposition to TM and TE polarizations at the reflecting point.**

Since E_z itself is the parallel component (TM), it does not need to be decomposed and hence to find its corresponding reflected field, it should be simply multiplied by Γ_{TM}.

After finding TM and TE components of reflected waves, they should be converted to previous global coordinates for further process:

$$\begin{cases} E_x' = E_{xTM}\cos(\psi) + E_{xTE}\sin(\psi) \\ E_y' = E_{yTM}\sin(\psi) + E_{yTE}\cos(\psi) \end{cases} \tag{3-17}$$

where E_x' and E_y' are the x and y components of the reflected electric field from wall5.

The same procedure is applicable for other walls. To find Γ_{TM} and Γ_{TE}, angles of incidence and transmission are required [27]:

$$\begin{cases} \Gamma_{TE} = \dfrac{\eta_2 \cos(\theta_i) - \eta_1 \cos(\theta_t)}{\eta_2 \cos(\theta_i) + \eta_1 \cos(\theta_t)} \\ \Gamma_{TM} = \dfrac{\eta_2 \cos(\theta_t) - \eta_1 \cos(\theta_i)}{\eta_2 \cos(\theta_t) + \eta_1 \cos(\theta_i)} \end{cases} \tag{3-18}$$

where (η_1, η_2), (θ_i, θ_t) are the intrinsic impedances of free space and wall and angles of incidence and transmission, respectively.

Referring to Figure 3.9, one can easily calculate angles of incidence and transmission for wall5 as follows:

$$\begin{cases} \theta_i = \dfrac{\pi}{2} - \arctan\dfrac{h_{Rx}}{B_5 A_5} \\ \theta_t = \arcsin\dfrac{k_1 \sin(\theta_i)}{k_2} \end{cases} \tag{3-19}$$

where (θ_i, θ_t), h_{Rx}, (k_1, k_2) are angles of incidence and transmission, height of Rx and wave number of air and walls, respectively.

3.3.5 Channel Capacity Calculation

Assuming that the channel is unknown to the transmitter and the total transmitted power is equally allocated to all N_T antennas, the capacity of the system is given by [6]:

$$C = \log_2\left(\det\left[I_{n_T} + \frac{SNR}{N_T} \times \frac{HH^*}{norm(HH^*)}\right]\right) \quad bps/Hz \tag{3-20}$$

where I_{n_T} is the identity matrix, $SNR=P_T/N_o$ is the average signal to noise ratio within the receiver aperture, N_T is the number of transmitter antennas, H is the $N_T \times N_R$ channel matrix and H^* is the conjugate transpose of H. To calculate H-matrix which is a 4×4 matrix here, baseband channel complex impulse response should be computed for scatterers, reflectors and direct path corresponding to each channel.

1) <u>Scatterers</u>

$$h_{scatterers} = \sum_{q=1}^{N_s} \frac{e^{-jk(\left|\vec{r}_{msq}\right| + \left|\vec{r}_{sqb}\right|)}}{\left(\left|\vec{r}_{msq}\right| \times \left|\vec{r}_{sqb}\right|\right)} [E_\theta(\vec{r}_{bs}) \cdot \vec{\ell}_{eff\theta} + E_\varphi(\vec{r}_{bs}) \cdot \vec{\ell}_{eff\varphi}] \tag{3-21}$$

where $\eta, i_0, N_s, \vec{r}_{msq}, \vec{r}_{sqb}, (E_\theta, E_\varphi), (\vec{\ell}_{eff\theta}, \vec{\ell}_{eff\varphi})$ are the characteristic impedance of the free space, input current, number of scatterers, distance vector from Tx (MS) to q^{th} scatterer, distance vector from Rx (BTS) to q^{th} scatterer, effective radiation pattern at Rx in θ and φ directions (radiation patterns of Tx and Rx are included in effective radiation pattern), effective lengths of the half-wavelength dipole in θ and φ directions, respectively.

Assuming that the half-wavelength dipole antenna is connected to a matched load and current distribution is sinusoidal, two components of effective complex length of dipole can be obtained from [28]:

$$\begin{cases} \vec{\ell}eff_{\theta} = \dfrac{\lambda}{\pi} \dfrac{E_{\theta}}{\left|E_0\right|} \\ \vec{\ell}eff_{\varphi} = \dfrac{\lambda}{\pi} \dfrac{E_{\varphi}}{\left|E_0\right|} \end{cases} \tag{3-22}$$

where E_{θ} and E_{φ} are the electric fields radiated by the half-wavelength dipole while it is in transmitting mode.

2) Reflectors

$$h_{reflectors} = \sum_{q=1}^{N_r} \frac{e^{-jk(\left|\vec{r}_{mrq}\right| + \left|\vec{r}_{rqb}\right|)}}{\left(\left|\vec{r}_{mrq}\right| \times \left|\vec{r}_{rqb}\right|\right)} [E_{\theta}(\vec{r}_{br}) \cdot \vec{\ell}_{eff\theta} + E_{\varphi}(\vec{r}_{br}) \cdot \vec{\ell}_{eff\varphi}] \tag{3-23}$$

where $N_r, \vec{r}_{mrq}, \vec{r}_{rqb}, (E_{\theta}, E_{\varphi}), (\vec{\ell}_{eff\theta}, \vec{\ell}_{eff\varphi})$ are the number of reflectors, distance vector from Tx to q^{th} reflector (wall), distance vector from Rx to q^{th} reflector, effective radiation pattern at Rx in θ and φ directions, effective lengths of the half-wavelength dipole in θ and φ directions, respectively.

3) Direct Path

To obtain direct field between Tx and Rx, the following equation is used:

$$h_{direct} = \frac{e^{-jk|\vec{r}_{mb}|}}{|\vec{r}_{mb}|}[E_\theta(\vec{r}_{bm}) \cdot \vec{\ell}_{eff\theta} + E_\varphi(\vec{r}_{bm}) \cdot \vec{\ell}_{eff\varphi}] \tag{3-24}$$

where $\vec{r}_{mb}, (E_\theta, E_\varphi), (\vec{\ell}_{eff\theta}, \vec{\ell}_{eff\varphi})$ are the distance vector from Tx to Rx, effective radiation pattern at Rx in θ and φ directions and the effective lengths of the half-wavelength dipole in θ and φ directions, respectively.

LOS and NLOS Cases

To obtain H-matrix entries for LOS scenario, for each of 16 channels $h_{scatterers}$, $h_{reflectors}$ and h_{direct} should be added up. For NLOS case, a blocking wall in the shape of a rectangle is assumed to be located between Tx and Rx as shown in Figures 3.10 and 3.11. This wall stops some of the radiated rays from Tx and does not let them to reach Rx. These blocked rays could come from either reflectors, scatterers or directly from Tx. Assuming that the blocking wall is located at $x=x_0$, to find out which rays from scatterers (or reflectors) are blocked; first their locations should be determined. If the wall is between Tx and scatterers (or reflectors), the following equations should be solved to find the y and z components of cross point shown in Figure 3.10:

$$\text{Scatterers:}\begin{cases}\dfrac{x_0 - x_{scat}}{y_{cross} - y_{scat}} = \dfrac{x_{Tx} - x_{scat}}{y_{Tx} - y_{scat}} \\ \dfrac{x_0 - x_{scat}}{z_{cross} - z_{scat}} = \dfrac{x_{Tx} - x_{scat}}{z_{Tx} - z_{scat}}\end{cases} \Rightarrow \quad \text{cross point}\left| \begin{matrix} x_0 \\ y_{cross} \\ z_{cross} \end{matrix} \right. \qquad (3\text{-}25)$$

$$\text{Reflectors:}\begin{cases}\dfrac{x_0 - x_{ref}}{y_{cross} - y_{ref}} = \dfrac{x_{Tx} - x_{ref}}{y_{Tx} - y_{ref}} \\ \dfrac{x_0 - x_{ref}}{z_{cross} - z_{ref}} = \dfrac{x_{Tx} - x_{ref}}{z_{Tx} - z_{ref}}\end{cases} \Rightarrow \quad \text{cross point}\left| \begin{matrix} x_0 \\ y_{cross} \\ z_{cross} \end{matrix} \right. \qquad (3\text{-}26)$$

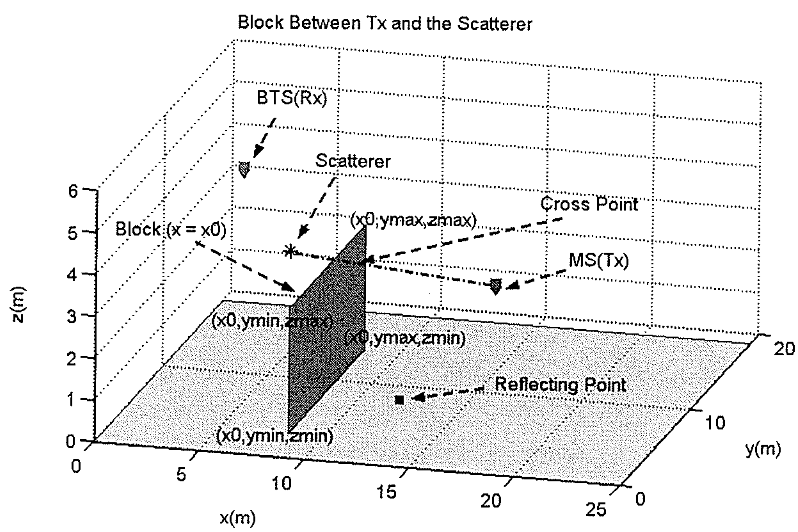

Figure 3.10 **Schematic for the case where the wall is located between Tx and the scatterer.**

If the wall is located between Rx and the scatterers (or reflectors) the following equations should be solved to find the cross points shown in Figure 3.11:

$$\text{Scatterers: } \begin{cases} \dfrac{x_0 - x_{scat}}{y_{cross} - y_{scat}} = \dfrac{x_{Rx} - x_{scat}}{y_{Rx} - y_{scat}} \\ \dfrac{x_0 - x_{scat}}{z_{cross} - z_{scat}} = \dfrac{x_{Rx} - x_{scat}}{z_{Rx} - z_{scat}} \end{cases} \Rightarrow \quad \text{cross point} \left| \begin{matrix} x_0 \\ y_{cross} \\ z_{cross} \end{matrix} \right. \qquad (3\text{-}27)$$

$$\text{Reflectors: } \begin{cases} \dfrac{x_0 - x_{ref}}{y_{cross} - y_{ref}} = \dfrac{x_{Rx} - x_{ref}}{y_{Rx} - y_{ref}} \\ \dfrac{x_0 - x_{ref}}{z_{cross} - z_{ref}} = \dfrac{x_{Rx} - x_{ref}}{z_{Rx} - z_{ref}} \end{cases} \Rightarrow \quad \text{cross point} \left| \begin{matrix} x_0 \\ y_{cross} \\ z_{cross} \end{matrix} \right. \qquad (3\text{-}28)$$

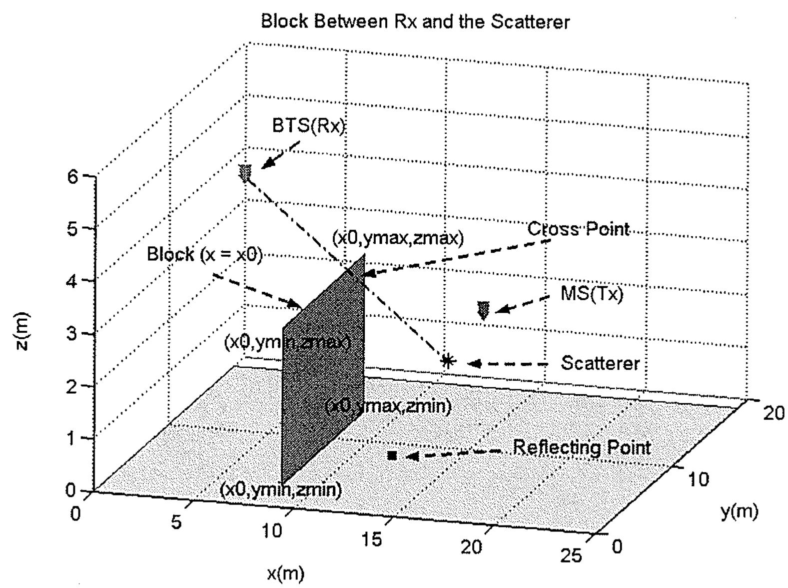

Figure 3.11 **Schematic for the case where the wall is located between Rx and the scatterer.**

If $(y_{\min-block} \le y_{cross} \le y_{\max-block})$ & $(z_{\min-block} \le z_{cross} \le z_{\max-block})$, referring to Figures 3.10 and 3.11, the corresponding ray should be ignored for calculating *H*-matrix entries.

3.3.6 Coordinate Transformations

To find the total electric field at Rx which is the last destination of the traveled wave, many coordinate transformations should be performed. Since, it is much easier to transform rectangular coordinates of local and global systems rather than spherical ones, before each transformation step, electric field in rectangular coordinate should be found. Equation (3-29) is used frequently while developing the mathematical model. It is a general formula to rotate a coordinate system and convert it to the other one by knowing the angles between their axes.

$$\underbrace{\begin{bmatrix} \hat{u}_1 \\ \hat{u}_2 \\ \hat{u}_3 \end{bmatrix}}_{New\_System} = \underbrace{\begin{bmatrix} \hat{a}_1 \cdot \hat{u}_1 & \hat{a}_2 \cdot \hat{u}_1 & \hat{a}_3 \cdot \hat{u}_1 \\ \hat{a}_1 \cdot \hat{u}_2 & \hat{a}_2 \cdot \hat{u}_2 & \hat{a}_3 \cdot \hat{u}_2 \\ \hat{a}_1 \cdot \hat{u}_3 & \hat{a}_2 \cdot \hat{u}_3 & \hat{a}_3 \cdot \hat{u}_3 \end{bmatrix}}_{Rotation\_Matrix} \underbrace{\begin{bmatrix} \hat{a}_1 \\ \hat{a}_2 \\ \hat{a}_3 \end{bmatrix}}_{Old\_System} \tag{3-29}$$

The given solution in (3-7) is for an $\vec{x}$ oriented field propagation along the $\vec{z}$-axis. However, these conditions will rarely be met since the same coordinate system is used for all scatterers. By employing a local coordinate system for each object, the mentioned solution can be applied.

Different local and global coordinates are shown in Figure 3.12 and defined as follows:

- *Gmain* ($x_{Gmain}, y_{Gmain}, z_{Gmain}$) is the global coordinate.
- *G1* (x_{G1}, y_{G1}, z_{G1}) is a parallel coordinate system with *Gmain* and its origin is on the center of Tx.

- *L1* (x_{L1}, y_{L1}, z_{L1}) is the local coordinate for Tx antenna and its origin is the same as that of *G1* and also for this coordinate system z_{L1} is chosen along the direction of Tx dipole and x_{L1} is defined on the plane of x_{G1} and y_{G1}.
- *L2* (x_{L2}, y_{L2}, z_{L2}) is the local coordinate for scatterers and its origin is on the scatterer center and for this coordinate system z_{L2} is chosen along the direction of r_{L1} and x_{L2} is chosen along the direction of θ_{L1}. (r_{L1}, θ_{L1}, φ_{L1}) are cylindrical coordinate components of each scatterer in respect to *L1* coordinate. It is worth mentioning that for each scatterer an *L2* coordinate is defined.
- *L3* (x_{L3}, y_{L3}, z_{L3}) is the local coordinate for Rx antenna the origin of which is on the center of Rx and also for this coordinate system z_{L3} is chosen along the direction of Rx dipole and x_{L3} is defined on a plane parallel to the plane of x_{Gmain} and y_{Gmain}.

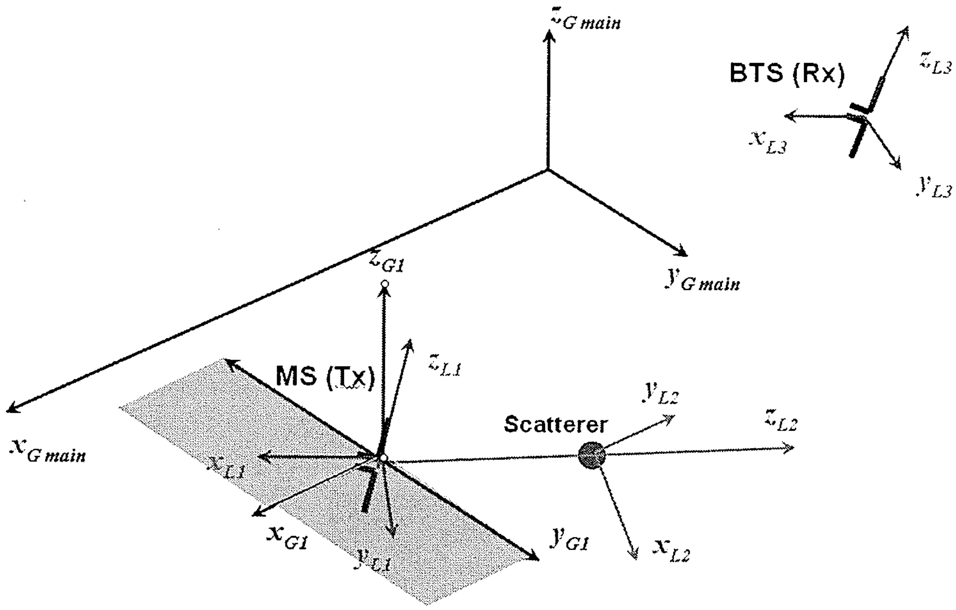

Figure 3.12 **Global and local coordinates and dipole antennas at both ends.**

The local coordinates *L1* and *L3* are defined to provide the possibility of using different polarizations for Tx and Rx antennas, respectively.

Now to fulfill the condition required for using the scattered formulas, *L1* should be converted to *L2* which is the local coordinate of each scatterer. If the scatterer is located at $(r_{L1}, \theta_{L1}, \varphi_{L1})$ in respect to *L1* coordinate, to convert *L1* coordinates into *L2* coordinates system, one can use:

$$\begin{bmatrix}\hat{x} & \hat{y} & \hat{z}\end{bmatrix}_{L2} = \begin{bmatrix}\hat{x} & \hat{y} & \hat{z}\end{bmatrix}_{L1} \begin{bmatrix} \cos\theta_{L1}\cos\varphi_{L1} & -\sin\varphi_{L1} & \sin\theta_{L1}\cos\varphi_{L1} \\ \cos\theta_{L1}\sin\varphi_{L1} & \cos\varphi_{L1} & \sin\theta_{L1}\sin\varphi_{L1} \\ -\sin\theta_{L1} & 0 & \cos\theta_{L1} \end{bmatrix} \tag{3-30}$$

where θ_{L1} and φ_{L1} are scatterer's coordinates referred to *L1*.

If the Tx antenna type is something other than dipole or generally, is an antenna with electric field in both θ and φ directions then the relation between the *L1* and *L2* coordinates is more complicated and the corresponding rotation matrix is as follows:

$$\begin{bmatrix} \hat{x} & \hat{y} & \hat{z} \end{bmatrix}_{L2} = \begin{bmatrix} \hat{x} & \hat{y} & \hat{z} \end{bmatrix}_{L1} \times \frac{1}{A} \times \tag{3-31}$$

$$\begin{bmatrix} E_\theta \cos\theta_{L1} \cos\varphi_{L1} - E_\varphi \sin\varphi_{L1} & -E_\varphi \cos\theta_{L1} \cos\varphi_{L1} - E_\theta \sin\varphi_{L1} & A \sin\theta_{L1} \cos\varphi_{L1} \\ E_\theta \cos\theta_{L1} \sin\varphi_{L1} + E_\varphi \cos\varphi_{L1} & -E_\varphi \cos\theta_{L1} \sin\varphi_{L1} + E_\theta \cos\varphi_{L1} & A \sin\theta_{L1} \sin\varphi_{L1} \\ -E_\theta \sin\theta_{L1} & +E_\varphi \sin\theta_{L1} & A \cos\theta_{L1} \end{bmatrix}$$

where E_θ, E_φ are the electric field components at each scatterer center referred to *L1* and θ_{L1} and φ_{L1} are scatterer's coordinates and $A = \sqrt{E_\theta^{\ 2} + E^2_{\ \varphi}}$. Equation (3-31) is simplified to rotation matrix in (3-30) if Tx antennas had electric field only in θ direction. Finally after all coordinate conversions, all the vectors which are necessary to find channel complex impulse response such as electric fields and effective lengths should be converted to the main global coordinate which is specified as G_{main} in Figure 3.12.

3.4 *Verifying the SISTER Model*

To verify the obtained results from developed model, *Wireless Insite* software by Remcom Inc. [5] is used. This software is a three-dimensional ray tracing tool for both indoor and outdoor applications which models the effects of buildings and terrain and generally the scatterers, on the propagation of electromagnetic waves.

In order to accomplish this verification, different steps have been taken. As Figure 3.13 indicates, first only a direct path between Tx and Rx is considered for a SISO system and received power is verified by both Friis equation and ray tracing tool.

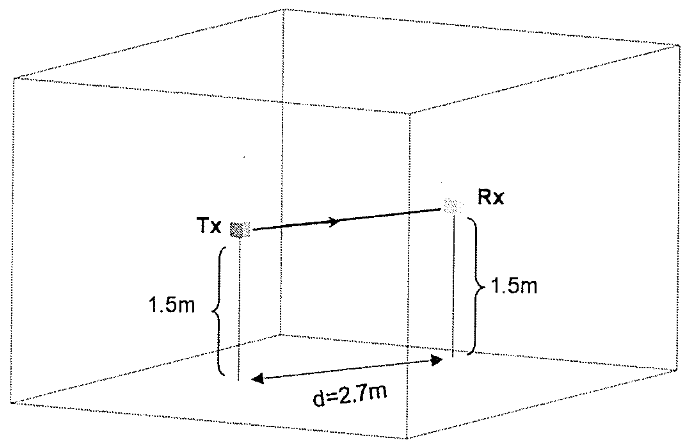

Figure 3.13 Ray tracing visualization of a SISO system considering direct path only.

It is assumed that a half wavelength dipole antenna (Gain=2.16dBi) is used at both ends, Tx-Rx distance is 2.7m, both Tx and Rx heights are 1.5m and transmitted power is 0dBm (1mW). For the mentioned system configuration, numerical results obtained from both proposed mathematical model and ray tracing are summarized in Table 3-1.

	$P_{received}$	Mag E_z (V/m)	Phase E_z (degree)
SISTER Model	-44.362 dBm (3.663×10^{-8} W)	0.117	76.917
Ray Tracing	-44.350 dBm (3.673×10^{-8} W)	0.117	73.496
Friis Equation	-44.337dBm (3.684×10^{-8} W)	-------	-------

Table 3-1 **Numerical results for a SISO system configuration shown in Figure 3.13.**

As it can be seen the result obtained from the SISTER model match perfectly with both ray tracing tool and also Friis transmission equation given in (3-32) [25]:

$$\frac{P_r}{P_t} = \left(\frac{\lambda}{4\pi \mathrm{R}} \right)^2 G_r G_t \tag{3-32}$$

where P_r, P_t, λ, R, G_r and G_t are received power, transmitter power, wavelength, Tx-Rx distance and Rx antenna gain and Tx antenna gain respectively.

In the next step (Figure 3.14) one wall is added to the previous system configuration and the reflected ray is evaluated as well.

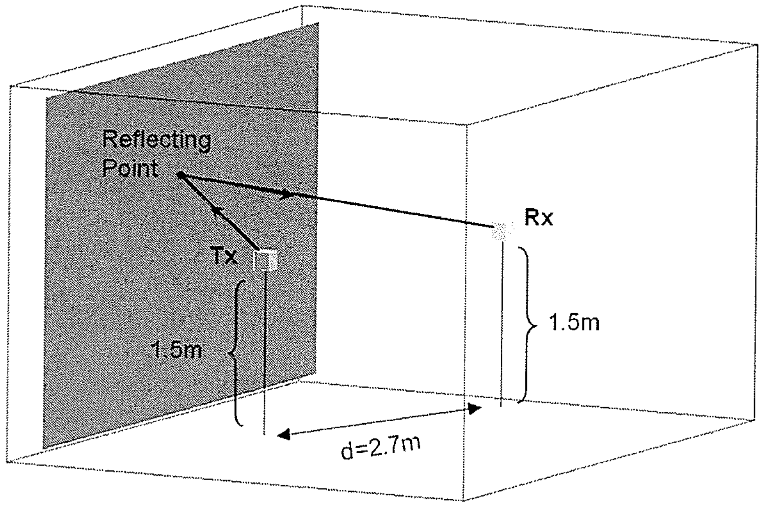

Figure 3.14 **Ray tracing visualization of a SISO system in an indoor environment considering reflection from one wall.**

For this case, summarized results can be found in Table 3-2 which again shows an acceptable match with those of the ray tracing.

The same procedure to validate the reflected field has been done for all six walls and all have shown good match.

	$P_{received}$	Mag E_z (V/m)	Phase E_z (degree)
SISTER Model	-48.442 dBm (1.432×10^{-8} W)	0.073	-115.719
Ray Tracing	-48.461 dBm (1.425×10^{-8} W)	0.073	-121.210

Table 3-2 **Numerical results for a SISO system configuration shown in Figure 3.14.**

As the final step to verify the results, channel capacity for the MIMO system configuration illustrated in Figure 3.15 is compared for both proposed model and ray tracing tool.

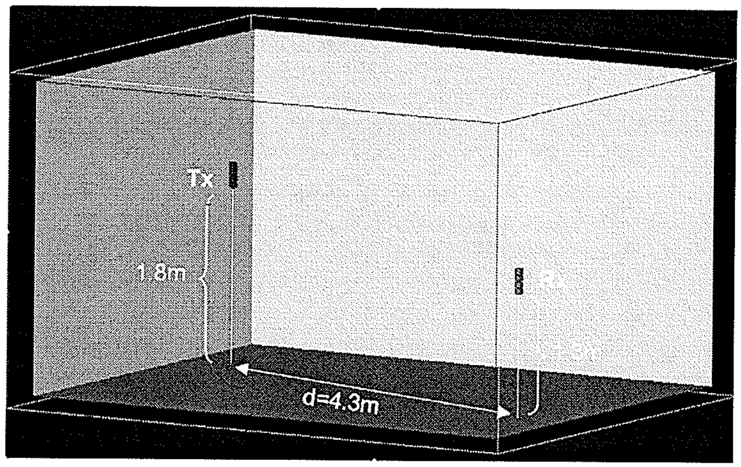

Figure 3.15 Ray tracing visualization of a 4×4-MIMO system in an indoor environment considering six walls.

Figure 3.16 shows the results for three cases:

1) Direct path only
2) Reflected paths only
3) Total paths

As these results show very good agreement is achieved.

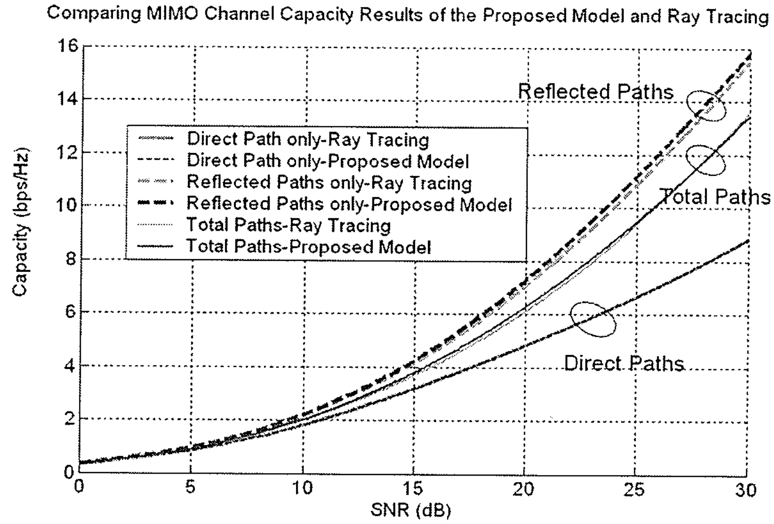

Figure 3.16 **Comparing MIMO channel capacity obtained from SISTER model and ray tracing tool for different rays.**

3.5 Chapter Summary

In this chapter, the SISTER model capabilities and assumptions were addressed. A simple shape of sphere is chosen for scatterers and to keep the simplicity only single interaction from each scatterer (or reflector) is considered. It is worth mentioning that to have fair comparison, for ray tracing simulation also, single interaction is chosen manually. Moreover, to characterize the indoor channel more accurately, the SISTER model was enhanced in such a way that it includes not only the scattered fields and reflection from the ground but also from the walls. This is due to the fact that for indoor environments the considerable amount of multipaths is generated by reflected waves from the walls.

In addition, all the mathematical expressions needed to model a wireless channel including scatterers and reflectors are presented in this chapter. Channel complex impulse response and the channel capacity equations are also given. Since the essential formulas for scattered field are based on specific conditions, many coordinate transformations are needed to perform to satisfy those conditions which are described in details.

Finally, it was explained that how the SISTER model is verified by comparing its results with ones obtained by a ray tracing tool. Different parameters such as received power, received electric field and channel capacity were compared and verified.

Chapter4: Numerical Results for Outdoor Environments

4.1 Chapter Introduction

The main objective of this chapter is to present, explain and discuss numerical results for outdoor environments obtained by changing different parameters which impact the channel capacity using the SISTER model.

4.2 Numerical Results

Before starting to evaluate the results it is worth mentioning that to be able to see the impact of changing parameters corresponding to scatterers, they should put high enough energy in calculating H-matrix entries. Therefore, for the outdoor environment scatterers' radius is chosen 10cm and as it was given in (3-12), scatterers' conductivity is chosen high enough to get sufficient scattered energy.

Outdoor system specifications are summarized in Table 4-1.

	Tx (MS) height	Rx (BTS) height	Relative height of Tx and Rx	Distance between Tx and Rx
Outdoor System	24λ (3m)	40λ (5m)	16λ (2m)	102λ (13m)

Table 4-1 Outdoor system specifications.

As it was mentioned in Chapter 3, different distributions for scatterers are applicable for the SISTER model. In this study, we chose the most common ones; uniform distribution and cluster form. Before presenting the results, the channel capacity for the well-known channels are considered and shown in Figure 4.1. As it can be seen, the minimum capacity expected for a 4×4-MIMO system in *SNR*=30 dB is 8 bps/Hz which belongs to highly correlated channels and the maximum is 32 bps/Hz which belongs to absolutely uncorrelated channels that can not be found in practice. Rayleigh channels, on the other hand, represent the environments which are rich in terms of multipath and offer high capacity which can be achieved in practice.

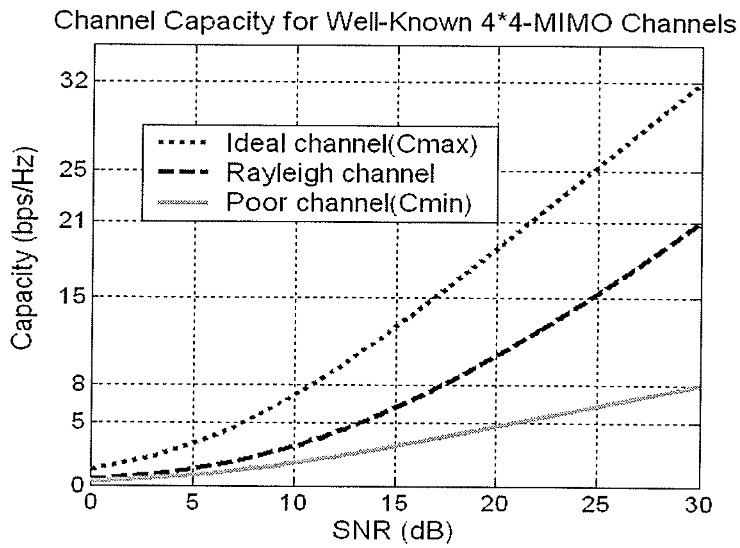

Figure 4.1 **Capacity for different 4×4-MIMO channels.**

4.2.1 Uniformly Distributed Scatterers Around Each End

In this scenario, scatterers are uniformly distributed around each of Tx and Rx and the results are obtained for total of 30 and 100 scatterers, around both ends.

4.2.1.1 Material of the Ground and Different Numbers of Scatterers

LOS Case

In this case, besides scattered fields, reflection from the ground and also direct path contribute in the calculation of total electric field at the receiver. Therefore, before pursuing the study of scatterers' impact on the capacity for different scenarios, the effect of ground's material is studied. In general, two types of low and high conductive grounds may be defined whose electrical conductivities and permittivities are as follows:

Low conductive ground: σ=0.001 (S/m) and ε_r=4

High conductive ground: $\sigma=10^7$ (S/m) and ε_r=25

For a system shown in Figure 4.2, channel capacity is computed for different ground's conductivities and the results are illustrated in Figure 4.3.

Figure 4.3 shows that for a ground with conductivity more than 100 S/m, capacity is mainly controlled by reflected path from the ground and scatterers do not contribute much in the channel capacity. For ε_r=4, if σ is less than 0.1 S/m, direct path is the dominant path, if σ is between 0.1 and 100 S/m, scatterers have impact on the channel and if σ is more than 100 S/m, direct path and reflection path from the ground are dominant paths.

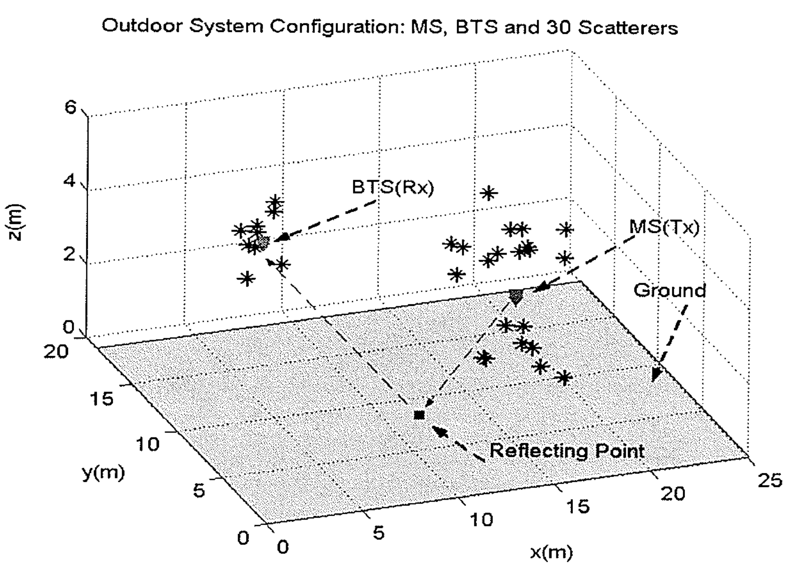

Figure 4.2 **Outdoor system configuration including Tx, Rx and 30 scatterers distributed uniformly around both ends in LOS scenario.**

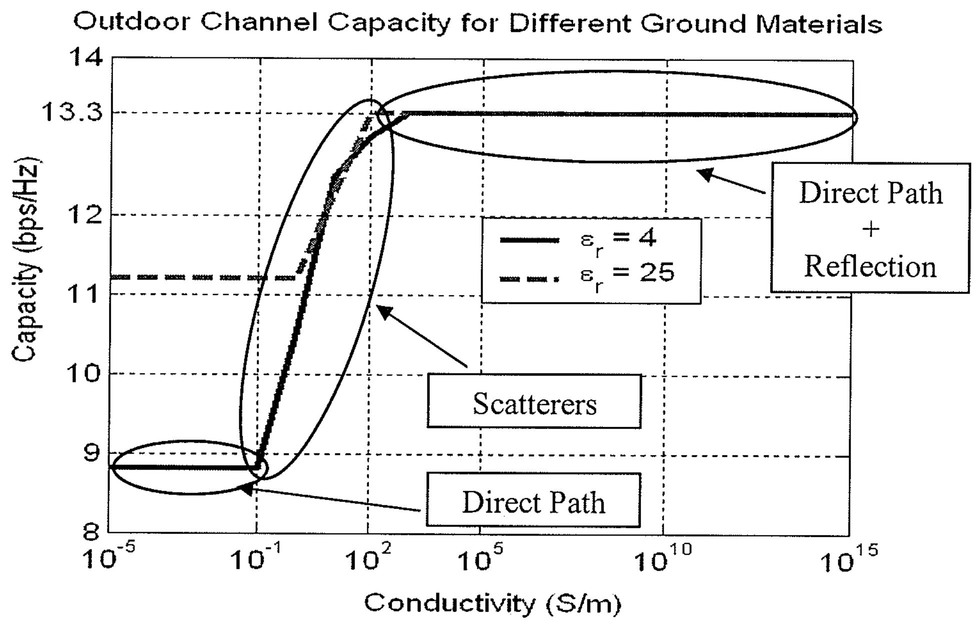

Figure 4.3 **Channel capacity at *SNR*=30dB for different grounds (ε_r=4, ε_r=25) in LOS case where 30 scatterers are uniformly distributed around both ends.**

As Figure 4.4 shows, for LOS scenario in the case of low conductive ground, reflection from the ground is so small that can be ignored comparing to the total scattered field and direct path and hence its presence does not affect capacity that much. In fact, it is not strong enough to suppress the effect of direct path's influence in reducing the capacity. On the other hand, reflection from the high conductive ground contributes as much as the direct path so its presence can somehow suppress the effect of direct path and hence increase the capacity comparing to the low conductive ground case.

Figure 4.4 also shows that for different numbers of scatterers, there is only small change in capacity. As it is expected, capacity is higher when scatterers are more which leads to less correlation between the channels.

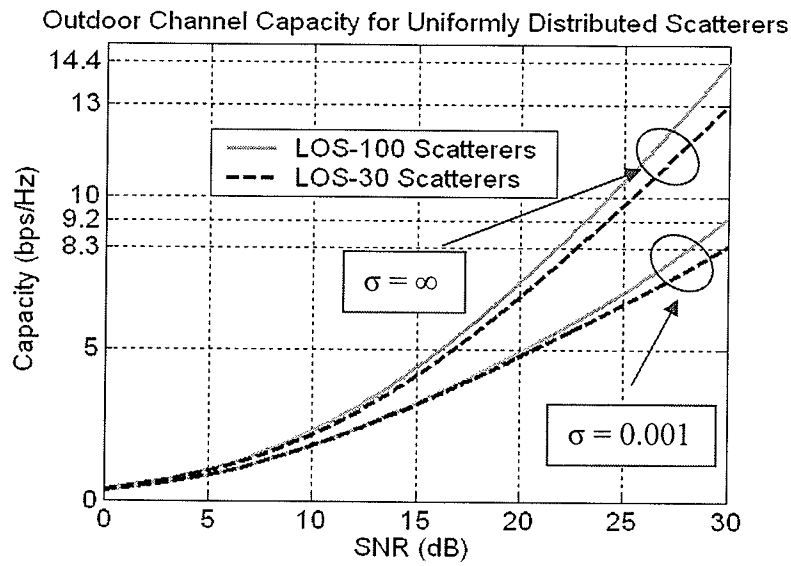

Figure 4.4 **Channel capacity for different number of scatterers distributed uniformly around both ends in LOS case (σ=ground's electrical conductivity).**

NLOS Case

For this case two scenarios are studied. First, blocking wall (height=4.5m) shown in Figure 4.5, is located in such a way that there is neither direct path between Tx and Rx, nor reflection from the ground. Although, some of scatterers are also blocked, capacity is increased comparing to LOS case since there is no direct path any more.

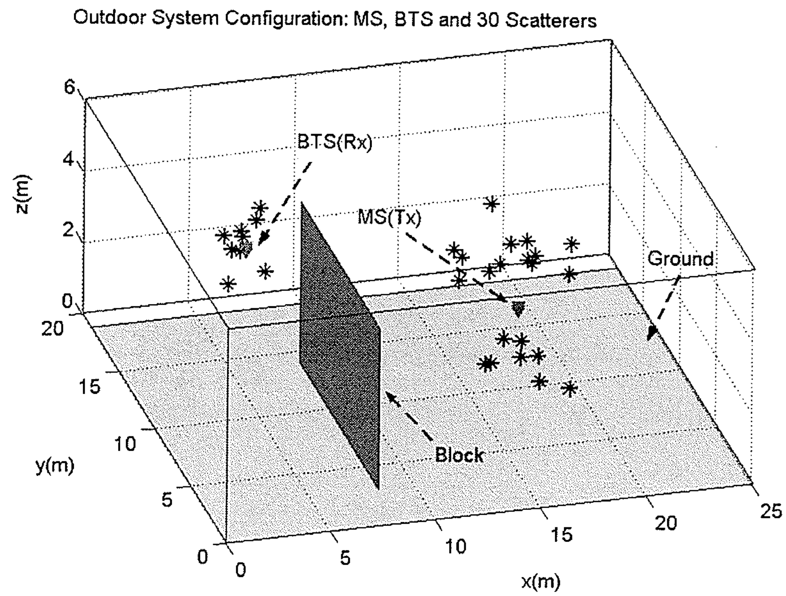

Figure 4.5 **Outdoor system configuration including Tx, Rx and 30 scatterers distributed uniformly around both ends in NLOS case.**

Figure 4.6 shows the capacity results for this case. The capacity is high while no dominant path exists. Moreover, for uniformly distributed around each of the Tx and Rx antennas, higher capacity can be achieved by increasing the number of scatterers as it is expected.

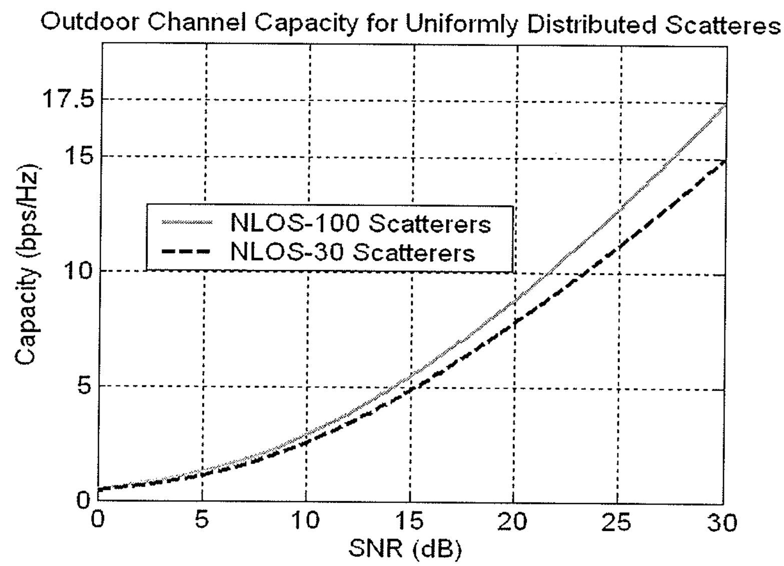

Figure 4.6 **Channel capacity for different number of scatterers distributed uniformly around both ends in NLOS case, no direct path and no reflection from the ground.**

In the next case, blocking wall is located in such a way that it just blocks the direct path and not the reflection from the ground. Figure 4.7 shows the capacity results for this case. It shows when the number of scatterer is not high (30 scatterers) reflection form the high conductive ground is the dominant path and so capacity is low. But when the number of scatterers is high enough (100 scatterers), they are able to lessen the effect of reflection from the ground and so in this case capacity is higher. For low conductive ground, on the other hand, since the reflection from the ground is so weak, no dominant path exists and hence for both 30 and 100 number of scatterers, channel capacity is high.

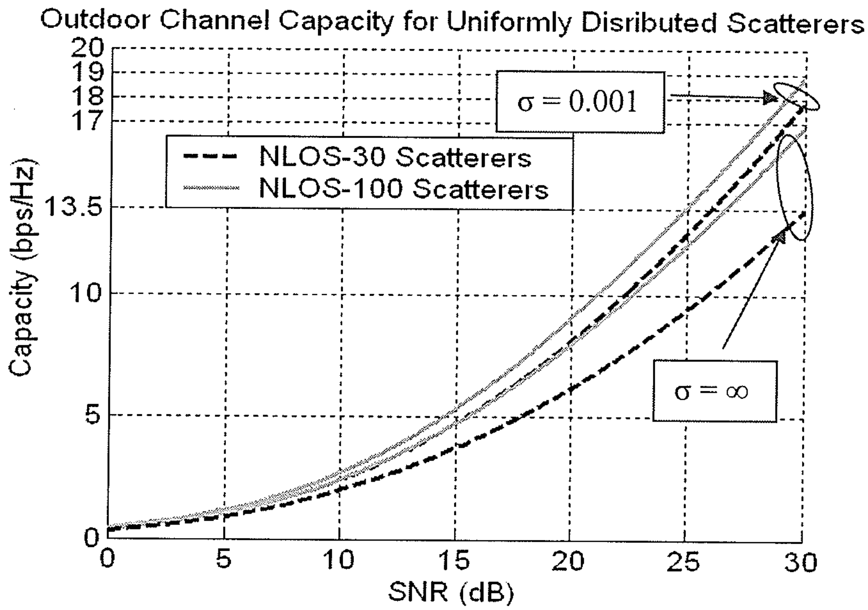

Figure 4.7 **Channel capacity for different number of scatterers distributed uniformly around both ends in NLOS case including reflection from the ground but not the direct path (σ=ground's electrical conductivity).**

4.2.1.2 MIMO Elements' Spacing

To study the impact of the number of MIMO elements and BTS antenna spacing, a system configuration illustrated in Figure 4.8 is considered. In this configuration, since it is needed to position the BTS antennas further in order to implement the larger spacings, scatterers are located in a further distance from the BTS antennas. For NLOS case particularly, the block should be high enough (block height=5.5m) to still block the direct path even after applying larger spacings.

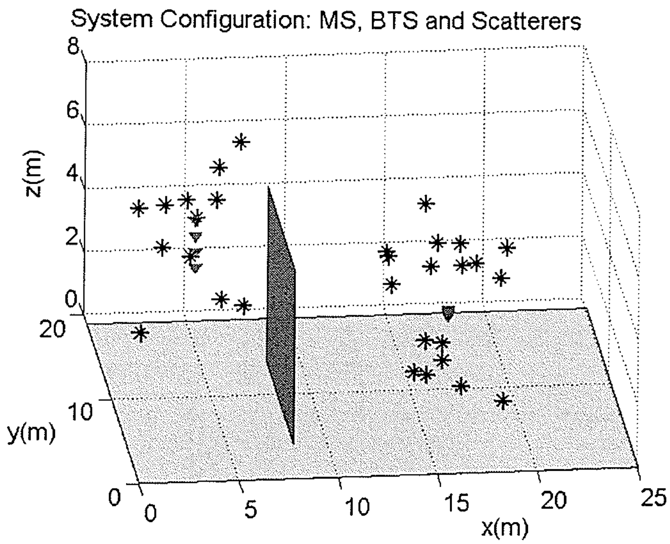

Figure 4.8 **Another system configuration for uniform distribution with larger BTS element spacing (BTS element spacing=4λ).**

For both LOS and NLOS cases, as Figures 4.9 and 4.10 indicate, increase in BTS element spacing leads to increase in channel capacity.

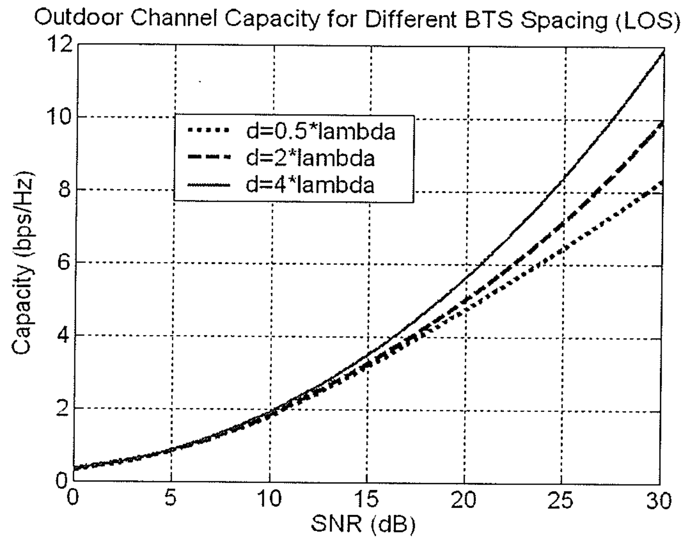

Figure 4.9 **Outdoor channel capacity for uniform distribution of 30 scatterers in LOS case, showing impact of changing BTS element spacing (d=BTS element spacing).**

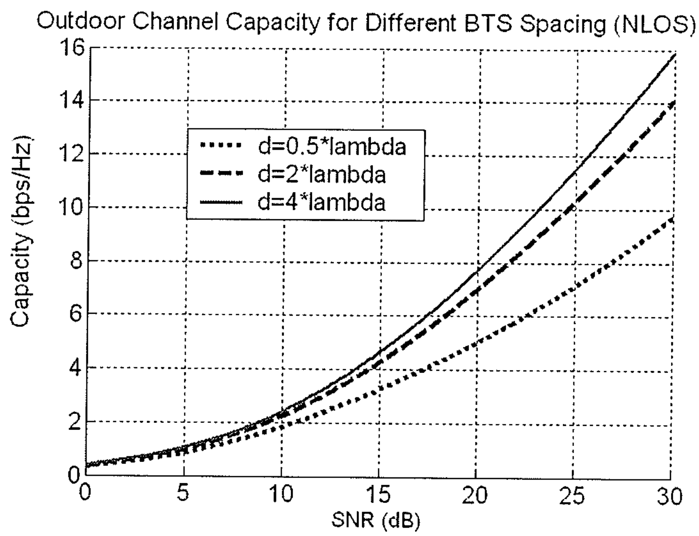

Figure 4.10 **Outdoor channel capacity for uniform distribution of 30 scatterers in NLOS case, showing impact of changing BTS element spacing (d=BTS element spacing).**

4.2.1.3 MIMO Elements' Number

Figures 4.11 and 4.12 show how the number of elements impacts a MIMO system in LOS and NLOS cases. In both cases as we expect, capacity is controlled by the minimum number of elements.

As it can be seen, in LOS case, there is not much difference between 4×4-MIMO with the rest of the MIMO systems since channels are so correlated due to the presence of the direct path. Conversely, in NLOS case, a significant difference between 4×4-MIMO with the rest of the MIMO systems can be observed.

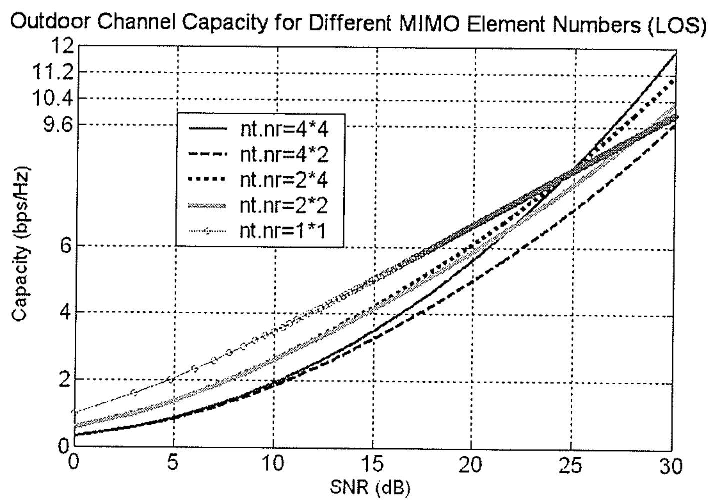

Figure 4.11 **Channel capacity for uniform distribution in LOS case, showing impact of changing the number of elements (BTS element spacing=4λ, nt=number of Tx antennas, nr=number of Rx antennas).**

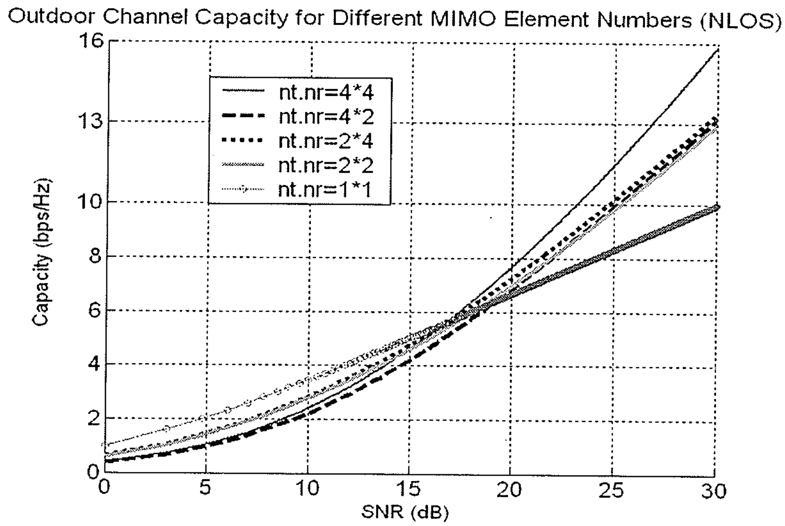

Figure 4.12 **Channel capacity for uniform distribution in NLOS case, showing impact of changing the number of elements (BTS element spacing=4λ, nt=number of Tx antennas, nr=number of Rx antennas).**

4.2.2 Cluster Distribution

4.2.2.1 Material of the Ground and Different Number of Scatterers

LOS Case

Figure 4.13 shows the scenario for LOS case.where the scatterers are distributed in six clusters.

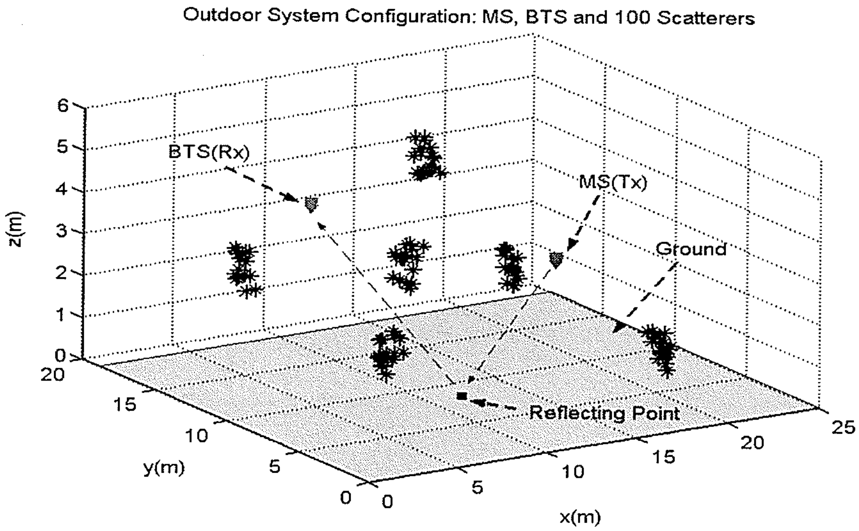

Figure 4.13 **Outdoor system configuration including Tx, Rx and 100 scatterers in 6 clusters for LOS case.**

As Figure 4.14 shows, the channels are so correlated that even large number of scatterers does not increase the capacity. It is because of two reasons; presence of direct path and cluster distribution of scatterers which makes them packed within a cluster. Furthermore, the reflection from the ground plays a significant role in lessening the effect of the direct path. As it is expected, the high conductive ground shows higher capacity comparing to low conductive one.

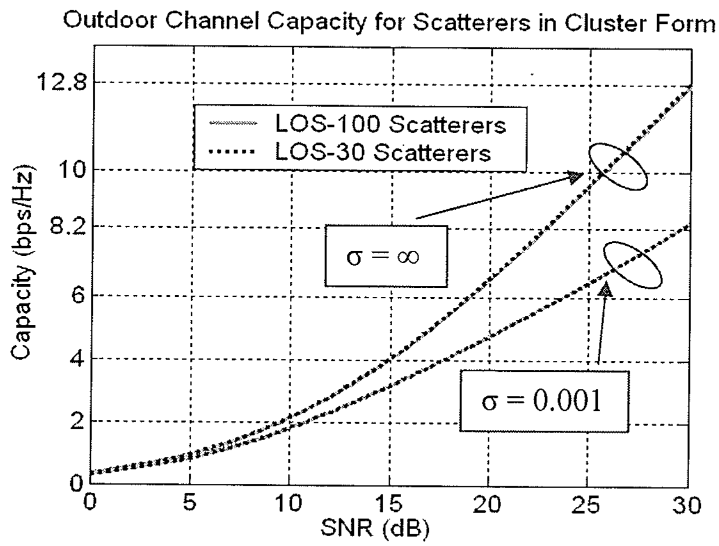

Figure 4.14 **Channel capacity for different number of scatterers in clusters for LOS case (σ=ground's electrical conductivity).**

NLOS Case

Figure 4.15 shows the scenario for NLOS case where the scatterers are distributed in six clusters. For this case two scenarios are studied. First, blocking wall (height=4.5m) is located in such a way that there is neither direct path between Tx and Rx, nor reflection from the ground.

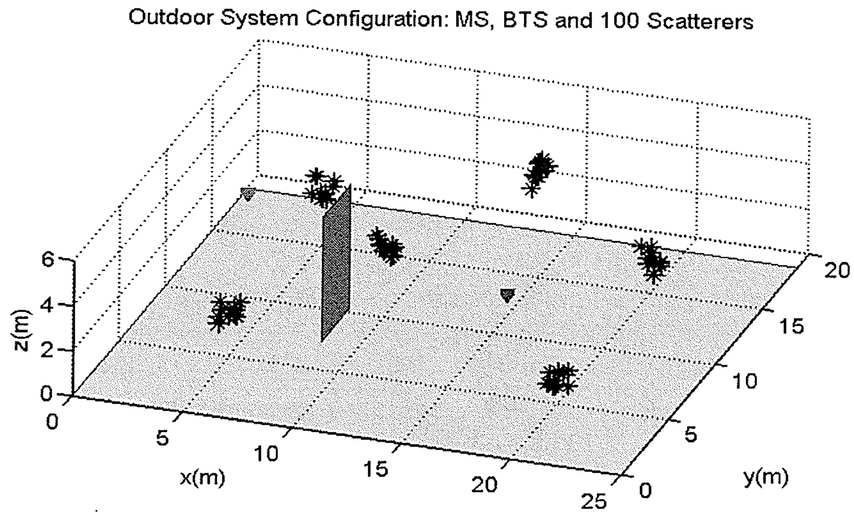

Figure 4.15 **Outdoor system configuration including MS, BTS and 100 scatterers in 6 clusters for NLOS case.**

Figure 4.16 shows the capacity for this case. Conversely to what was seen in LOS case, it shows a higher capacity for larger number of scatterers.

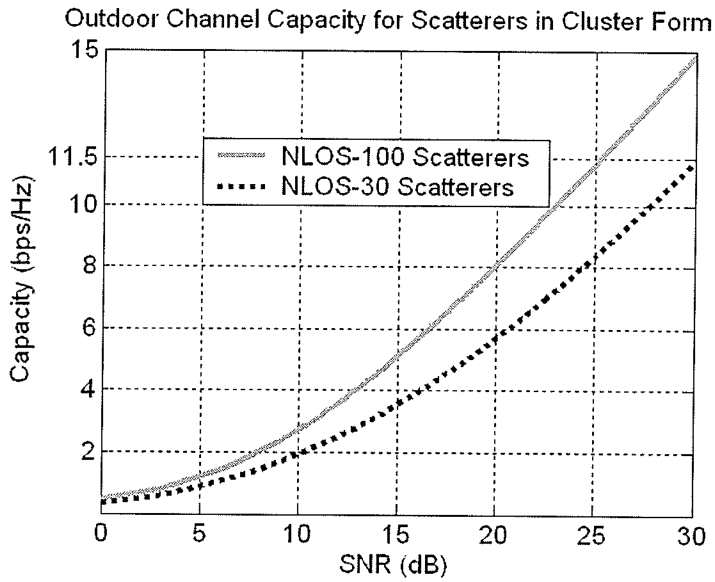

Figure 4.16 **Channel capacity for different number of scatterers in 6 clusters for NLOS case, no direct path and no reflection from the ground.**

In the next case, blocking wall is located in such a way that it just blocks the direct path and not the reflection from the ground. Figure 4.17 shows capacity for this case. As it is expected, high conductive ground make a dominant path and results in reduction in capacity. On the other hand, low conductive ground is so weak that it can not make a dominant path and therefore leads in increase in channel capacity.

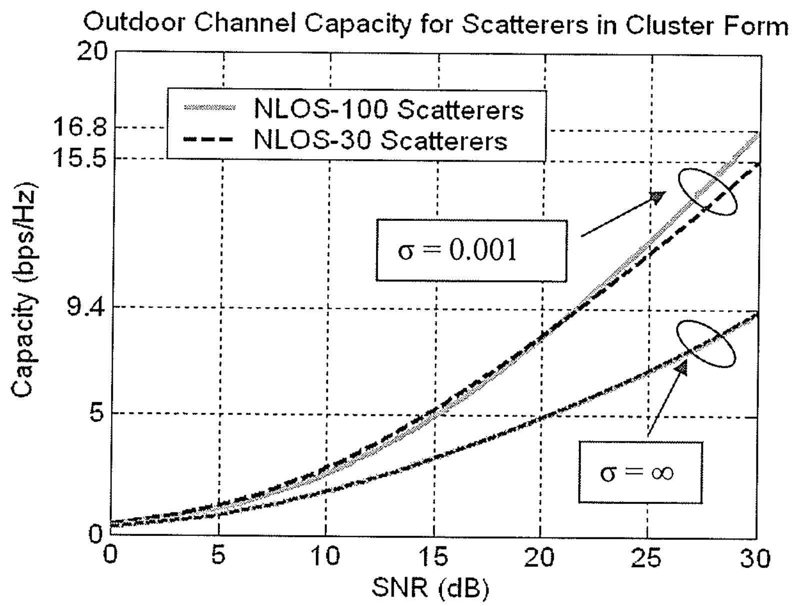

Figure 4.17 **Channel capacity for different number of scatterers in 6 clusters for NLOS case, including reflection from the ground but not the direct path (σ=wall's electrical conductivity).**

Comparing the results obtained for two cases of uniform and cluster forms, by using space diversity, one can find that generally, cluster form shows lower capacity since the correlation between the channels is higher. However, as it will be seen in the next section, by applying angle diversity method, one can direct each beam towards different clusters and decrease the correlation between the channels and improve the capacity.

4.2.2.2 Comparing Space and Angle Diversity Methods

To compare space and angle diversity methods for a 4×4-MIMO system, a scenario consisting of four clusters is considered shown in Figure 4.18.

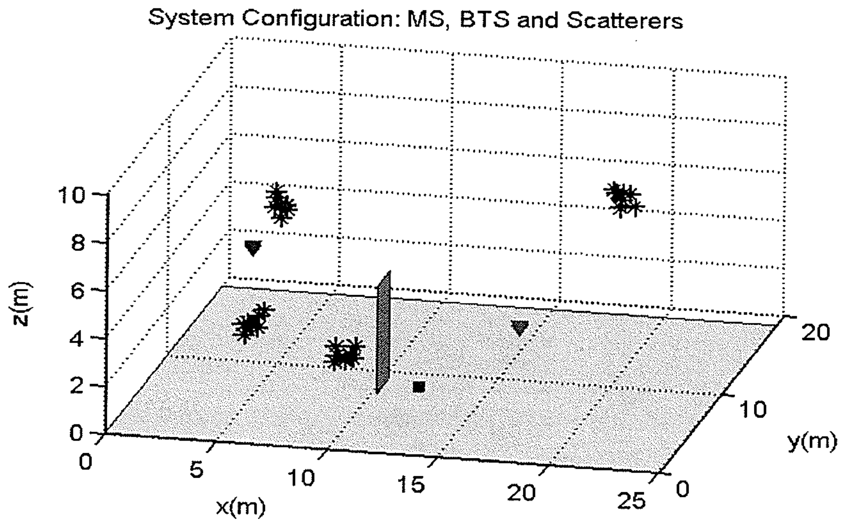

Figure 4.18 **Outdoor system configuration including MS, BTS and 30 scatterers in 4 clusters.**

In space diversity case, 4 antenna elements with the same amplitudes and phases are used while in angle diversity they have the same amplitudes but not the same phases. Four simultaneous beams with different scan angles are assumed.

Figure 4.19 shows the normalized pattern of a single dipole antenna with respect to elevation angle of θ.

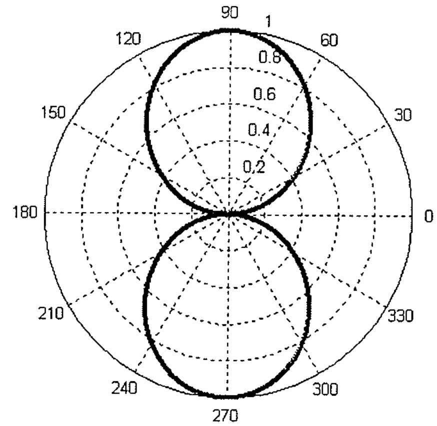

Figure 4.19 **Normalized pattern of dipole antenna in the *z* direction with respect to elevation angle.**

Figure 4.20 shows the normalized pattern of 4 dipoles with different electric progressive phases and scanning angles of 40°, 70°, 110°, 140°. Similar beams with different scanning angles are used in angle diversity method at BTS and MS sides. The position of clusters defines the scanning angles. In other words, as Figure 4.18 shows, there are 4 clusters in the scenario; therefore at both MS and BTS, 4 beams are directed towards these four clusters. It is possible to have more clusters and have different scanning angles.

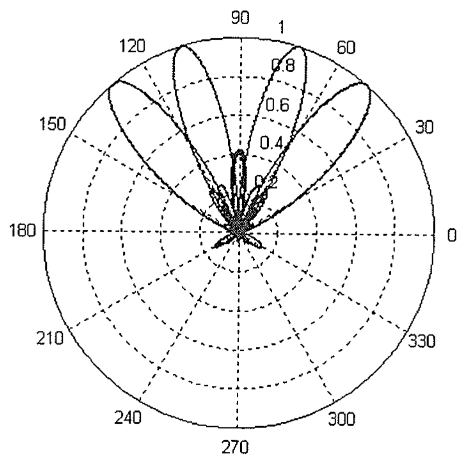

Figure 4.20 **Normalized pattern of an array of 4 dipole antennas with electric phase difference in the *z* direction respect to elevation angle (element spacing=0.5λ).**

To compare space and angle diversity methods, two cases were studied. The length occupied by antenna elements is the same for both space and angle diversity methods. It is essential to keep the array length the same if we intend to have a fair comparison between the two methods in terms of system size and length.

In the first case, antenna array length at both ends is 0.75λ and in the second case, at MS side, it is 0.75λ and at BTS side, it is 6λ. In the second case, for space diversity method, there are 4 antennas at BTS with the spacing of 2λ while for angle diversity method, there are 13 antennas at BTS side with the spacing of 0.5λ.

Case1:

Assumptions made for space and angle diversity methods in Case1 are summarized in Table 4-2.

	Number of elements at BTS	Number of elements at MS	BTS element spacing (*d-rx*)	MS element spacing (*d-tx*)
Space Diversity	4	4	0.5λ	0.5λ
Angle Diversity	4	4	0.5λ	0.5λ

Table 4-2 Assumptions for space and angle diversity methods in Case1.

For both methods, there are 4 antennas at MS and 4 antennas at BTS with the same spacing.

Array length=L_{array}
Number of array elements=N_{array}
Element spacing=d

$$L_{array}=(N_{array}-1)\times d \tag{4-1}$$

where at both MS and BTS sides for both methods, d=0.5λ, N_{array}=4 and L_{array}=0.75λ.

For space diversity in this case, channel capacity is calculated as follows:

$$C(SNR)=\log_2(\det(I+\frac{SNR}{N_T}\times\frac{H\cdot H^*}{norm(H\cdot H^*)})) \tag{4-2}$$

For angle diversity in this case, channel capacity is calculated as follows:

$$C(SNR)=\log_2(\det(I+(G_{Tx}\times G_{Rx})\frac{SNR}{N_T}\times\frac{H\cdot H^*}{norm(H\cdot H^*)})) \tag{4-3}$$

where C is the channel capacity, I is the Identity matrix, SNR is the signal to noise ratio, N_T is number of transmitter antennas (or beams) and H is the channel matrix.

Factor ($G_{Tx} \times G_{Rx}$) in (4-3) shows the array gain of angle diversity method. When an array consists of elements with the spacing of 0.5λ, then its gain is equal to the number of elements if antenna losses are ignored ($G_{Tx}=N_T=4$, $G_{Rx}=N_R=4$ and $G_{total}=4\times4=16$). This is required to take into account while comparing capacities of two methods in terms of *SNR*. Figure 4.21 shows 4 beams which are made at MS side for angle diversity in both Cases 1 and 2. Figure 4.22 also shows 4 beams which are made at BTS side for angle diversity in Case1.

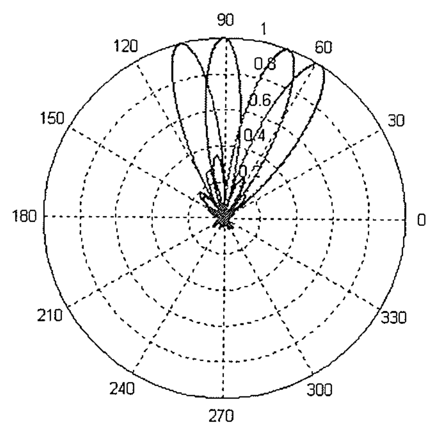

Figure 4.21 **Four multibeams of MS (Tx) which are pointed towards four clusters located in different θ angles (N-array=4, beam angles=62°, 70°, 91°, 105°).**

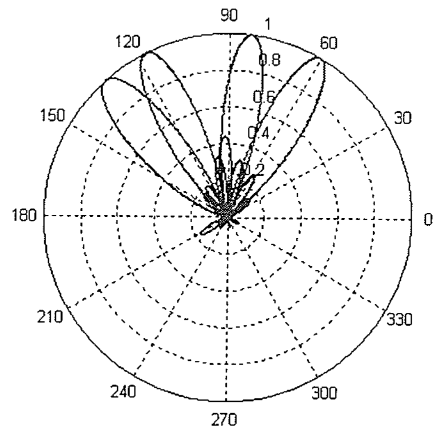

Figure 4.22 **Four multibeams of BTS (Rx) which are pointed towards four clusters located in different θ angles (N-array=4, beam angles=60°, 83°, 117°, 132°).**

Table 4.3 and Figure 4.23 show singular values of *H*-matrix and capacity results for both methods in LOS case, respectively.

	Singular Value1	Singular Value2	Singular Value3	Singular Value4
Space Div.	1.0000	0.0016	0.0004	0.0000
Angle Div.	1.0000	0.0024	0.0008	0.0000

Table 4-3 **Singular values for 30 scatterers in 4 clusters for LOS in Case1.**

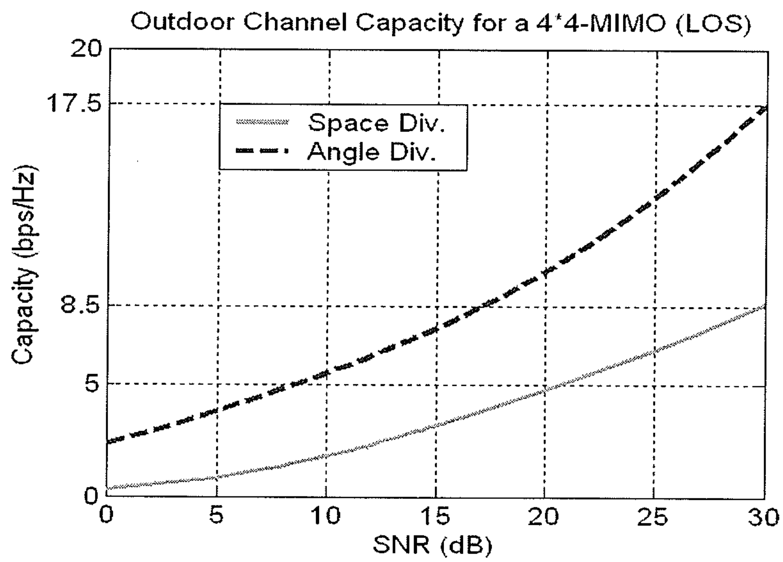

Figure 4.23 **Channel capacity for 30 scatterers in 4 clusters for LOS in Case1.**

Table 4.4 and Figure 4.24 show singular values of *H*-matrix and capacity results for both methods in NLOS case, respectively.

	Singular Value1	Singular Value2	Singular Value3	Singular Value4
Space Div.	1.0000	0.4424	0.0062	0.0003
Angle Div.	1.0000	0.4481	0.0007	0.0000

Table 4-4 **Singular values for 30 scatterers in 4 clusters for NLOS in Case1.**

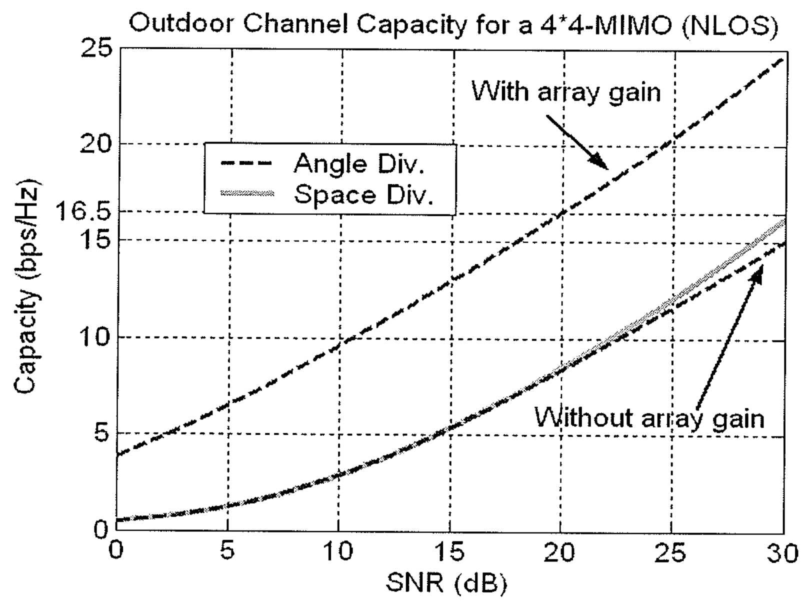

Figure 4.24 **Channel capacity for 30 scatterers in 4 clusters for NLOS in Case1.**

As Figures 4.23 and 4.24 show, array gain that is achieved in angle diversity method lets this method surpass space diversity method significantly. Even though angle diversity is showing better channel orthogonality, improperly chosen angles caused not to get the maximum achievable capacity for the angle diversity.

For NLOS case, the rays from Tx towards clusters behind the block are stopped which cause reduction in the number of channels. Another reason which has caused getting undesirable results for angle diversity method in both LOS and NLOS cases for Case1 is the overlapping beams.

Therefore, we tried different antenna patterns (other than half wavelength dipole) whose Half Power Beam Widths (HPBW) are different at both MS and BTS sides. The results for LOS case are given in Figures 4.25 and 4.26. As the results show, applying antennas with greater HPBW in space diversity method gives better results. It is reasonable since by greater HPBW, antenna is capable to transmit/receive more multipaths which results in increase in capacity.

On the other hand, for angle diversity method, we expect to have better results for lower HPBWs since lower HPBWs result in less overlap among the lobes and correlation among the channels. As Figure 4.26 shows, conversely to our expectation, for lower HPBWs, no better results are achieved. This may be explained by taking into account that using antenna patterns whose HPBWs are less than 70° leads in reduction in beams' power in desirable scanning angles which are closer to endfire direction which ultimately decreases the number of channels. Therefore, it does not seem a good way to choose an antenna with low HPBW to increase the capacity in the circumstances where array arrangement should be kept the same and at the same time it is required to scan the angles close to endfire direction.

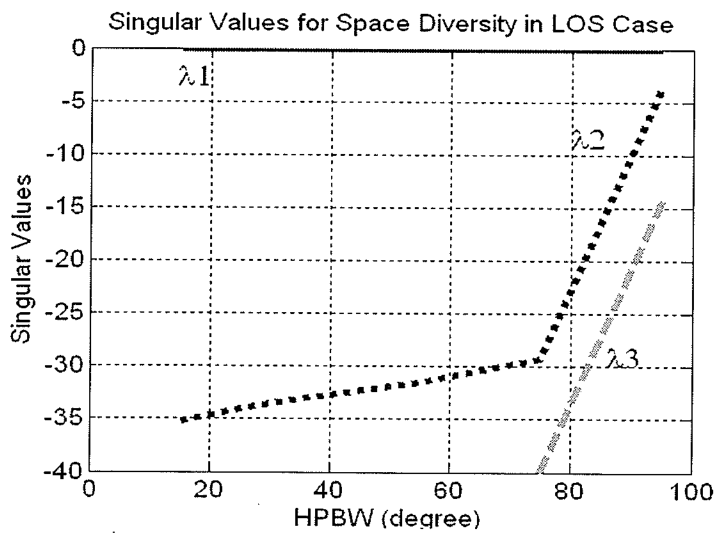

Figure 4.25 **Singular values for space diversity in LOS scenario for Case1.**

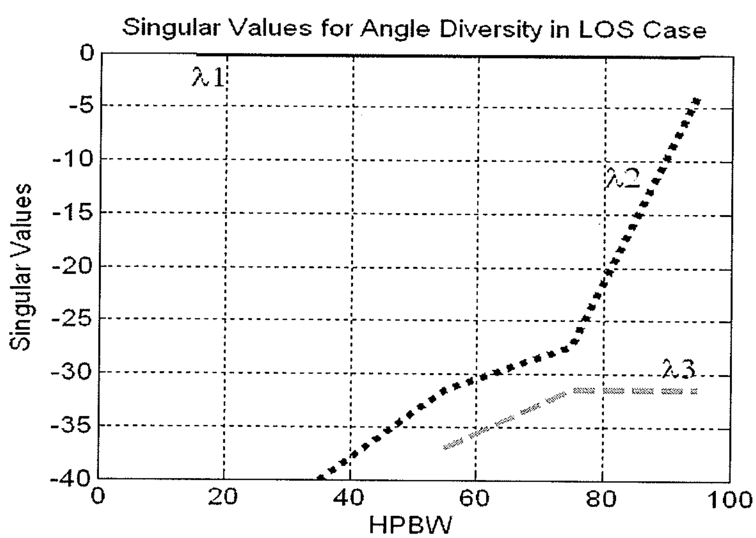

Figure 4.26 **Singular values for angle diversity in LOS scenario for Case1.**

Referring to Figure 4.21, we can see that four beams at MS side have great overlaps. It can be the main reason for unexpected results for Case1 in LOS scenario. Therefore, we tried other scanning angles which are shown in Figure 4.27. These angles are chosen based on having more isolation from each other and less overlap. The results for this scenario are given in Table 4-5 and Figure 4.28.

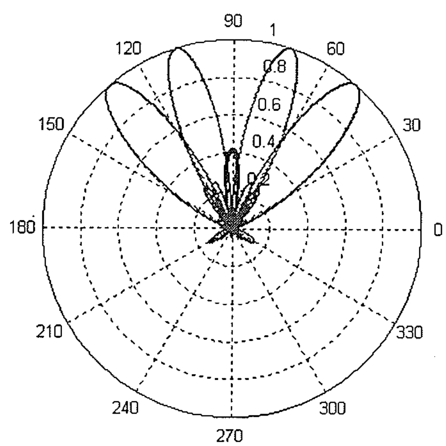

Figure 4.27 **New scanning angles for MS (Tx) which have less overlap comparing to previous one in LOS scenario (N-array=4, beam angles=50°, 74°,108°,132°).**

	Singular Value1	Singular Value2	Singular Value3	Singular Value4
LOS Case	1.0000	0.0058	0.0011	0.0000
NLOS Case	1.0000	0.2673	0.0025	0.0000

Table 4-5 **Singular values for angle diversity method with new scanning angles for MS in Case1.**

Comparing obtained results with Figures 4.23 and 4.24 and Tables 4-3 and 4-4, one may realize that the results for new scanning angles are almost the same for NLOS case but for LOS case, an improvement has been achieved. Therefore, we can conclude that in angle diversity method it is very critical to choose right beam angles with the least overlap in LOS case and in fact by choosing them properly significant improvement can be achieved which will let this method surpass the space diversity.

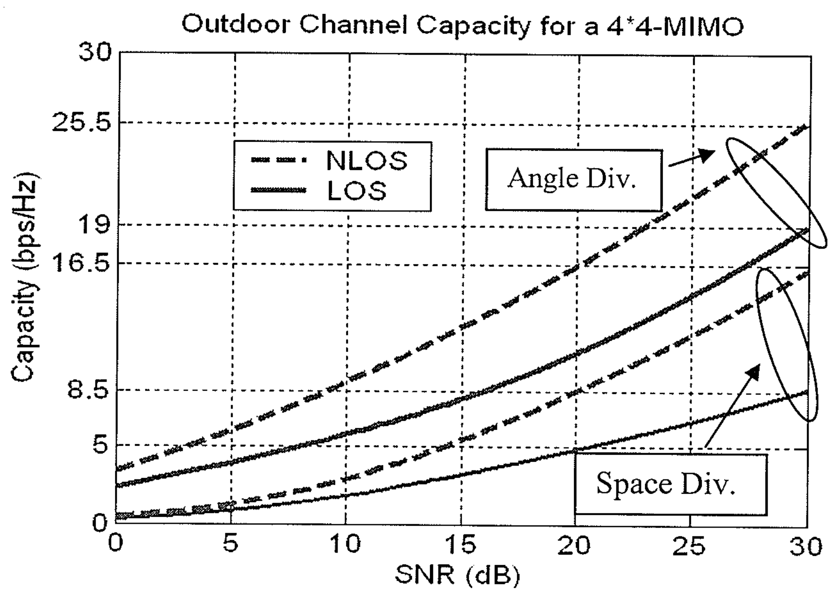

Figure 4.28 **Channel capacity for new scanning angles Case1.**

<u>Case2:</u>

Assumptions which are made for space and angle diversity methods in Case2 are summarized in Table 4-6.

	Number of elements at BTS	Number of elements at MS	BTS element spacing (*d-rx*)	MS element spacing (*d-tx*)
Space Diversity	4	4	2λ	0.5λ
Angle Diversity	13	4	0.5λ	0.5λ

Table 4-6 Assumptions for space and angle diversity methods in Case2.

For angle diversity, number of antennas at both sides is chosen so that the antenna array length is the same for both methods, at BTS it is 6λ and at MS it is 0.75λ.

Referring to equation (4-3), the array gain of angle diversity is $13\times4=52$. It is required to take this gain into account while comparing capacities of two methods in terms of *SNR*.

Figure 4.29 also shows 4 beams which are made at BTS side for angle diversity with 13 antenna elements in Case2.

In this case the beams are much narrower comparing to Case1.

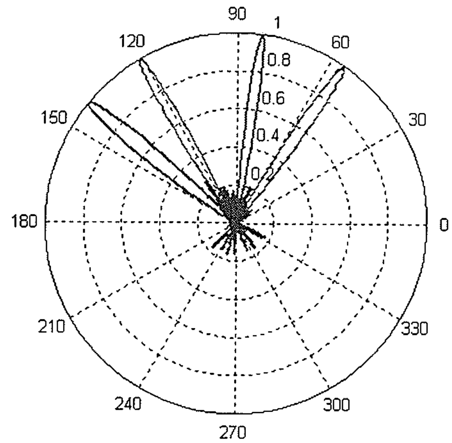

Figure 4.29 **Four multibeams of BTS (Rx) which are pointed towards four clusters located in different θ angles for Case2 (N-array=13, beam angles=55°, 83°, 120°, 141°).**

Table 4-7 and Figure 4.30 show singular values of *H*-matrix and capacity results for both methods in LOS case. For Case2 in LOS scenario, angle diversity gives much more desirable results comparing to space diversity. It is due to the use of larger number of antennas in angle diversity comparing to space diversity method in Case2. In fact, the use of more antennas makes it possible to have narrower beams which subsequently lead to have less interference from other channels and also larger array gain which results in higher capacity. The same is true for NLOS scenario. The results for NLOS scenario is given in Table 4-8 and Figure 4.31.

In conclusion, if there is a possibility to have a larger spacing as much as 6λ at BTS side and if we are willing to get a higher capacity regardless of cost issues, it is wiser to fill the available space by as many as antennas possible with the spacing of 0.5λ rather than just using 4 antennas with the larger spacing of 2λ. However, more antennas cost more and it is necessary to compromise between higher capacity and cost.

	Singular Value1	Singular Value2	Singular Value3	Singular Value4
Space Div.	1.0000	0.0058	0.0004	0.0000
Angle Div.	1.0000	0.0152	0.0095	0.0000

Table 4-7 Singular values for 30 scatterers in 4 clusters for LOS in Case2.

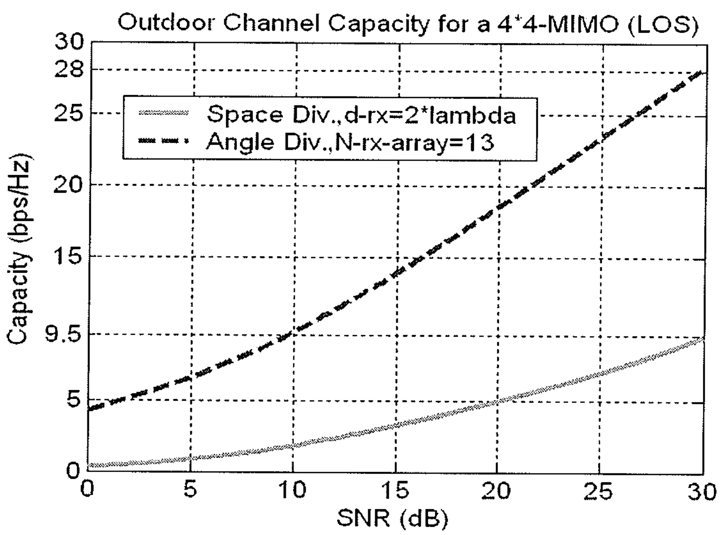

Figure 4.30 Channel capacity for 30 scatterers in 4 clusters for LOS in Case2.

	Singular Value1	Singular Value2	Singular Value3	Singular Value4
Space Div.	1.0000	0.0601	0.0017	0.0003
Angle Div.	1.0000	0.5277	0.0023	0.0000

Table 4-8 Singular values for 30 scatterers in 4 clusters for NLOS in Case2.

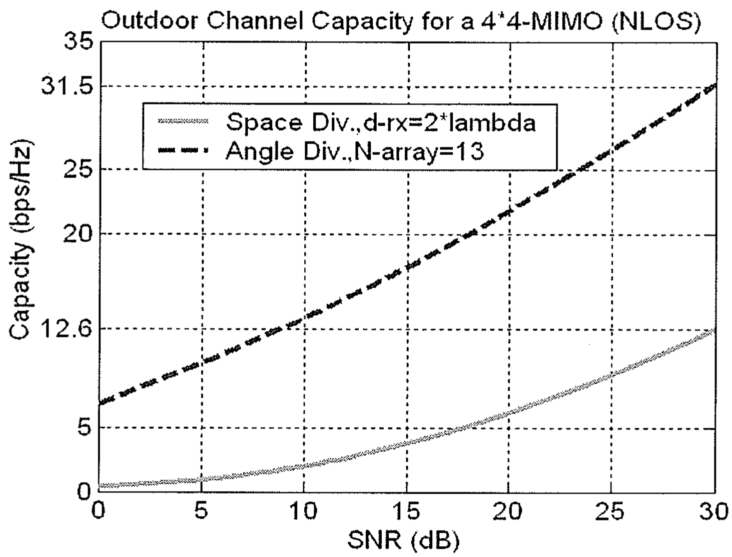

Figure 4.31 **Channel capacity for 30 scatterers in 4 clusters for NLOS in Case2.**

4.2.2.3 Impact of Number of Clusters on Channel Capacity

Since the presence of LOS path makes the channels highly correlated, it is not possible to study the number of clusters impact on the channel capacity. A scenario for NLOS case, similar to what was shown in Figure 4.15 is considered. To consider the effects of number of clusters, clusters in this configuration are located in such a way to avoid getting blocked by the defined obstacle in the middle of the study area. Figure 4.32 shows that for a certain amount of *SNR*, as the number of clusters increases, at first, channel capacity increases but after a while it stays constant.

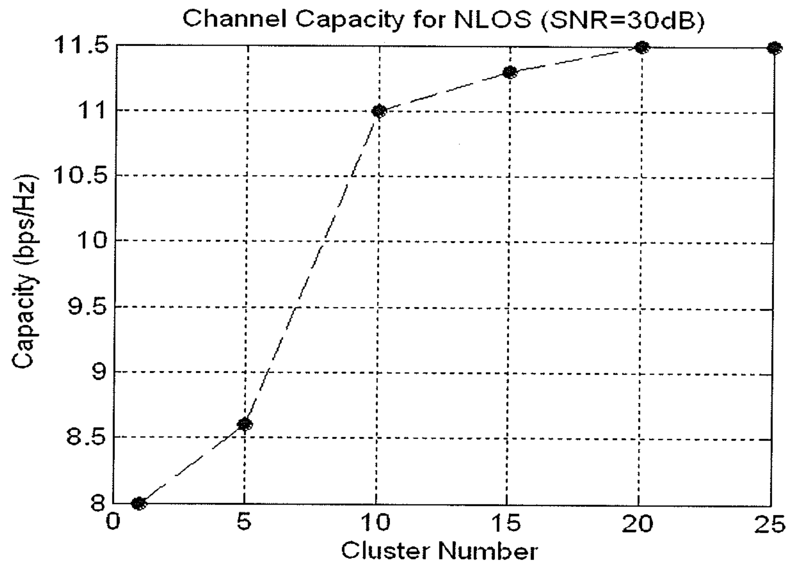

Figure 4.32 **Channel capacity at *SNR*=30 dB for different numbers of clusters which contain 10 scatterers each.**

4.3 Chapter Summary

In this chapter two different distributions of uniform and cluster form for scatterers were studied in a typical outdoor environment. In this study, relative height of Tx and Rx was 2m and their distance was about 13m.

For both kinds of distribution, results for LOS and NLOS cases were evaluated. Impacts of number of scatterers, number of MIMO elements, Rx element spacing and ground's material were studied.

Finally space and angle diversity methods were compared for two cases; in the first case, antenna array length at both ends was 0.75λ and in the second case, at MS side, it was 0.75λ and at BTS side, it is 6λ. In the second case, for space diversity method, there were

4 antennas at BTS with the spacing of 2λ while for angle diversity method; there were 13 antennas at BTS side with the spacing of 0.5λ.

Chapter5: Numerical Results for Indoor Environments

5.1 Chapter Introduction

The main objective of this chapter is to present, explain and discuss numerical results for indoor environments obtained by changing different parameters which impact the channel capacity using the SISTER model.

5.2 Different Scenarios

Two typical indoor environments, an office and an amphitheater area are studied. The main focus is on the office area where communication has greater importance.

A Typical Office Area

For a typical office area, system specifications are summarized in Table 5-1.

	Tx height	Rx height	Relative height of Tx and Rx	Distance between Tx and Rx	Room's dimension	scatterers' radius	scatterers' number
Office	10.4λ (1.3m)	14.4λ (1.8m)	4λ (0.5m)	32.24λ (4.3m)	5×4×3(m3)	0.1m	30

Table 5-1 A typical office system specifications.

For indoor environments similar to outdoor ones, two distributions, uniform and cluster form are studied. The only difference is that, here for the uniform distribution, scatterers are uniformly distributed in the cube which represents the indoor environment. While in the outdoor, they were uniformly distributed around each of Tx and Rx.

5.2.1 Uniform Distribution

To model uniform distribution for indoor environments, 30 scatterers are uniformly distributed in an area enclosed by a cube shown in Figure 5.1.

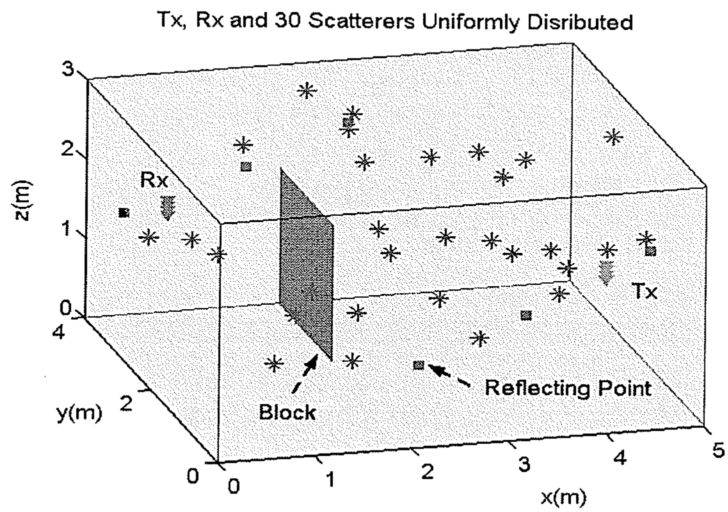

Figure 5.1 **System configuration of an office area including Tx, Rx and 30 scatterers distributed uniformly for NLOS scenario.**

5.2.1.1 Number of Scatterers

Increasing number of scatterers from 30 to 100 in this area has shown growth in channel capacity for both NLOS and LOS cases as it is shown in Figure 5.2.

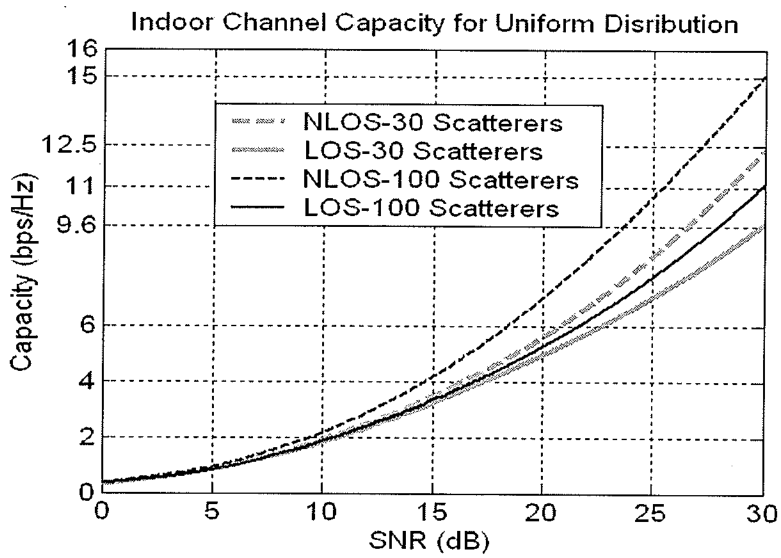

Figure 5.2 **Indoor channel capacity for different numbers of scatterers distributed uniformly.**

For indoor environments, in addition to scattered fields and direct path, reflections from six walls also contribute in the calculation of final electric field for LOS case. For NLOS case some of the reflections, depending on the location of blocking wall may contribute in the calculations.

It is worth noting that in indoor environments, reflected fields have greater importance comparing to outdoor environments since for indoor six reflecting objects are considered whereas for outdoor only one is contributing. Depending on the phase of each of these reflected paths at Rx, their summation may increase or decrease the correlation between the channels. As Figure 5.3 shows, reflections from the walls somehow lessen the direct path dominance in LOS case but their presence in NLOS case decreases the capacity.

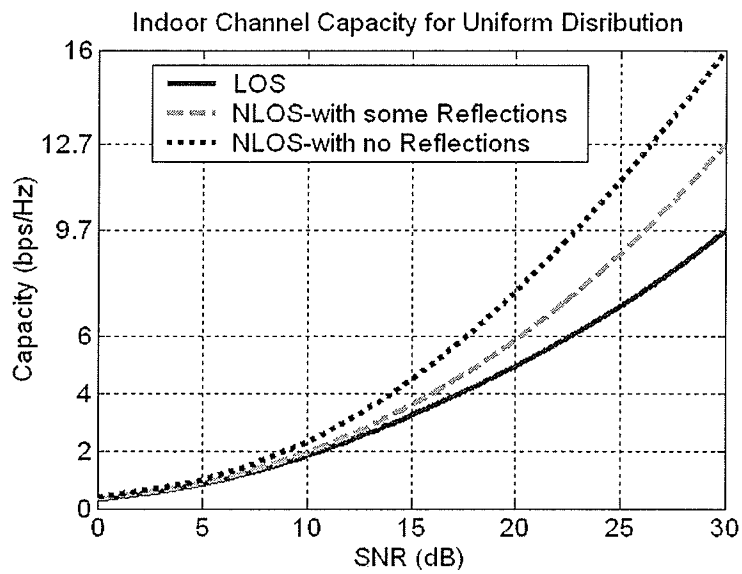

Figure 5.3 **Indoor channel capacity for 30 scatterers distributed uniformly.**

5.2.1.2 Material of the Walls

Material of the walls can significantly change the capacity since it has impact on the power and the direction of the reflected fields. To examine how the material of the walls impacts the capacity, two different kinds of walls, high and low conductive ones are studied. Figure 5.4 indicates the channel capacity considering only reflected fields in the calculation. It shows, choosing high conductive material for the walls influences the power and phase of the reflected fields in such a way that ultimately it makes more uncorrelated channels comparing to the case of choosing low conductive walls. Therefore, as Figure 5.5 shows, high conductive walls have increased the channel capacity for both LOS and NLOS cases, adding the scattered and direct path in the capacity calculation.

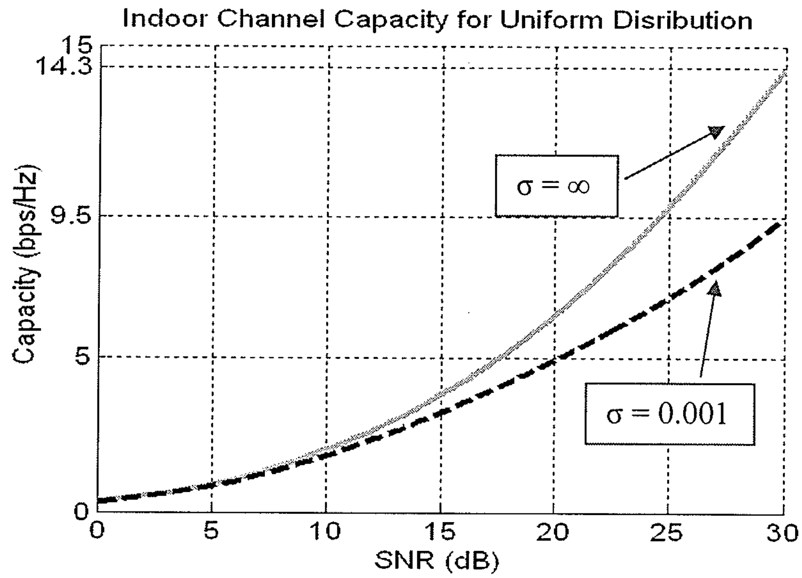

Figure 5.4 Indoor channel capacity considering only reflections from the walls (σ=wall's electrical conductivity).

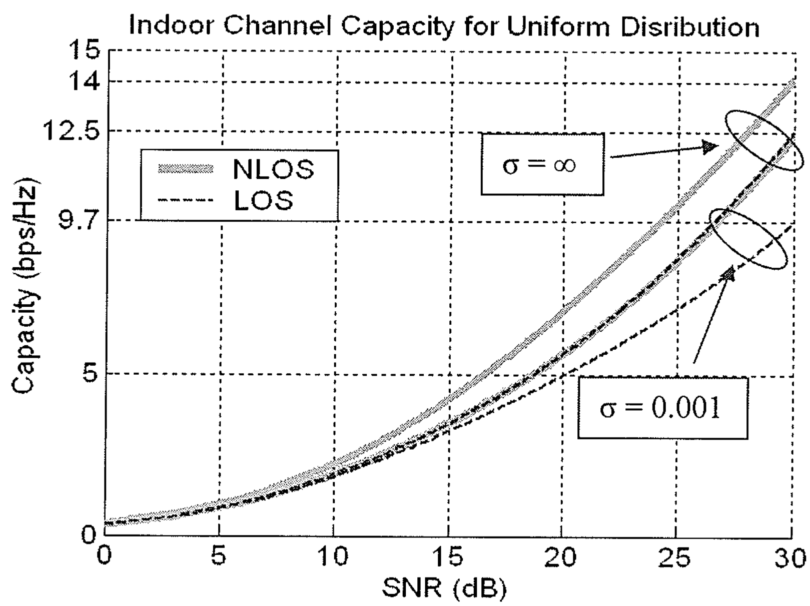

Figure 5.5 Channel capacity for different walls (σ=wall's electrical conductivity).

5.2.1.3 Rx Elements' Spacing

Figures 5.6 and 5.7 show how the spacing of Rx elements impacts the channel capacity for LOS and NLOS cases, respectively. For both cases, the more the spacing of Rx elements is, the higher the capacity is. Obtaining the same results for outdoors, we can conclude that larger spacing results in higher capacity in general.

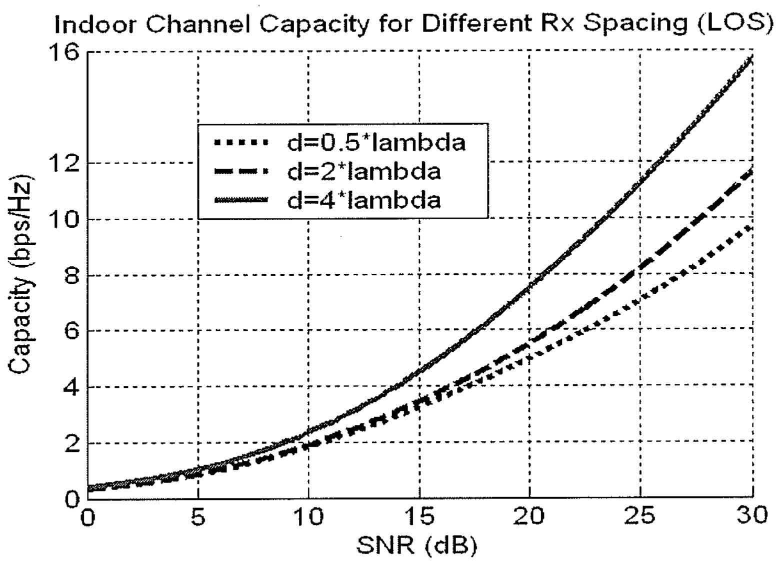

Figure 5.6 **Indoor channel capacity for uniform distribution in LOS case, showing impact of changing Rx element spacing (Tx element spacing=0.5λ, d=Rx element spacing).**

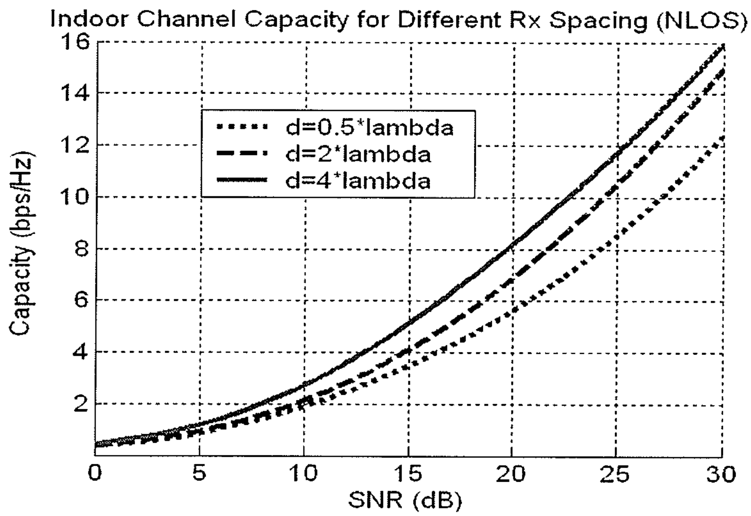

Figure 5.7 **Indoor channel capacity for uniform distribution in NLOS case, showing impact of changing Rx element spacing (Tx element spacing=0.5λ, d=Rx element spacing).**

5.2.1.4 MIMO Elements' Number

Figures 5.8 and 5.9 show how the number of MIMO elements impacts the channel capacity for LOS and NLOS cases, respectively. For LOS case in lower *SNRs*, SISO works better than the rest. For higher *SNRs* they give the same results. In fact in LOS case the channel is highly correlated, particularly for lower *SNRs*, and adding the number of elements introduces even more correlation among the channels.

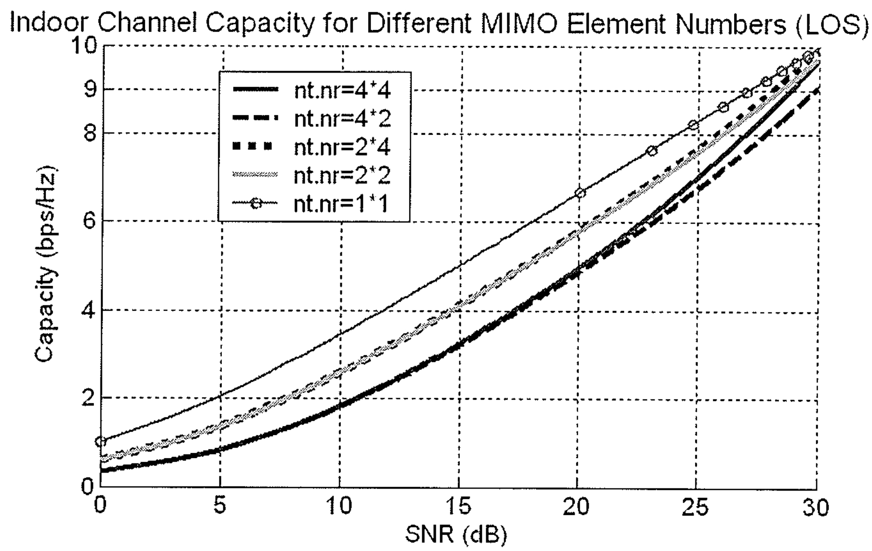

Figure 5.8 **Channel capacity for uniform distribution in LOS case, showing impact of changing the number of elements (Rx element spacing=0.5λ, nt=number of Tx antennas, nr=number of Rx antennas).**

For NLOS case, similar results are obtained for lower *SNRs* but for higher *SNRs* 4×4-MIMO works best.

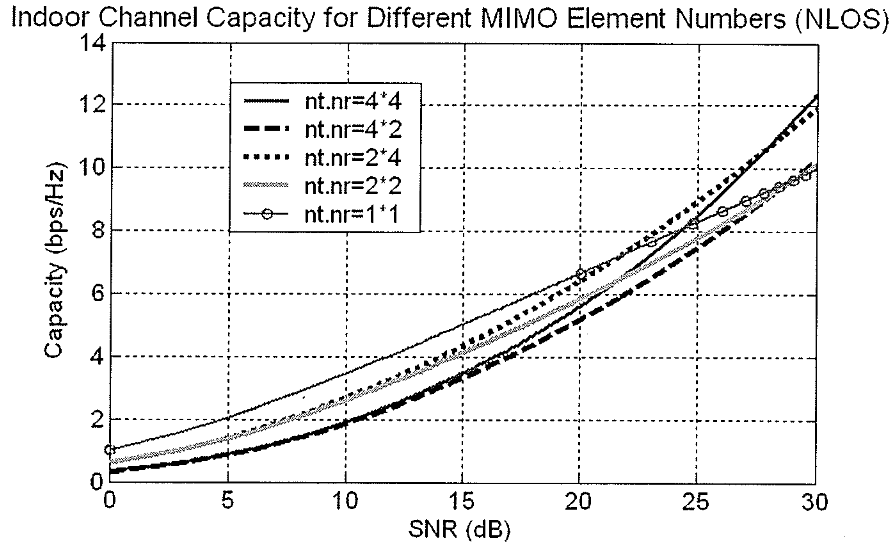

Figure 5.9 **Channel capacity for uniform distribution in NLOS case, showing impact of changing the number of elements (Rx element spacing=0.5λ, nt=number of Tx antennas, nr=number of Rx antennas).**

5.2.1.5 Tx Different Positions

In this section, the impact of Tx position is investigated. Two different locations, one in the middle (Figure 5.10) and the other in the corner (Figure 5.11) of the office are chosen.

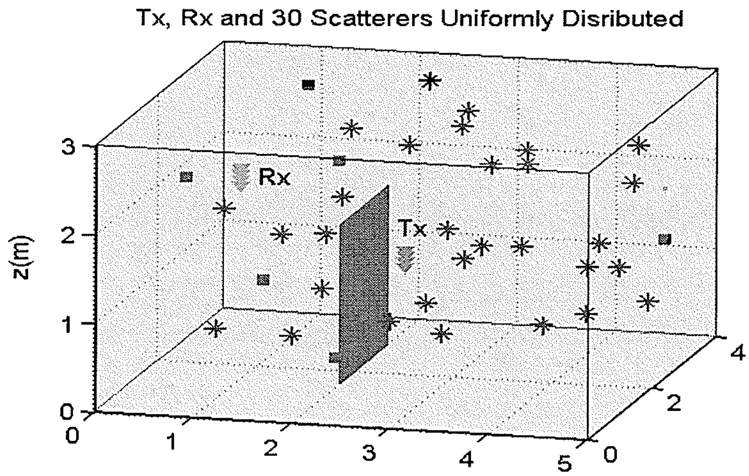

Figure 5.10 System schematic for NLOS case where Tx is in the middle of the office area.

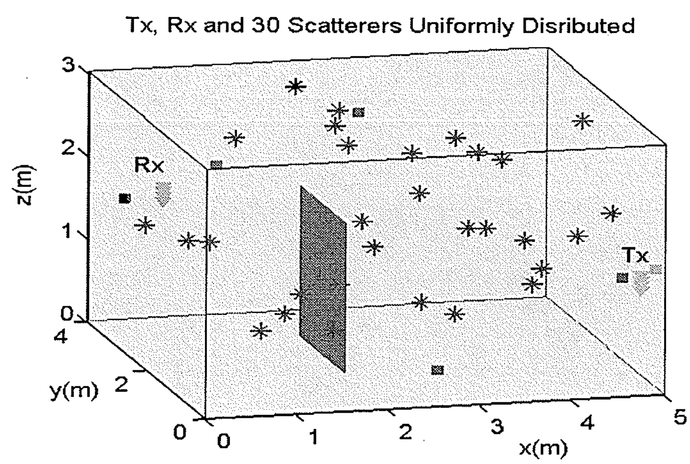

Figure 5.11 System schematic for NLOS case where Tx is in the corner of the office area.

Figures 5.12 and 5.13 show that for both cases of LOS and NLOS channel capacity is higher when Tx is in the middle. It can be due to the fact that when Tx is in the corner it can just transmit towards limited directions effectively and this makes channels more correlated whereas when it is in the middle, it can transmit to all the directions evenly and make more uncorrelated cannels.

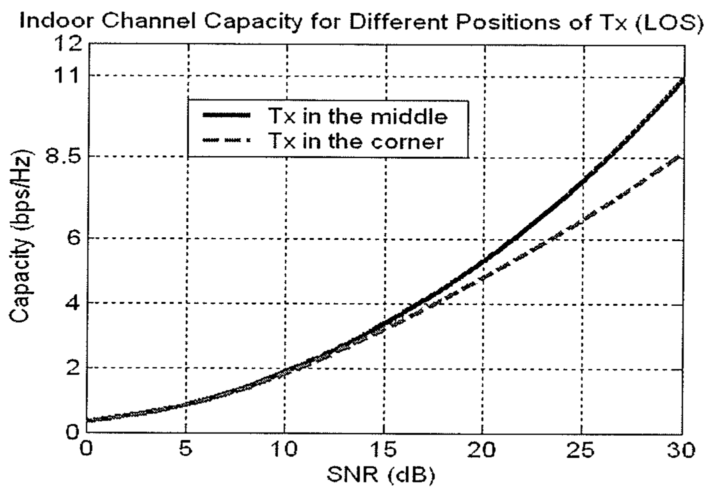

Figure 5.12 **Channel capacity for different positions of Tx in LOS case.**

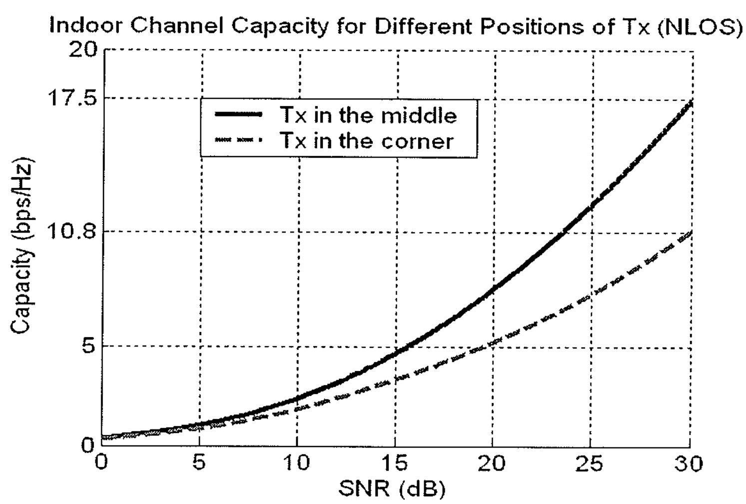

Figure 5.13 **Channel capacity for different positions of Tx in NLOS case.**

5.2.1.6 Comparing Space and Angle Diversity Methods

In this section space and angle diversity methods are compared. Four selected beams which are used for angle diversity method are shown in Figure 5.14.

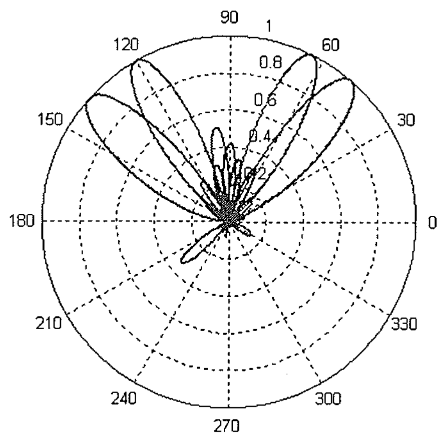

Figure 5.14 **Selected beams for both Tx and Rx in the 4×4-MIMO system (beam angles=48°, 65°, 130°, 138°).**

Referring to equation (4-3), the array gain of angle diversity method is 4×4=16. It is required to take into account while comparing capacities of two methods in terms of *SNR*. The composition of singular values are given in Table 5-2. It shows for both LOS and NLOS cases, angle diversity surpasses space diversity method in terms of channel orthogonality. Moreover, it offers array gain which again leads in an increase in the capacity shown in Figures 5.15 and 5.16.

	Singular Value1	Singular Value2	Singular Value3	Singular Value4
Space Div. (LOS)	1.0000	0.0067	0.0008	0.0000
Angle Div. (LOS)	1.0000	0.1120	0.0011	0.0005
Space Div. (NLOS)	1.0000	0.0208	0.0087	0.0002
Angle Div. (NLOS)	1.0000	0.2252	0.0658	0.0000

Table 5-2 **Singular values for 30 scatterers uniformly distributed for the 4×4-MIMO system.**

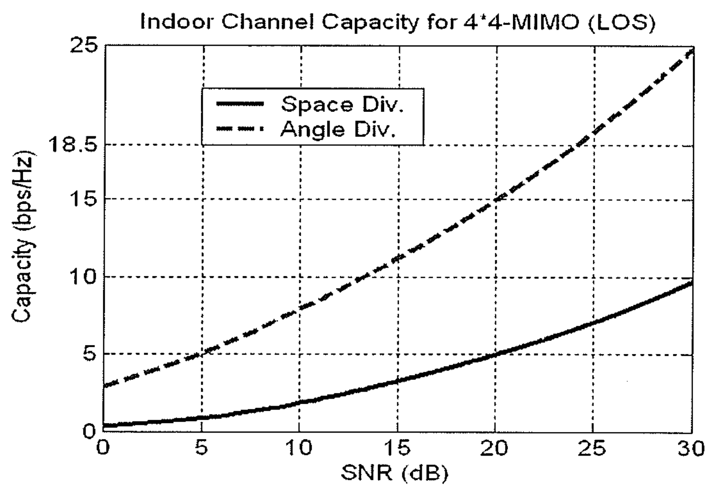

Figure 5.15 **Channel capacity for 30 scatterers uniformly distributed for LOS case in the 4×4-MIMO system.**

It is also more convenient to apply angle diversity method since there is not a huge difference between LOS and NLOS capacities if the beams are selected properly while this is not true for space diversity. Furthermore, applying angle diversity helps to lessen the interference from other available systems in an indoor environment which is a real concern nowadays. However, the price which should be paid to gain all these achievements is selecting the right beams.

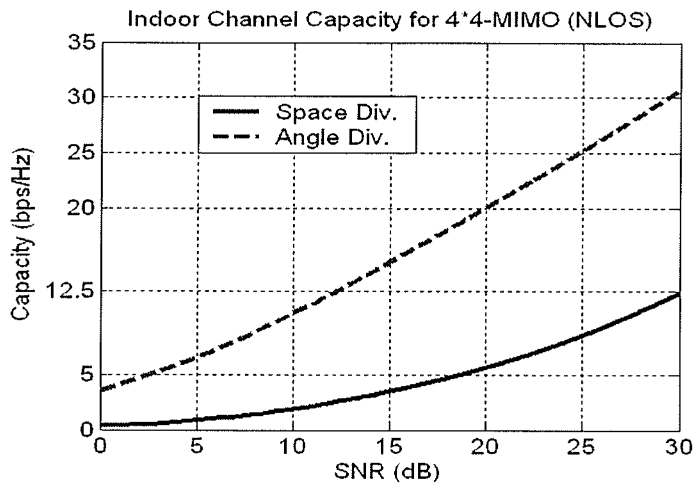

Figure 5.16 **Channel capacity for 30 scatterers uniformly distributed for NLOS case in the 4×4-MIMO system.**

Trying different scanning angles here, it is realized that particularly for LOS case higher capacity can be achieved by choosing angles far away from the direct path (Figure 5.14) which in most cases is approximately around horizontal plane (θ=90°).

5.2.1.7 Comparing 2×2-MIMO and 4×4-MIMO Systems

Referring to results shown in Figure 5.8, it is motivating to check whether 2×2-MIMO system gives desirable results or not. To implement a 2×2-MIMO system, total antenna length is kept the same as the 4×4-MIMO system which is $3\lambda/2$. For space diversity, instead of 4 elements, there are 2 elements at each end with the spacing of $3\lambda/2$. For angle diversity, there are two elements with λ spacing. Each element consists of 2 dipoles with $\lambda/2$ spacing.

To study angle diversity method for this 2×2-MIMO system in LOS case where 30 scatterers are uniformly distributed (Figure 5.1), two beams are directed towards the reflecting points of ceiling and the floor which actually are the two angles far from the direct path (Figure 5.17). For NLOS case, however, since no direct path exists, there is more freedom to find the desirable angles. Therefore, as it is shown in Figure 5.17, different angles for the LOS case are chosen for beams which one of them is not that far from the horizontal plane.

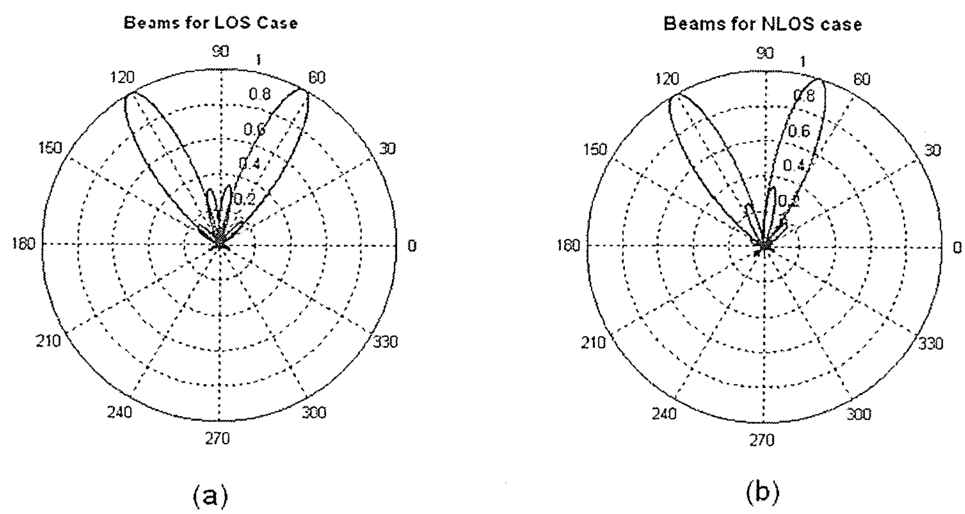

Figure 5.17 **Selected angles for the 2×2-MIMO in LOS and NLOS cases for both Tx and Rx (beam angles for (a)=62°, 121°, beam angles for (b)=72°, 119°).**

Results for the 2×2-MIMO system are given in Table 5-3 and Figure 5.18.

As these results show, for the 2×2-MIMO system similar to what was obtained for the 4×4-MIMO system, angle diversity works better for both LOS and NLOS cases.

Comparing 2×2-MIMO and 4×4-MIMO systems for space diversity method when scatterers are uniformly distributed, it is wiser to use a 2×2-MIMO system since it offers almost the same capacity with a lower cost.

	Singular Value1	Singular Value2	Singular Value3	Singular Value4
Space Div. (LOS) 4×4-MIMO	1.0000	0.0067	0.0008	0.0000
Angle Div. (LOS) 4×4-MIMO	1.0000	0.1120	0.0011	0.0005
Space Div. (NLOS) 4×4-MIMO	1.0000	0.0208	0.0087	0.0002
Angle Div. (NLOS) 4×4-MIMO	1.0000	0.2252	0.0658	0.0000
Space Div. (LOS) 2×2-MIMO	1.0000	0.0094	-------	-------
Angle Div. (LOS) 2×2-MIMO	1.0000	0.1529	-------	-------
Space Div. (NLOS) 2×2-MIMO	1.0000	0.0011	-------	-------
Angle Div. (NLOS) 2×2-MIMO	1.0000	0.1816	-------	-------

Table 5-3 Comparing singular values for the 2×2-MIMO and 4×4-MIMO systems.

Although angle diversity for 4×4-MIMO system shows better performance, still 2×2-MIMO system gives desirable results. In fact, the selected beams shown in Figure 5.17 are not necessarily the optimum ones and it is possible to find angles which give even more desirable results and comparable to what is obtained by angle diversity for 4×4-MIMO system.

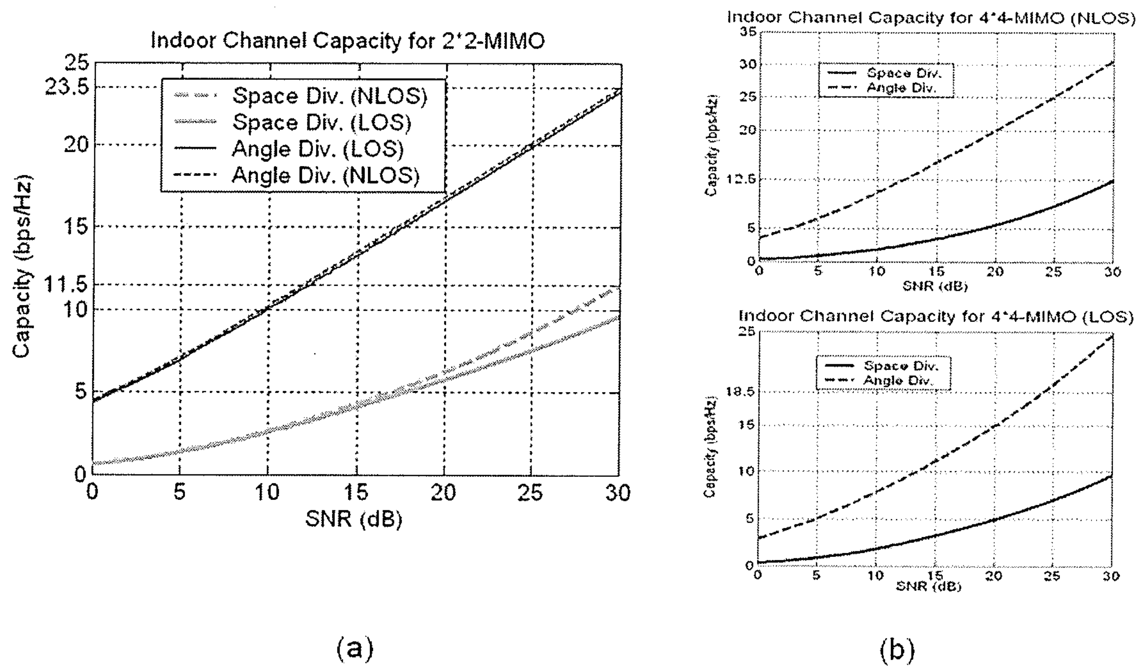

Figure 5.18 **Comparing channel capacity for 2×2-MIMO and 4×4-MIMO systems: (a) 2×2-MIMO system (b) 4×4-MIMO system.**

5.2.1.8 Comparing 2×2-MIMO and 4×4-MIMO Systems for Specific Tx Positions

2×2-MIMO and 4×4-MIMO systems are also compared for specific positions of middle and corner of the office area and the corresponding results are given in Figures 5.19 and 5.20 and Tables 5-4 and 5-5.

	Singular Value1	Singular Value2
Space Div. (LOS)	1.0000	0.0068
Angle Div. (LOS)	1.0000	0.0051
Space Div. (NLOS)	1.0000	0.0312
Angle Div. (NLOS)	1.0000	0.0378

Table 5-4 **Singular values for 2×2-MIMO where Tx is located in the corner of the office.**

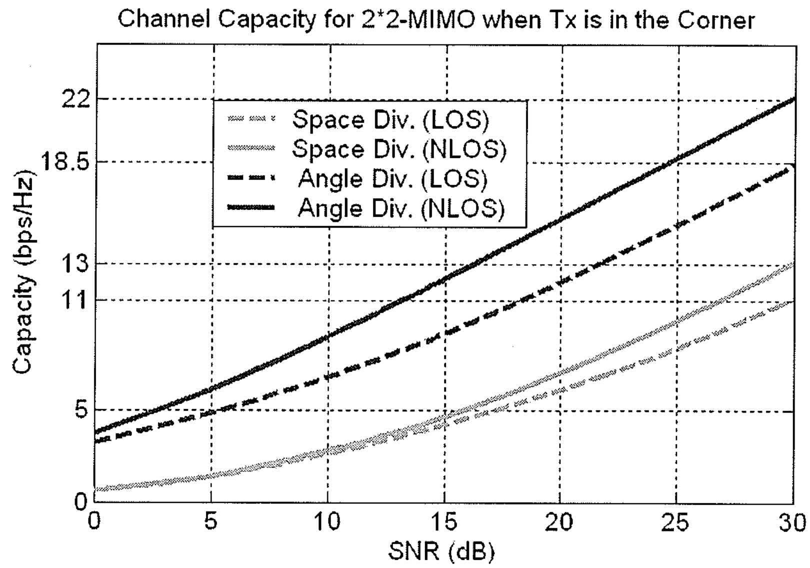

Figure 5.19 **Channel capacity for the 2×2-MIMO where Tx is located in the corner of the office.**

As these results show, for both positions angle diversity shows higher capacity. Here as well, scanning angles which are far away from the horizontal plane, particularly for LOS case show better results.

	Singular Value1	Singular Value2
Space Div. (LOS)	1.0000	0.0492
Angle Div. (LOS)	1.0000	0.5707
Space Div. (NLOS)	1.0000	0.1151
Angle Div. (NLOS)	1.0000	0.7663

Table 5-5 **Singular values for the 2×2-MIMO where Tx is located in the middle of the office.**

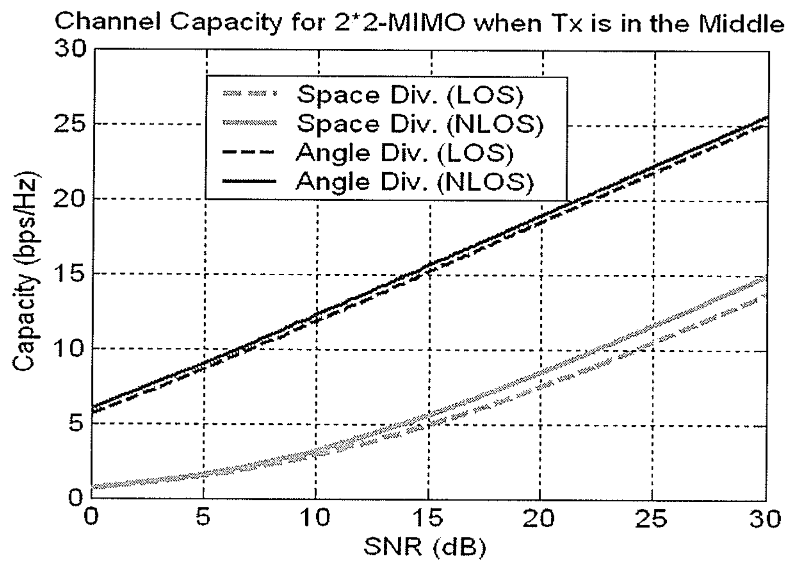

Figure 5.20 **Channel capacity for the 2×2-MIMO where Tx is located in the middle of the office.**

5.2.2 Cluster Distribution

To study cluster distribution, four clusters are located in different positions in the office area as it is shown in Figure 5.21.

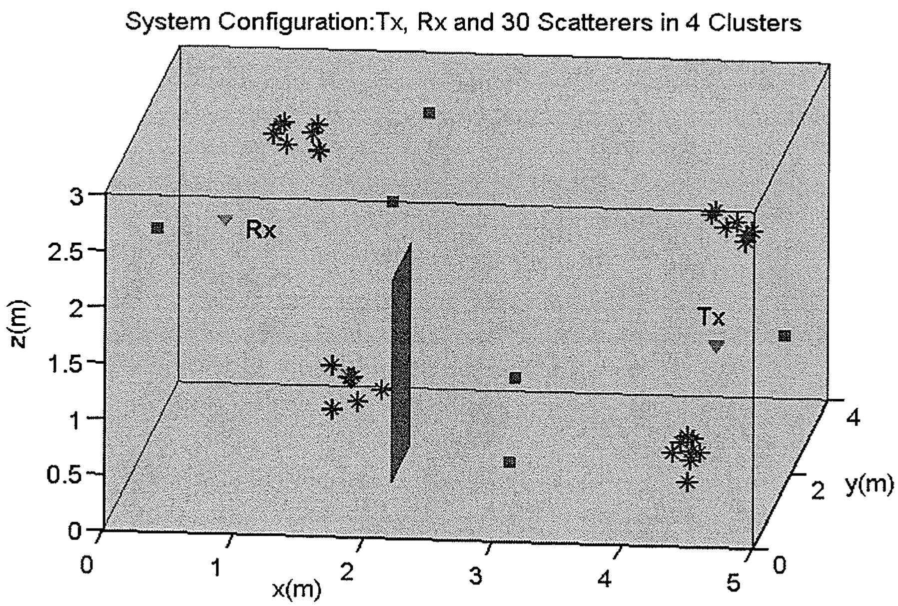

Figure 5.21 **System schematic for NLOS case for cluster distribution of scatterers.**

5.2.2.1 Comparing Space and Angle Diversities

In this section, space and angle diversity methods are compared for office area where scatterers are in cluster form.

As it is shown in Figure 5.22, first non-optimum beams are chosen, each of which are directed towards each of four clusters' angles. As it can be seen, they are close to each other and have some overlaps. These overlaps cause increase in the correlation among the channels and show decrease in channel capacity (Figure 5.23), therefore they are changed in such a way that have less overlap while they are not directed to clusters any more.

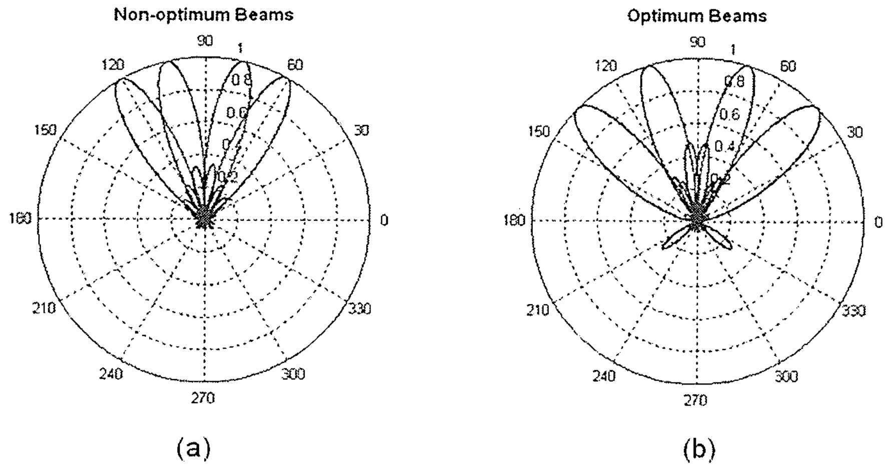

Figure 5.22 **Beams for the 4×4-MIMO system (beam angles for (a)=61°, 77°, 103°, 121°, beam angles for (b)=43°, 73°, 108°, 136°).**

The final results are given in Table 5-6 and Figure 5.23. As expected, the beams with less overlap significantly increase the capacity. However, it is worth reminding that here linear array and dipole antenna are used which both lead to have omnidirectional patterns. It is probable to get even more desirable result for original selected beams, if antennas with higher directivity or planar array are used.

	Singular Value1	Singular Value2	Singular Value3	Singular Value4
Space Div. (LOS)	1.0000	0.0052	0.0008	0.0002
Angle Div. (LOS)	1.0000	0.0025	0.0007	0.0000
Angle Div. (LOS)_improved	1.0000	0.0045	0.0014	0.0005
Space Div. (NLOS)	1.0000	0.0884	0.0302	0.0037
Angle Div. (NLOS)	1.0000	0.0802	0.0153	0.0013
Angle Div. (NLOS)_improved	1.0000	0.1888	0.0621	0.0205

Table 5-6 **Singular values for the 4×4-MIMO system.**

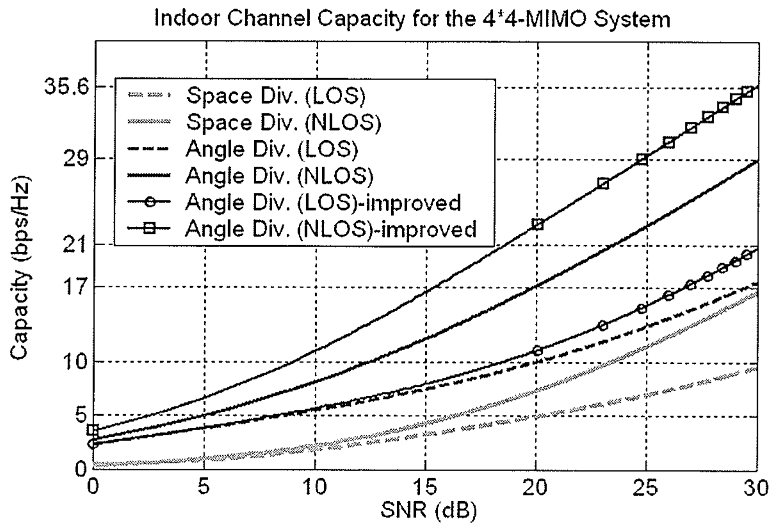

Figure 5.23 **Channel capacity for 30 scatterers in cluster form in the 4×4-MIMO system.**

5.2.2.2 Comparing 2×2-MIMO and 4×4-MIMO Systems

For cluster form of scatterers also, 2×2-MIMO and 4×4-MIMO systems are compared and corresponding results are given in Figure 5.24 and Table 5-7. As these results show, only for space diversity in LOS case, 2×2-MIMO works better than 4×4-MIMO. In the rest of the cases when scatterers are in cluster form, 4×4-MIMO surpasses 2×2-MIMO system.

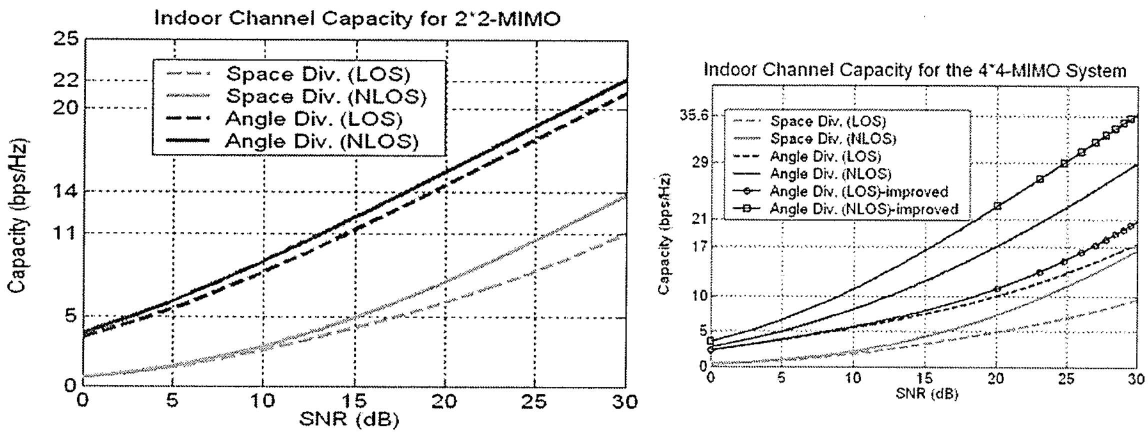

Figure 5.24 Comparing channel capacity for 2×2-MIMO and 4×4-MIMO systems.

	Singular Value1	Singular Value2	Singular Value3	Singular Value4
Space Div. (LOS) 4×4-MIMO	1.0000	0.0052	0.0008	0.0002
Angle Div. (LOS) 4×4-MIMO	1.0000	0.0025	0.0007	0.0000
Angle Div. (LOS)_improved 4×4-MIMO	1.0000	0.0045	0.0014	0.0005
Space Div. (NLOS) 4×4-MIMO	1.0000	0.0884	0.0302	0.0037
Angle Div. (NLOS) 4×4-MIMO	1.0000	0.0802	0.0153	0.0013
Angle Div. (NLOS)_improved 4×4-MIMO	1.0000	0.1888	0.0621	0.0205
Space Div. (LOS) 2×2-MIMO	1.0000	0.0063	-------	-------
Angle Div. (LOS) 2×2-MIMO	1.0000	0.0351	-------	-------
Space Div. (NLOS) 2×2-MIMO	1.0000	0.0529	-------	-------
Angle Div. (NLOS) 2×2-MIMO	1.0000	0.0691	-------	-------

Table 5-7 Comparing singular values for 2×2-MIMO and 4×4-MIMO systems.

Amphitheater Area

Figure 5.25 shows system schematic of a typical amphitheater area of $10 \times 7 \times 5\ m^3$ which encloses Tx, Rx and 120 scatterers representing the chairs.

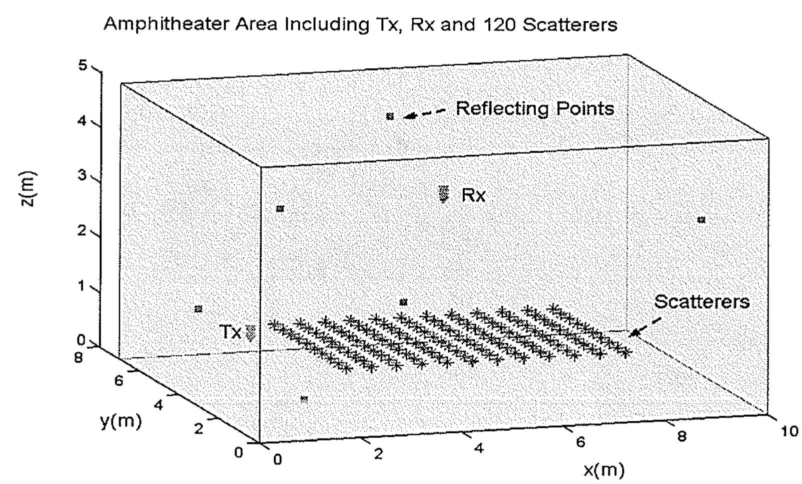

Figure 5.25 **System configuration of an amphitheater area including Tx, Rx and 120 scatterers.**

For a typical amphitheater area, system specifications for two cases are summarized in Table 4-1. For two cases Tx heights and locations are different. In Case1, Tx is located at a lower height among the chairs and in the Case2 it is far from the chairs and is located at a higher height.

	Tx height	Rx height	Relative height of Tx and Rx	Distance between Tx and Rx	Room's dimension
Amphitheater (Case1)	6.8λ (0.85m)	28λ (3.5m)	21.2λ (2.65m)	23λ (2.87m)	10×7×5(m3)
Amphitheater (Case2)	10.4λ (1.3m)	28λ (3.5m)	17.6λ (2.2m)	36.8λ (4.6m)	10×7×5(m3)

Table 5-8 A typical amphitheater system specifications.

Scatterers' characteristics are also given in Table 5-9.

	Radius	Number	Height
Scatterers (Chairs)	10cm	120	80cm

Table 5-9 Scatterers' characteristics for amphitheater area.

For the Case1 where Tx is among the chairs, scanning beams at Tx and Rx are shown in Figures 5.26 and 5.27 for 4×4-MIMO and 2×2-MIMO systems, respectively. As Figure 5.26 shows, the chosen beams for 4×4-MIMO have high overlaps which occurred because of scanning towards endfire direction. As Table 5-10 and Figure 5.28 show in spite of the presence of these overlaps still angle diversity surpasses space diversity method for 4×4-MIMO system. Comparing space and angle diversities for 2×2-MIMO systems also shows better performance of angle diversity.

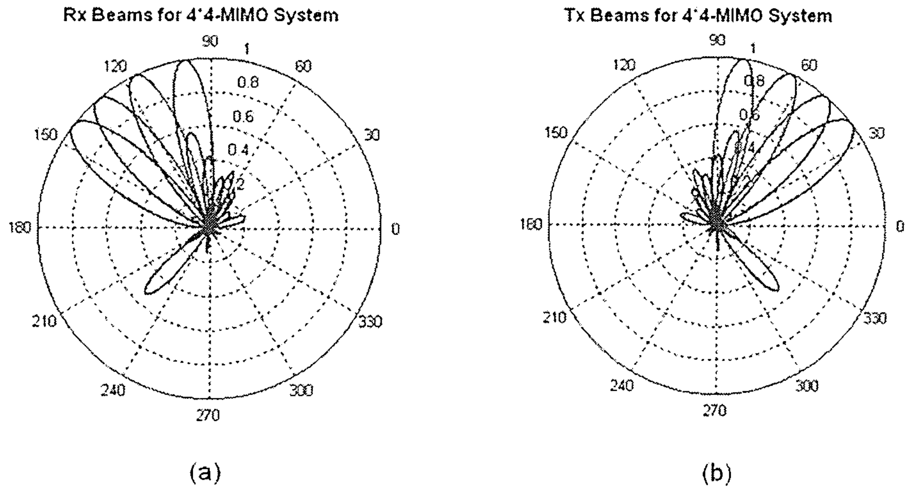

Figure 5.26 Beams for the scenario where Tx is located among the chairs for the 4×4-MIMO System (beam angles for (a)=100°, 117°, 131°, 143°, beam angles for (b)=38°, 50°, 63°, 81°).

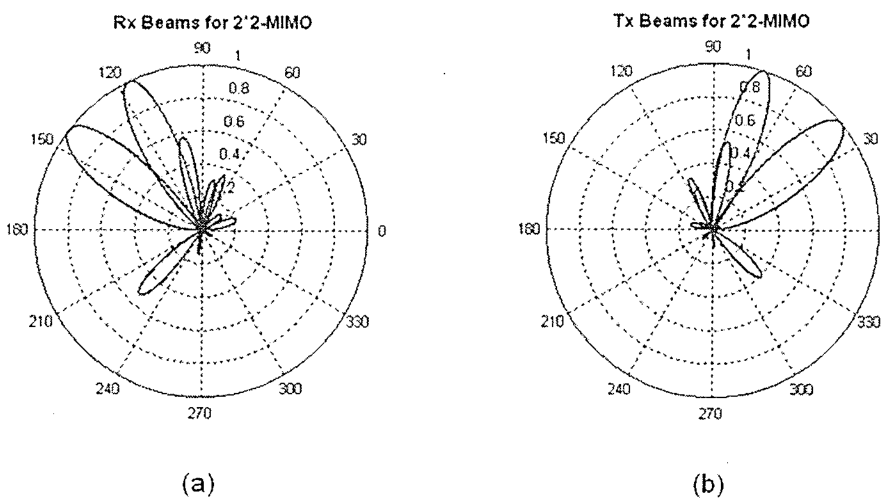

Figure 5.27 Beams for the scenario where Tx is located among the chairs for the 2×2-MIMO System (beam angles for (a)=117°, 144°,, beam angles for (b)=40°, 73°).

	Singular Value1	Singular Value2	Singular Value3	Singular Value4
Space Div. (4×4-MIMO)	1.0000	0.0651	0.0051	0.0000
Angle Div. (4×4-MIMO)	1.0000	0.0609	0.0391	0.0000
Space Div. (2×2-MIMO)	1.0000	0.0603	-------	-------
Angle Div. (2×2-MIMO)	1.0000	0.0943	-------	-------

Table 5-10 Singular values for the scenario where Tx is located among the chairs.

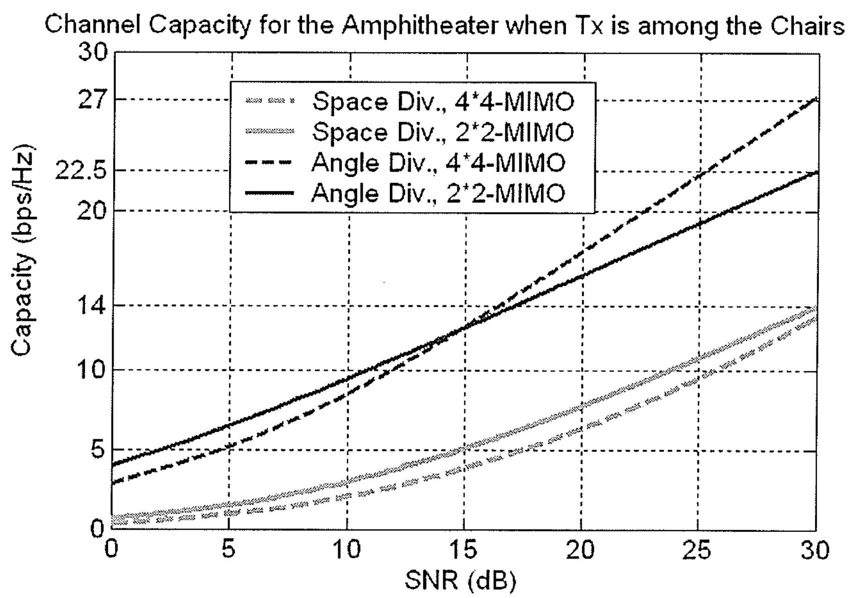

Figure 5.28 Channel capacity for the scenario where Tx is located among the chairs.

For the Case2 where Tx is far from the chairs, scanning beams at Tx and Rx are shown in Figures 5.29 and 5.30 for 4×4-MIMO and 2×2-MIMO systems, respectively. Figure 5.31 and Table 5-11 show overall capacity for both 4×4-MIMO and 2×2-MIMO systems.

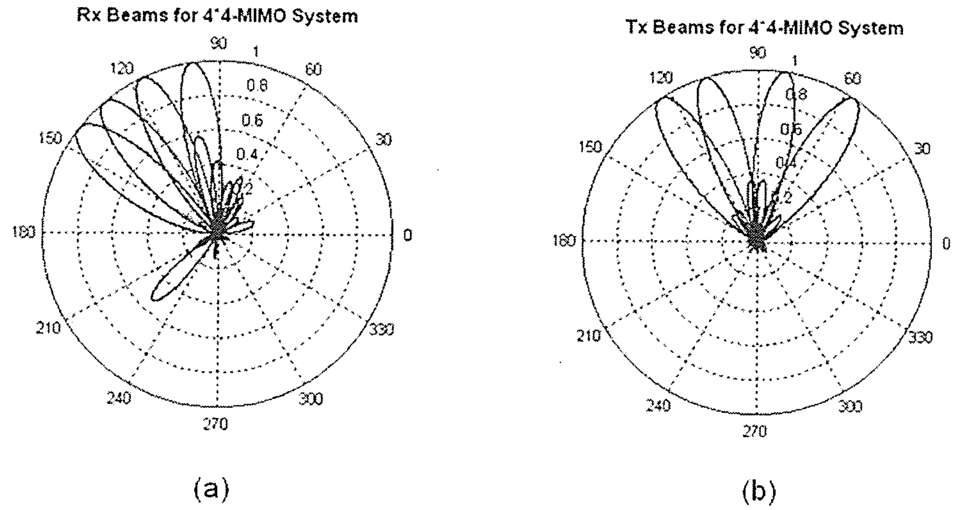

Figure 5.29 **Beams for the scenario where Tx is located far from the chairs for the 4×4-MIMO System (beam angles for (a)=100°, 117°, 131°, 143°, beam angles for (b)=57°, 82°, 106°, 123°).**

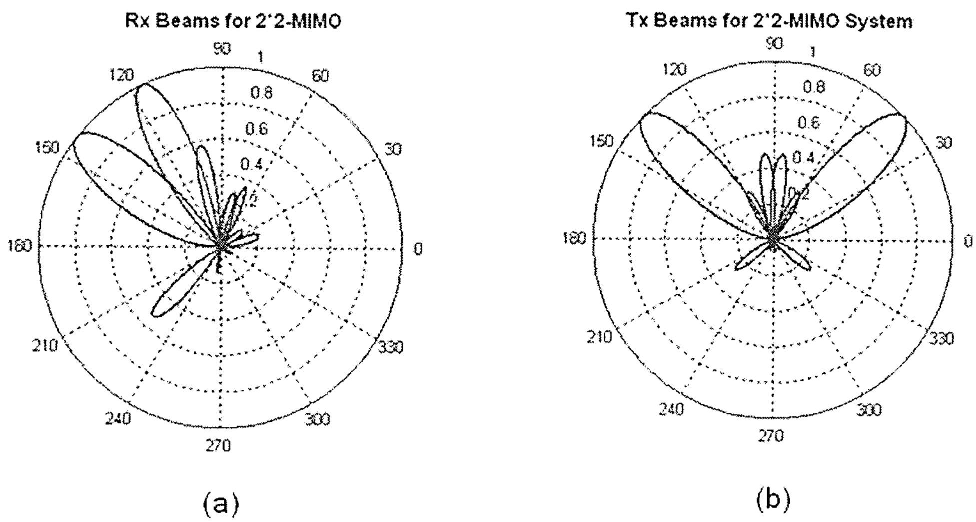

Figure 5.30 **Beams for the scenario where Tx is located far from the chairs for the 2×2-MIMO System (beam angles for (a)=116°, 142°, beam angles for (b)= 45°, 135°).**

	Singular Value1	Singular Value2	Singular Value3	Singular Value4
Space Div. (4×4-MIMO)	1.0000	0.0880	0.0080	0.0010
Angle Div. (4×4-MIMO)	1.0000	0.0806	0.0067	0.0000
Space Div. (2×2-MIMO)	1.0000	0.2037	-------	-------
Angle Div. (2×2-MIMO)	1.0000	0.1151	-------	-------

Table 5-11 Singular values for the scenario where Tx is located far from the chairs.

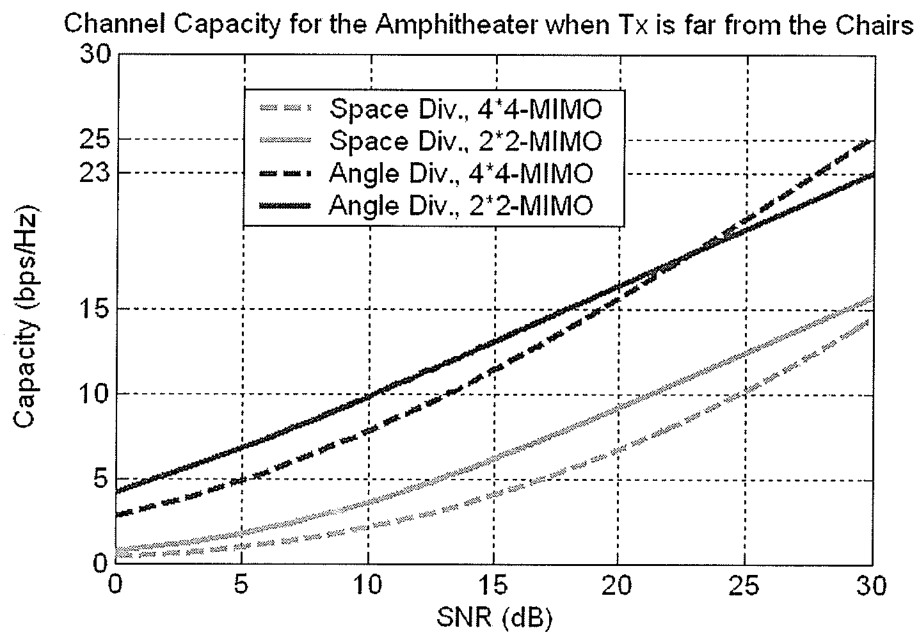

Figure 5.31 Channel capacity for the scenario where Tx is located far from the chairs.

5.3 Chapter Summary

In this chapter two different distributions of uniform and cluster form for scatterers were studied in two typical indoor environments of an office and an amphitheater.

For both kinds of distribution, results for LOS and NLOS cases were evaluated. Impacts of number of scatterers, number of MIMO elements, Rx element spacing, Tx position and wall's material were studied for LOS and NLOS cases.

Moreover, space and angle diversity methods for different MIMO systems were compared.

Chapter6: Conclusions and Future Works

6.1 Chapter Introduction

In this chapter, model properties, thesis contribution, conclusions of the outdoor and indoor results, model shortcomings and future works for this study are addressed.

6.2 The SISTER Model

In this thesis a mathematical model to characterize wireless communication channel for outdoor and indoor environments is developed which falls into semi-deterministic channel model category. This model is based on electromagnetic scattering and reflecting and fundamental physics and mathematics, and in fact, it bridges the gap between the complicated wave propagation of radio signals and the idealized models using statistical channel properties for analyzing MIMO systems.

The formulas used in this model consist of reflected and scattered fields, antenna pattern and channel capacity calculations and coordinate transformations. Electromagnetic scattering was considered in the model by choosing simple shape of sphere for scatterers and including their scattering properties in the calculations.

To keep the SISTER model simple, we considered only single interaction from each scatterer (or reflector) and neglected the interactions between scatterers (or reflectors). The achieved accuracy is acceptable since the main objective of developing such models is not characterizing the wireless channel perfectly and including all the details. Conversely, these simple modelings are suitable for designing at preliminary stages to let the designer to specify the procedure guidelines properly and hence stay on the right track for a better design and faster implementation of the system. Therefore, it is required to keep these models as simple and fast as possible.

Finally, the SISTER model is validated by *Wireless Insite,* a three dimensional ray tracing tool by Remcom Inc.

6.3 Thesis Contribution

The proposed model is applicable to arbitrary antennas and suitable for channel prediction studies for both indoor and outdoor environments. In the SISTER model, different distributions for scatterers and in the case of indoor environments, different dimensions for a room can be assumed. The corresponding algorithm calculates the direct path, reflected and scattered electric fields and finally computes the channel capacity in a very short time. In the SISTER model, different distributions for the scatterers, reflection from the ground for outdoors and from the walls for indoors and also antenna array factor are included in channel complex impulse response calculations.

6.4 Results and Conclusions

Based on the results for the outdoor environments, reflection from the high conductive ground can increase the capacity for LOS case since it lessens direct path dominance. Conversely, low conductive ground does not have significant impact on the channel capacity.

For indoor environments as well, reflected fields from the walls are added up and have significant impact on the channel capacity which is comparable to the direct path. In the presence of direct path, strong reflected field can increase the capacity as it lessens the effect of direct path; conversely, if direct path does not exist, strong reflected field can act like a virtual dominant path and reduce the channel capacity.

As a result, environments with high conductive walls can show higher channel capacity in LOS case if the multipaths are added in such a way that they increase the orthogonality.

For both indoor and outdoor environments with uniform distribution of scatterers, if using space diversity is the only possible choice, for lower SNRs it is wiser to use a 2×2-MIMO system rather than a 4×4-MIMO system but for higher SNRs probably 4×4-MIMO systems surpass 2×2-MIMO systems. For the cluster form of the scatterers in indoors, higher performance can be achieved by 4×4-MIMO system comparing to 2×2-MIMO system applying space diversity.

Generally, in LOS case, space diversity does not show satisfactory results even for a 4×4-MIMO system when the element spacing at both ends is $\lambda/2$. However, if it is possible to increase the element spacing at even one end, considerable improvement can be achieved. Although, the better alternative to improve the channel capacity is applying angle diversity or beam selection method. This technique is a promising solution in MIMO systems whose main advantage comparing to its other counterparts is that it allocates high capacity not to all the points but to the desired ones which results in minimum interference for undesired areas. This is quite beneficial especially in indoor environments where interference is a real concern.

As this study shows, for an office area, for instance, with either uniform or cluster form distribution for scatterers, if the right angles for the beams are selected, the best performance can be achieved by 4×4-MIMO applying angle diversity method.

To obtain narrow beams needed in this method, antenna array can be used as MIMO elements at both Tx and Rx sides.

The main challenge in these systems is finding the optimal angles where the different beams should be directed towards. As our study suggests acceptable results can be obtained by directing the beams towards the clusters of scatterers or reflecting points from the walls (of course those which are not in horizontal plane such as ceiling and floor reflecting points) to increase the probability of orthogonality between different paths, though they are not necessarily the best ones. If the clusters or reflecting points are located in the same elevation angles with respect to Tx and Rx or are close to horizontal plane where usually direct path exists, obviously they are not good choices for the direction of the beams. When right angles are selected, LOS capacity might be as high as NLOS capacity as the results have confirmed. It is predicted to find right angles much easier by employing planar array instead of linear array since they give large directivities by directing beams in only half sphere.

Another important issue is the beams' overlap. Even if the beams are selected properly still it is probable not to get desirable results due to the beams' overlap. Therefore, as the results have confirmed, the best beam angles are those which are far from the direct path direction (horizontal plane) and have the least overlap with each other. To lessen the effect of overlap, different antenna polarization for the adjacent beams can be used. For NLOS case, while selecting scanning angles, it should be taken into account that the blockage can affect some beams and reduce the number of channels. This happens for instance, if beams are directed towards the clusters which are behind the block.

According to the results, if there is a possibility to have a larger spacing at least at one end and if we are willing to get a higher capacity regardless of cost issues, it is wiser to use more antenna elements in order to decrease HPBW which ultimately leads to decrease in beams' overlap and increase in capacity.

Another challenging problem as it was seen for the amphitheater environment, for instance, is scanning the angles towards the endfire which leads in changing the scanning angles and pushing them close to each other which ultimately increases the overlap. To solve these kinds of problems, other array arrangements can be used to change the desirable direction from endfire to broadside.

6.5 The SISTER Model Shortcomings

As the shortcomings of the model, two following items can be addressed:

1. Since the model is developed based on assuming single interaction from each scatterer (or reflector) it would not be as accurate for large size scatterers which are located close to each other. This is due to the fact that large packed scatterers can have a significant contribution in making great amount of energy at the receiver even after multiple interactions between themselves which are neglected in the SISTER model.
2. The derivative order of the Associated Legendre function which is used in scattered field calculation is dependent on the size of the scatterers. As the run time of the program mainly depends on taking this derivative, for larger scatterers and obviously for large number of scatterers, it will rise up. Therefore, the run time puts limits on the number and size of scatterers.

6.6 Future Works

Future works for this study are summarized as follows:

1. This model can be enhanced in such a way that it includes multi-reflections to be applicable for areas such as hallways.

2. MS mobility can also be taken into account by including the Doppler shift effects, to model a non stationary channel.
3. While in calculations wherever needed, we only considered exact center frequency, the SISTER model is only applicable for narrowband channels. As a next step, it can be improved to include wideband channels as well.
4. According to the results, to achieve high performance in angle diversity method it is critical to have directional antennas. Planar arrays are good candidates since they make it possible to gain large directivities by directing beams in only half sphere. Therefore, as the next step, model can be enhanced to be applicable to planar arrays as well as linear ones.

6.7 Chapter Summary

In this chapter, the SISTER model properties were reviewed once again and its strengths as the thesis contribution were addressed. General conclusions for outdoor and indoor environments were evaluated and challenges in getting higher performance were discussed. Finally, the SISTER model's shortcomings and the future works for this study were expressed.

References

[1] R. Goodwins, ZDNet Company at UK, "Finding MIMO", October 14, 2003. http://comment.zdnet.co.uk/0,39020505,39117125-2,00.htm

[2] D. Gesbert, "Background on MIMO research, "Univ. Oslo, Norway, http://heim.ifi.uio.no/~gesbert/mimo_research.html

[3] URL: http://en.wikipedia.org/wiki/Multiple-input_multiple-output_communications

[4] D. Gesbert, H. Bolcskei, D.A. Gore, A.J. Paulraj, "Outdoor MIMO wireless channels: models and performance prediction," *Communications, IEEE Trans.* vol. 50, pp. 1926 – 1934, no. 12, Dec. 2002.

[5] Remcom Inc. Technical Staff, *Wireless Insite*, Remcom Inc., version 2.0.5, 2004.

[6] J. Foschini, M. Gans "On the limit of wireless communications in a fading environment when using multiple antennas," *Wireless Personal Communications*, vol. 6, no. 3, pp. 311-335, 1998.

[7] M.A. Jensen, J.W. Wallace, "A review of antennas and propagation for MIMO wireless communications," *Antennas and Propagation, IEEE Trans.* vol. 52, no. 11, Nov. 2004, pp. 2810 – 2824.

[8] J.C. Liberty JR., T.S. Rappapaort, *Smart Antennas for Wireless Communications*. Upper Saddle River, NJ: Prentice Hall, 1999.

[9] V. Tarokh, N. Seshadri, A.R. Calderbank, "Space-time codes for high data rate wireless communication: performance criterion and code construction," *IEEE Transactions on Information Theory*, vol. 44, no. 2, pp. 744-65, March 1998.

[10] S. A. Alamouti, "A simple transmit diversity technique for wireless communication," *IEEE Journal on Selected Areas on Communications*, vol. 16, Oct. 1998.

[11] C. C. Martin, J. H. Winters, and N. R. Sollenberger, "MIMO radio channel measurements: performance comparison of antenna configurations," in *Proc. IEEE 54th Veh. Technol. Conf.*, vol. 2, pp. 1225–1229, Atlantic City, NJ, Oct. 2001.

[12] A. F. Molisch, J. H. Winters, and M. Z. Win, "Capacity of MIMO systems with antenna selection," in *Proc. IEEE Int. Conf. Commun.*, vol. 2, pp. 570–574, Helsinki, Finland, June 2001.

[13] S. Sandhu, R. U. Nabar, D. A. Gore, and A. Paulraj, "Near-optimal selection of transmit antennas for a MIMO channel based on Shannon capacity," in *Proc. 34th Asilomar Conf. Signals, Systems and Computers*, vol. 1, pp. 567–571, Pacific Grove, CA, Oct.-Nov. 2000.

[14] R.W. Heath JR., S. Sandhu, and A. Paulraj, "Antenna selection for spatial multiplexing systems with linear receivers," *IEEE Commun. Lett.*, vol. 5, pp. 142–144, Apr. 2001.

[15] R. A. Andrews, P. P. Mitra and R. deCarvalho, "Tripling the capacity of wireless communications using electromagnetic polarization," *Nature*, vol. 409, pp. 316–318, Jan. 2001.

[16] J. B. Andersen and B. N. Getu, "The MIMO cube – a compact MIMO antenna," in *Proc. 5th Int. Symp. on Wireless Personal Multimedia Communications*, vol. 1, pp. 112–114, Honolulu, HI, Oct. 2002.

[17] R.G. Vaughan, "Polarization diversity in mobile communications," *IEEE Trans. Veh. Technol.*, vol. 39, pp. 177–186, Aug. 1990.

[18] J. P. Kermoal, L. Schumacher, F. Frederiksen, and P. E. Mogensen, "Polarization diversity in MIMO radio channels: experimental validation of a stochastic model and performance assessment," in *Proc. IEEE 54*th *Veh. Technol. Conf.*, vol. 1, pp. 22–26, Atlantic City, NJ, Oct. 2001.

[19] R. Janaswamy, "Effect of element mutual coupling on the capacity of fixed length linear arrays," *IEEE AntennasWireless Propagat. Lett.*, vol. 1, no. 1, pp.157–160, 2002.

[20] R.G. Vaughan, J.B. Andersen, "Antenna diversity in mobile communications," *IEEE Trans. Veh. Technol.*, vol. VT-36, pp.147–172, Nov.1987.

[21] T. Svantesson, "Correlation and channel capacity of MIMO systems employing multimode antennas," *IEEE Trans. Veh. Technol.*, vol. 51, pp. 1304–1312, Nov. 2002.

[22] C. Waldschmidt, T. Fugen, and W. Wiesbeck, "Spiral and dipole antennas for indoor MIMO-systems," *IEEE Antennas Wireless Propagat. Lett.*, vol. 1, no. 1, pp.176–178, 2002.

[23] T. Svantesson, *Antenna and Propagation from a Signal Processing Perspective*, PhD dissertation, Chalmers University of Technology, Sweden 2001.

[24] A. E. Forooshani and S. Noghanian, "Comparison of space and angle diversity techniques for Indoor MIMO System," *IEEE AP Symposium, Albuquerque, NM, USA,* Jul. 2006.

[25] C. Balanis, *Antenna Theory Analysis and Design*, John Wiley & Sons, Inc., New York, 1988.

[26] C. Balanis, *Advanced Engineering Electromagnetics*, John Wiley & Sons, Inc., New York, 1989.

[27] S.M. Wentworth, *Fundamentals of Electromagnetics with Engineering applications*, 111 River Street, Hoboken, NJ: John Wiley & Sons, 2005.

[28] Robert E. Collin, *Antennas and Radiowave Propagation,* McGraw-Hill, New York, 1985.